



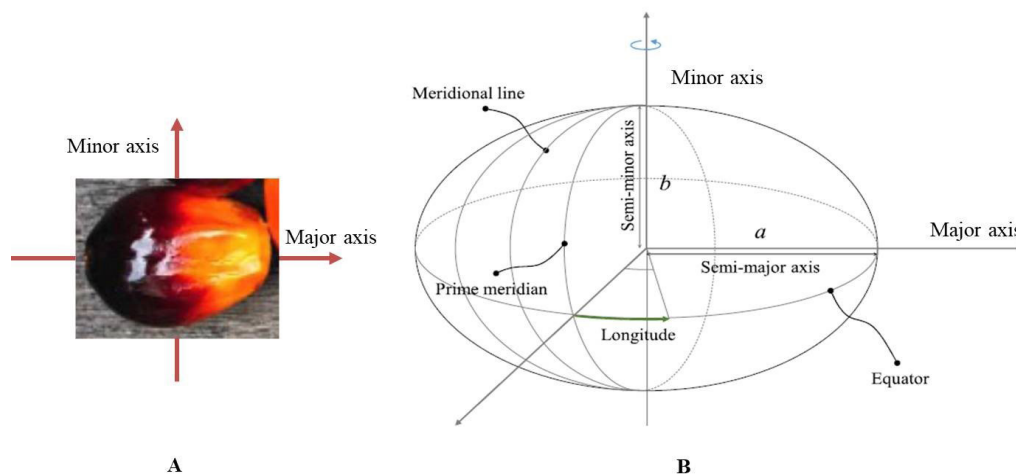
SQUJS

Sultan Qaboos University Journal for Science

ISSN (Print Edition): 1027-524 X; ISSN (Online Edition): 2414-536 X

Volume 28, Issue 2, 2023

Indexed in Google Scholar, DOAJ, CrossRef, EBSCO, Jgate, LOCKSS, and Al Manhal



A: Palm oil fruit showing its oval shape with major and minor axes [33], B: Parameters of the ellipsoid model of the earth [34] (see p. 5, Figure 2).

Contents

- The Intended Blessed Tree in the Quran - Is it Olive Tree or Palm Oil Tree?
- Impact of Climate Change on Rare Species in Arid Environments
- An Efficient Sensor Based on Anodic Activation of Graphene Oxide for Sensitive and Selective Determination of Dopamine in Blood Serum
- Preparation and Characterization of Iron Oxide Nano-Adsorbent by *Enteromorpha Flexuosa* Algae Obtained from Yanbu Red Sea, Saudi Arabia
- Analysis of Fractional Linear Multi-Steps Methods of Order Four From Super-Convergence
- Knowledge and Attitude Towards COVID-19 and Associated Mental Health Status Among Students of Sultan Qaboos University, Oman

SULTAN QABOOS UNIVERSITY JOURNAL FOR SCIENCE

(Formerly: SQU Journal for Scientific Research - Science and Technology)

The Sultan Qaboos University Journal for Science publishes original contributions covering the full range of fundamental and applied sciences, including mathematics, statistics, chemistry, physics, biology, biotechnology, environmental, earth sciences and computer sciences as well as related disciplines. Papers should present the results of original research that have not been previously published. In addition, the Journal publishes review articles on topics of particular interest. The Journal welcomes also articles related to applied aspects of science with relevance to the needs of local Omani society. Examples of applied studies of local interest include: geological and geophysical case studies and fieldwork results from different areas of Oman; local biological surveys, distributions and case studies; and design, implementation and evaluation of IT solutions for the local industry. All papers will be peer reviewed.

SQU ACADEMIC PUBLICATIONS BOARD

Prof. Amer Saif Al-Hinai, Chairman of Academic Publications Board

Prof. Farouq Sabri Mjalli

Prof. Samir Al-Adawi

Prof. M. Shafiur Rahman

Prof. Said Al-dhafri

Prof. Muhammad S. Khan

Dr. Saleh Al-Brashdi

Prof. Mohammed N. Al-Suqri

Dr. Ghazi Ali Al-Rawas

Mr. Jamal Al-Gheilani

SQUJS EDITORIAL BOARD

Editor-in-Chief, Prof. Muhammad S. Khan

Editors: Prof. Rachid Sbiaa

Dr. Michael Barry

Associate Editors

Prof. Abderezak Touzene

Prof. Ahmad J. Al-Salman

Prof. Iftikhar Ahmed

Prof. Moh'd T.S. Alodat

*Prof. Mohammad M. Rahman

Prof. A.M. Jarrah, Yarmouk University, Jordan

Prof. Wael Ismail, Arabian Gulf University, Bahrain

Prof. Ercan Ozcan, Istanbul Technical University, Turkey

Prof. Imran Ali, Central University New Delhi, India

*Online manager

Dr. Nawal Al-Rasbi

Prof. Nazife Koca

Prof. Rachid Sbiaa

Dr. Rengaraj Selvaraj

Dr. Sedky Hassan

Dr. Talal K. Al-Hosni

Prof. Kalyan Das, Indian Institute of
Technology Bombay, India

Prof. Haikel Jelassi, National Center for Nuclear
Sciences and Technologies, Tunis

INTERNATIONAL ADVISORY BOARD

Prof. Asif M. Khan, University of Peshawar, Pakistan

Prof. Deniz Sunar Cerci, Adiyaman University, Turkey

Prof. Huda Mahmoud, Kuwait University

Prof. Kuppapalle Vajravelu, University of
Central Florida, USA

Prof. Paul R. Raithby,

University of Bath, UK.

Prof. Yogendra Prasad Chaubey, Concordia,
University, Canada

Editorial Assistant: Laila Al-Anboursy

Cover Page Designer: Laila Al-Anboursy

Date of issue: December 2023

The Journal is not responsible for opinions printed in its publications; they represent the views of the individuals to whom they are credited and are not binding upon the Journal.

All correspondence should be addressed to the Journal Office of Sultan Qaboos University Journal for Science, P.O. Box 36, Muscat 123, Sultanate of Oman. Tel: (968) 2414-2251, Email: squjs@squ.edu.om.

ISSN (print edition): 1027-524X; ISSN (online edition): 2414-536X

Edited and designed by the Journal Editorial Office, College of Science, Sultan Qaboos University.

CONTENTS

BIOLOGY

- The Intended Blessed Tree in the Quran - Is it Olive Tree or Palm Oil Tree? 1
Mostafa Koutb
- Impact of Climate Change on Rare Species in Arid Environments 9
Hamada E. Ali

CHEMISTRY

- An Efficient Sensor Based on Anodic Activation of Graphene Oxide for Sensitive and Selective Determination of Dopamine in Blood Serum 17
*Al-Ghafri L.^a, Al-Hatmi N.^a, Joudi S.A^b and Khudaish E.A.^{*a}*
- Preparation and Characterization of Iron Oxide Nano-adsorbent by *Enteromorpha Flexuosa* Algae obtained from Yanbu Red Sea, Saudi Arabia 28
*Alaa Elmi¹, Rafat Afifi Khattab², Omar M.L. Alharbi³, Gunel Imanova⁴, Imran Ali^{*1,5}*

MATHEMATICS

- Analysis of Fractional Linear Multi-Step Methods of Order Four from Super-Convergence. 44
*Khadija Al-Hasani and H.M. Nasir**

STATISTICS

- Knowledge and Attitude Towards COVID-19 and Associated Mental Health Status among Students of Sultan Qaboos University, Oman 56
M. Mazharul Islam^{1,3}, Ronald Wesonga^{1,3}, Iman Al Hasani^{1,3}, Afra Al Manei^{2,3}*

GUIDE TO AUTHORS

The Intended Blessed Tree in the Quran - Is it Olive Tree or Palm Oil Tree?

Mostafa Koutb

Current Address: Department of Biology, Faculty of Applied Science, Umm Al-Qura University, 715 Makkah, Saudia Arabia. Permanent address: Department of Botany and Microbiology, Faculty of Science. Assiut University, 71516 Assiut, Egypt. Email: mmkoutb@uqu.edu.sa.

ABSTRACT: This article aims to provide an alternative scientific interpretation for verse 35 in Surat An-Nur. This verse addresses the very famous simile in the Quran which describes the light of Allah. In this verse Allah mentioned that 'Allah (is the) light (of) the heavens and the earth. (The) example (of) His Light (is) like a niche in it (is) a lamp; the lamp (is) in a glass, the glass as if it were a star brilliant (which) is lit from a tree blessed - an olive, not (of the) east and not (of the) west, would almost its oil glow, even if not touched it fire' 'Despite all the most commentators who have addressed this verse singled the olive tree as the blessed tree, the intended tree still has one characteristic that is enigmatic. Regarding this characteristic 'not east and not west', all previous interpretations directed this characteristic to the compass directions. But they did not give any logical and acceptable justification. Dealing with this verse with another linguistic concept, particularly with three words in the verse 'zaytūnatin, sharqiyyatin, and gharbiyyatin' can change the story of the intended blessed tree. The first word in the Arabic language could be considered as an adjective for exaggeration meaning a high oil producer rather than the genus olive. More interestingly, this word has been mentioned as an indefinite noun without 'Al' which makes the noun definite when it is used as a prefix; therefore, in this case, it is not specific to olive but it could refer to any tree producing high amount of oil. The second word 'sharqiyyatin' comes from the verb 'sharek', which in Arabic means, particularly for dates, that they became reddish in color as a sign of maturity. The third word 'gharbiyyatin' derives its meaning from the verb 'gharb' which means it became black. When these new meanings are applied to the verse, the first word will now mean any tree with high oil production. The other two words, will mean reddish and black colors of the fruit not the east and west directions. These two characteristics could be considered to be distinguishable features for palm oil tree not for olive trees. In this paper two additional evidences supporting this idea have been addressed. Therefore, the palm oil tree, particularly the subspecies *nigrescens* could be a potential candidate for the blessed tree in the Quran.

Keywords: Palm oil tree; Olive tree; Scientific interpretation of Quran; Carotenoids; Almost glow.

الشجرة المباركة في القرآن - هل هي شجرة الزيتون أم شجرة نخيل الزيت؟

مصطفى قطب

المخلص: هذا البحث محاولة لطرح تفسير علمي بديل للآية القرآنية 35 من سورة النور. هذه الآية تتناول المثل القرآني المشهور الذي يصف نور الله. في هذه الآية يقول الله تعالى 'اللَّهُ نُورُ السَّمَوَاتِ وَالْأَرْضِ مِثْلُ نُورِ كَمِشْكَاةٍ فِيهَا مِصْبَاحٌ الْمِصْبَاحُ فِي زُجَاجَةٍ الزُّجَاجَةُ كَأَنَّهَا كَوْكَبٌ دُرِّيٌّ يُوقَدُ مِنْ شَجَرَةٍ مُبَارَكَةٍ زَيْتُونَةٍ لَا شَرْقِيَّةٍ وَلَا غَرْبِيَّةٍ يَكَادُ زَيْتُهَا يُضِيءُ وَلَوْ لَمْ تَمْسَسْهُ نَارٌ' (النور-35). على الرغم من أن كل المفسرين الذين فسروا هذه الآية ذكروا أن الشجرة المباركة المقصودة في المثل قد تكون هي شجرة الزيتون إلا أن هناك صفة في هذه الشجرة ما زالت غامضة. هذه الصفة هي أن هذه الشجرة تتميز بأنها لا شرقية ولا غربية، وحيث أن كل التفسيرات السابقة وجهت هذه الصفة إلى الإتجاهات الجغرافية الأصلية إلا أنها لم تقدم مبررات مقبولة لهذا التفسير. لكن بالتعامل مع هذه الصفة - من وجهة نظر لغوية مختلفة، وتحديدًا بالمعنى اللغوي للكلمات الثلاث: زيتونة و شرقية و غربية ، يمكن أن يغير فهمنا لقصة الشجرة المباركة. الكلمة الأولى وهي 'زيتونة' في اللغة العربية تعني صيغة مبالغة دلالة على كثرة إنتاج الزيت وجدير بالذكر أن هذه الكلمة ذكرت في هذه الحالة بصيغة النكرة وهي تعني العموم وليست خاصة لجنس معين. بينما الكلمة الثانية وهي 'شرقية' جذر هذه الكلمة هو 'شرق' وهي تحمل معان عدة وخصوصًا عندما تستخدم للبلح أي 'شرق البلح' تعني أحمر لونه وهذه إشارة للنضج. والكلمة الثالثة هي 'غربية' وجذر هذه الكلمة في اللغة هو 'غرب' وهي أيضا لها معان عدة منها غرب الشيء يعني أصبح أسود اللون. وعند تطبيق هذه المعاني على الشجرة المباركة ، فإنها تؤول إلى معنى 'كثرة إنتاج الزيت'، وأن لون ثمرتها لا حمراء ولا سوداء هو لشجرة نخيل الزيت وليست شجرة الزيتون فقط. هناك أدلة أخرى تثبت هذه الفكرة ستتم مناقشتها في البحث. ومن

¹ اللَّهُ نُورُ السَّمَوَاتِ وَالْأَرْضِ مِثْلُ نُورِ كَمِشْكَاةٍ فِيهَا مِصْبَاحٌ الْمِصْبَاحُ فِي زُجَاجَةٍ الزُّجَاجَةُ كَأَنَّهَا كَوْكَبٌ دُرِّيٌّ يُوقَدُ مِنْ شَجَرَةٍ مُبَارَكَةٍ زَيْتُونَةٍ لَا شَرْقِيَّةٍ وَلَا غَرْبِيَّةٍ يَكَادُ زَيْتُهَا يُضِيءُ وَلَوْ لَمْ تَمْسَسْهُ نَارٌ! (النور- 35)

Elaeis guineensis nigrescens ثم يمكن القول بأن الشجرة المباركة في هذه الآية قد تكون هي شجرة نخيل الزيت وخصوصا تحت النوع .subspecies

الكلمات المفتاحية: شجرة نخيل الزيت؛ لا شرقية ولا غربية؛ لا حمراء ولا سوداء لون الثمرة الناضجة؛ كاروتينيدات؛ يكاد زيتها بضيء.



1. Introduction

Generally, similes in the Quran are very crucial and popular as an eloquent language style to simplify the meaning for humankind. One of these similes is represented in the Verse 35 in Surat An-Nur. In this verse Allah mentioned that 'Allah (is the) light (of) the heavens and the earth. (The) example (of) His light (is) like a niche in it (is) a lamp; the lamp (is) in a glass, the glass as if it were a star brilliant (which) is lit from a tree blessed - an olive, not (of) the east and not (of) the west, would almost its oil glow, even if not touched it fire' (An-Nur - 35). The oil palm tree, also known as '*Elaeis guineensis Jacq*', is a plant that grows well in tropical regions. The oil palm tree was developed and used as an agricultural crop [1]. The use of palm oil in food dates back to 5000 BC, as evidenced by the discovery of the oil in the tomb at Abydos in Egypt [2]. Oil palm can accumulate up to 90% oil in its mesocarp, the highest level observed in the plant kingdom. In contrast, the closely related date palm accumulates almost exclusively sugars [3]. Oil palm can produce higher amounts of oil than other oil-producing species (about nine times more than soy and 4.5 times more than rapeseed) per unit of land area [4]. Oil palm is now the most productive oil crop in the world (3.5 tons/ha/y), with 36% of global production [5]. Most palm oil is derived from the mesocarp which, can comprise up to 90% of the dry weight. This is, by far, the highest oil content reported for any plant tissue [3]. The fuel properties of optimized biodiesel were found to be comparable to those of diesel and were in accordance with the latest biodiesel standards. The calorific value of optimized Tung seed biodiesel was 9100 Kcal/Kg which is lower than diesel fuel [6]. The flash and fire point of palm seed biodiesel were determined to be 180 °C and 194 °C, respectively which are higher than diesel fuel.

Regarding the value of palm tree as a genus in the Quran, it has been mentioned 20 times throughout the Quran, while the olive tree was mentioned five times in addition to this time under investigation. If I could prove that the intended tree in this verse is the palm tree, it will be recorded in the Quran 21 times. Moreover, the palm tree also gained the attention in Sunnah, as Narrated Ibn `Umar: 'The Prophet (PBUH) said, 'Amongst the trees, there is a tree, the leaves of which do not fall and is like a Muslim. Tell me the name of that tree?' Everyone started to think about the trees in the desert areas. And I thought of the date palm tree. The others then asked, 'Please inform us what is that tree, O Allah's Messenger (PBUH)?' He replied, 'It is the date-palm tree'. Additionally, Anas ibn Malik reported that the Prophet, may Allah bless him and grant him peace, said, 'If the Final Hour comes while you have a shoot of a plant in your hands and it is possible to plant it before the Hour comes, you should plant it.' Although several plant species can propagate by shoots when this process is mentioned in the Arabic language, it is understood by default to be about the palm tree. Accordingly, all the above hints recorded about the palm tree in the Quran and Sunnah reflect the important value of this tree. As mentioned above, regarding the common interpretations of the verse under investigation, all previous interpretations directed this character to the compass directions. But they did not give any plausible and acceptable justification. Most of the previous scholars directed the word 'zaytūnatin' to the genus olive and the words 'sharqiyyatin, gharbiyyatin' have been directed to east and west directions [7,8]. Also, some scholars have mentioned that this tree is a desert tree, others mentioned that in the middle of the trees, and others mentioned that it is not an earth tree rather it paradise tree [8,9]. Moreover, when Allah wanted to specify olive itself, he mentioned in Surat Al-Tin 'By the fig, and the olive' (Al-Tin – 1) and in Arabic 'wal-fīni wal-zaytūn'.

In this current paper, I try to give a new vision about the intended blessed tree in this verse by using other alternative Arabic meanings to the linguistically accepted words 'zaytūnatin', 'sharqiyyatin' and 'gharbiyyatin'. Additionally, by directing the pronoun in 'not east and not west' to the palm oil fruit and particularly to its color orientation. This must not be understood as swimming against water current, because all the previous commentators reported that the intended blessed tree in this verse is the olive tree rather it is considered to be a different insight and concept for a new interpretation. Recently, a new insight as a scientific interpretation of the verse 43 in Surat Al-kaḥf has been introduced, although all previous commentators have provided a completely different concept of interpretation [10]. Therefore, in this manuscript I am trying to give an alternative interpretation to this verse with plausible justifications that might change the story of the candidate for the blessed tree in the Quran from the olive tree to the palm oil tree.

2. Fruit color and ripening

One of the main challenges in the fruit industry is to identify the right fruit to harvest. To preserve and maintain the quality of palm oil products, it is crucial to harvest the palm oil fresh fruit bunch (FFB) at the right stage [11]. According to Fadilah, *et al.* [12], most palm oil fruits grading is based on two, three or four stages that are unripe, reddish black as under-ripe, red as ripe, and reddish orange as over-ripe. Other research by [13,14,15] focused on two stages, which are ripe and unripe of FFB and achieved high accuracy results.

Some researchers have determined and evaluated the maturity of oil palm fruits using a variety of techniques, including hyperspectral imaging [16,17], fluorescence detection [18,19], computer vision and an optical sensor [20,21], inductive detection [22,23], near-infrared spectroscopy [24,25], laser detection [25], and lidar detection [26]. Advanced color-based machine vision was able to categorize distinct fruits into correct groups with an accuracy of 90% [27,28]. Further studies have been conducted with high accuracy values, including 95.48% [29], 97.9% [30] and 98.70% [31].

3. Not east and not west

First, the fruit of the palm oil tree is the intended by this description in the verse 'tree blessed - an olive, not (of the) east and not (of the) west', despite Allah mentioned apparently the tree. There are three clues that can support this approach, first, the fruit can be used to represent the whole tree as Allah mentioned in the story of Adam and Eve. 'Then when they both tasted the tree' (Al-A'raf – 22), in this case, it could be they tested the fruit or not. Secondly, Allah mentioned that this tree is 'zaytūnatin' which means highly produced oil and the source of oil production is the fruit not the whole tree. Thirdly, when Allah mentioned that 'is lit from a tree blessed' this means the lamp is lit by the oil and not by the whole tree, so the oil in this case represented the tree as the fruit can.





The Arabic verb 'sharek' which is the source of the word 'sharqiyyatin', has various lexical meanings, including the east direction and particularly, for dates means colored reddish, and in reference to the face it refers to reddish shyness. In addition, the word 'Asharqiyy' in Arabic means the red pigment [32]. Moreover the word 'shark' does not always refer to the east direction as Prophet Mohamed (PBUH) mentioned in Hadith An-Nawwas b. Sam'an said he heard the Apostle (PBUH) say: 'On the Day of Resurrection the Qur'an and those who acted according to it will be brought with Surat Al-Baqara and Al 'Imran preceding them. The Messenger of Allah (PBUH) likened them to three things, which I did not forget afterwards. He (the Holy Prophet) likened them to two clouds, or two black canopies with 'shark' (light) between them, or like two flocks of birds in ranks pleading for one who recited them'. In this case, the word 'shark' in Arabic means 'light' or 'silt' or 'barrier between.' On the other hand the verb 'gharb', which is the root of the word 'gharbiyyatin' in Arabic language, also has several meanings, including west direction and for an object means it became blackish. As Allah mentioned 'And in the mountains (are) tracts, white and red (of) various [their] colors, and intensely black' (Fatir – 27). In Arabic, the term 'gharābību' means black, and it has the same root in the language with the word 'gharbiyyatin'. Moreover the word 'Algharb' in Arabic means a big, green tree from which a black material like tar is produced to stain the camels [32]. Therefore, applying the color meaning to these words on what is mentioned in the verse 'not east and not west' will suggest the fruit color is non-pure reddish or non-pure blackish, but rather a combination of the two colors (reddish and black) within the same fruit. It is interesting to note that the Quran frequently uses this type of description, like when Allah mentioned in the description of the cow belonging to the Bani (children of) Israel, that 'It is a cow not old and not young' (Al-Baqarah - 68). The fact that this color exactly matches the color of fruit in its mature stage is more interesting (Figure 1).



Figure 1. Fruit exocarp colour phenotypes. (a) Individual oil palm fruits of a subspecies of *nigrescens* fruit bunch. Unripe fruits are deep-violet to black at the apex (visible in the bunch), and undergo minimal colour change upon ripening [33].

Fruit colour is an important trait in terms of fruit harvesting and, therefore, oil yield. Most oil palms are produced from the type of *nigrescens* or *virescens* fruit [33]. The *nigrescens* variety of oil palm makes up the majority of oil palm production. Fadilah, *et al.* [12] developed an interesting categorization of the ripeness stage into four groups: unripe purplish black, under-ripe reddish black, ripe red, and overripe reddish orange (table 1).

Table 1. The ripeness stage of palm oil FFB by Malaysian Palm Oil Board [12].

Image	Stage	Color characteristic
	Unripe	Purplish Black
	Under-ripe	Reddish black
	Ripe	Red
	Overripe	Reddish orange

4. Another evidence could support this interpretation

As it has been mentioned above, the Arabic verbs 'sharek' and 'ghareb' have several meanings, including the compass directions east and west. Even if we apply this meaning in the verse, it will also lead to the conclusion that the description of 'not east nor west' may apply to the fruit's color. This exact description describes the color orientation on the individual fruit. Let's suppose you were requested to describe the palm oil fruit colored with two different colors, using just two words. Indeed, it would be a very difficult job to express this situation in two words. Now, if we take into consideration the oblate ellipsoidal rotation of the earth around its minor axis in front of the sun, it has four directions, two of which are north and south on the minor axis up and down ends, while the other two are east and west. If we divide the ellipsoidal shape of the earth longitudinally along the minor axis, two halves eastern and western hemispheres will be revealed. If we apply this description to the fruit, which has an ellipsoid shape that is almost identical to that of the Earth's shape, its mature ovary has a minor axis capped by the stigma and at the posterior end an ovarian base detached from the receptacle in the inflorescence. So, if we divide this fruit in half along its minor axis, it will give two parts, east and west, comparable to the Earth. As Allah mentioned only the two words 'not east and nor west' that means the orientation of the two colors of the fruit should not be distributed in these two parts. The orientation of the colors - regardless the kind of color must be oriented in these two directions along their minor axes, which are east and west as indicated in figure 2. Therefore, based on the combination of the aforementioned descriptive features, we could suggest that intended blessed tree is the palm oil tree.

THE INTENDED BLESSED TREE IN QURAN IS IT OLIVE TREE OR PALM OIL TREE?

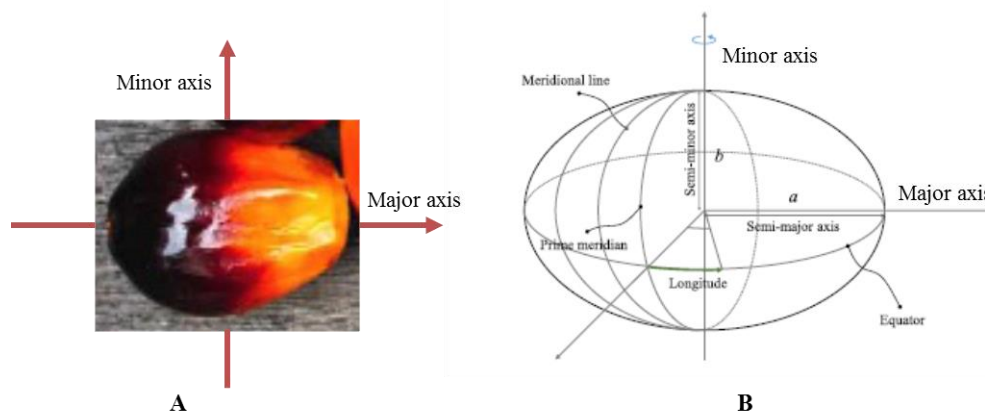


Figure 2. A: Palm oil fruit showing its oval shape with major and minor axes [33], B: Parameters of the ellipsoid model of the earth [34].

5. Correlation between red and black colors in Sunnah and their significance

These two colors, red and black, appeared together several times in the speech of our Prophet. For example, Jabir b. 'Abdullah al-Ansari reported: the Prophet (PBUH) said: 'I have been conferred upon five (things) which were not granted to anyone before me (and these are): Every apostle was sent particularly to his own people, whereas I have been sent to all the red and black'. The red and black people in this hadith refer to all people on the planet Earth, that might refer to the eastern and western people. Again, Abu Nadrah reported: the Messenger of Allah, peace and blessings be upon him, said during the middle of the day at the end of the pilgrimage, 'O people, your Lord is one, and your father Adam is one. There is no favor of an Arab over a foreigner, nor a foreigner over an Arab, nor red skin over black skin, nor black skin over red skin, except by righteousness. Have I not delivered the message?' They said, 'The Messenger of Allah has delivered the message.' This example also emphasizes the strong relationship between the colors, red and black. Generally in the Arabic language, when the expression 'black and red' is used, it often refers to all humanity on the planet. This expression might categorize all people into two groups: red and black. The red group might refer to the eastern people, while the black group might refer to the western one.

6. 'Would almost its oil glow, even if not touched it fire'

In this verse, Allah describes the oil of this blessed tree as an oil that is almost glowing. In Arabic, the verb 'yakādu' means 'it is close to happen', while the verb 'yuḏū' means 'illuminate or emit radiation'. That means its oil is close to illuminating or emitting radiation, even if it hasn't been touched by fire. The latter phenomenon could be attributable mainly to the presence of carotenoids in crude palm oil. Carotenoids are a diverse class of metabolites belonging to the family of terpenoids. These lipid-soluble compounds include oxygenated xanthophylls and non-oxygenated carotenes [35].

Crude palm oil is a complex mixture consisting of over 99% glycerides, which are the major component of the oil. The minor components include carotenoids, tocopherols, tocotrienols, phytosterols and phosphatides [36]. Red palm oil (RPO) is produced from crude palm oil through a milder refining process that enables the retention of most of the carotenes and vitamin E in the refined oil [37]. RPO is a refined palm oil with a high carotene content of approximately 524-542 mg/kg [38,39]. Moreover, it has been reported that red palm olein (RPOo) is the richest plant source of carotenoids, with a vitamin E content of 810 ppm, mostly in the form of tocotrienol. Vitamin E and β -carotenes play an important role as antioxidants that provide the oil with oxidative stability [40,41]. Interestingly, tocol compounds and β -carotene levels in virgin coconut, virgin olive, sunflower oil, and a mixture of olive and perilla oils are lower than in RPO [42-46].

Carotenoids affect the oil characteristics causing it to emit radiation. After light absorption to their bright S_2 state, carotenoids rapidly decay to the optically dark S_1 state. However, ultrafast spectroscopy experiments have shown the signatures of another dark state, termed S_X [47]. Upon photoexcitation, the generated S_2 state decays into S_1 in a few hundred femtoseconds, which then relaxes back to S_0 over a picosecond time scale [48]. It is difficult to produce the lowest energy triplet state, T_1 , of a carotenoid by direct absorption of light into that state. Instead, it is usually formed through energy transfer from another triplet species, e.g. triplet chlorophyll, intersystem crossing, the radiation less interconversion of singlet states and triplet states [49]. Triplet states are inefficient producers of luminescence [50].

There are a number of fundamentally sound reports of fluorescence from carotenoids [51-53], although until recently, it was largely believed that carotenoids were non-fluorescent. Indeed, many reports in the literature of carotenoid fluorescence can be attributed to fluorescent impurities in the samples [54]. When sensitive fluorescence spectrometers were used in sample analysis emission from carotenoids which typically have very weak quantum yields

on the range of 10^{-4} to 10^{-5} fluorescence could be observed [54,55]. Most carotenoids exhibit $S_2 \rightarrow S_0$ emission. Fluorescence associated with the $S_1 \rightarrow S_0$ transition is rarer (Figure 4).

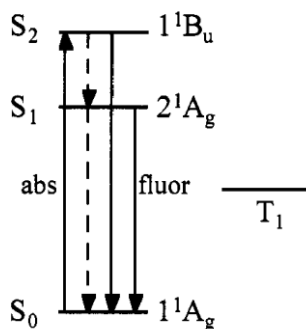


Figure 4. Energy level scheme of carotenoids. S_0 , S_1 and S_2 are singlet states, T_1 is the lowest lying triplet state [55].

7. Conclusion

In this article, I tried to give an alternative interpretation for the verse 35 in Surat An-Nur by rethinking the lexical meanings of Arabic words that provide us with some hints that the palm oil tree is the intended blessed tree in the Quran a scenario that is not exclusively restricted to olive tree. This finding was mainly attributed to its possession of highest oil production value in the plant kingdom, as well as to the specific colors of the fruit, the orientation of these colors on the pulp of the fruit, and to the high amount of carotenoids that might be responsible for making its oil almost glow or close to illuminating. Finally, it can be concluded that the intended blessed tree in Surat An-Nur verse 35 is the palm oil tree. Accordingly, the English translation of this part of the verse under investigation should be changed as follows '(which) is lit from a blessed tree— a palm oil, not red and no black, would almost make its oil glow, even if not touched by fire'. Indeed such similes that Allah provided to people through the Quran are very important for mankind and their understanding and knowledge. Therefore Allah mentioned that 'And these (are) the examples, We present them to the people so that they may give thought.(Al-Ankabut - 43). But not all people have the ability to understand these examples, as Allah mentioned in the Quran 'We site these examples for people, but none understand them except the knowledgeable ones (scientists) (Al-Hashr – 21).

Conflict of interest

The authors declare no conflict of interest.

Acknowledgment

The author greatly acknowledges Dr. Ahmed Abo Elwafa, Assistant Professor, Department of Arabic Linguistics, and Arabic Morphology and Syntax, College of Arabic Language and Literature, Umm Al-Qura University, Makkah, Saudi Arabia for the fruitful discussion on the lexical meanings of Arabic words.

References

1. Zolfagharnassab, S., Shariff, A.R.B.M., Ehsani, R., Jaafar, H.Z. and Aris, I.B. Classification of Oil Palm Fresh Fruit Bunches Based on Their Maturity Using Thermal Imaging Technique. *Agriculture*. 2022, **12**, 1779.
2. Raymond, W.D. The oil palm industry. *Tropical Science* 1961, **3**, 69-89.
3. Bourgis, F., Kilaru, A., Cao, X., Ngando-Ebongue, G.F., Drira, N., Ohlrogge, J.B. and Arondel, V. Comparative transcriptome and metabolite analysis of oil palm and date palm mesocarp that differ dramatically in carbon partitioning. *Proc. Natl. Acad. Sci. USA*. 2011, **108(30)**, 12527-12532. doi: 10.1073/pnas.1106502108.
4. Ngando-Ebongue, G.F., Ajambang, W.N., Koon, P., Lalu Firman, B. and Arondel, V. Breeding of the oil palm: Past, present and prospects. *Technological Innovations in Major World Oil Crops*. 2011, **1**, 7.
5. Gorey, N., Ghosh, S., Srivastava, P. and Kumar, V. Characterization of Palm Oil as Biodiesel IOP Conf. Series: *Materials Science and Engineering* 2017.
6. Al-Qurtubi, 'Al-Jami Li-Ahkam al-Qur'an'. Dar al-Taqwa, London, 2003.
7. Ibn Kathir, 'Tafsir al-Qur'an al-azim', Dar-us-Salam. Riyadh, 2000.
8. Al-Tabari, *Jaami' al-Bayan fee Ta'weel Ayy al-Qur'an*. Dar al-Ma'arif, Cairo, 1954.
9. Koutb, M. Water breakdown during photosynthesis and transpiration in plants as a scientific miracle in Qur'an. *Journal Interdisciplinary Qur'anic Studies* 2022, **1(2)**, 105-121.

THE INTENDED BLESSED TREE IN QURAN IS IT OLIVE TREE OR PALM OIL TREE?

11. Sabri, N., Ibrahim, Z. and Isa, D. Evaluation of color models for palm oil fresh fruit bunch ripeness classification. *Indonesian Journal of Electrical Engineering and Computer Science* 2018; **11(2)**, 549-557. <https://doi.org/10.11591/ijeecs.v11.i2.pp549-557>.
12. Fadilah, N., Mohamad-Saleh, J., Halim, Z.A., Ibrahim, H. and Ali S., S.S. Intelligent Color Vision System for Ripeness Classification of Oil Palm Fresh Fruit Bunch. *Sensors*. 2012, **12**, 14179-14195.
13. Roseleena, J., Nursuriati, J., Ahmed, J. and Low, C. Assessment of palm oil fresh fruit bunches using photogrammetric grading system. *International Food Research Journal*. 2011, **18**, 999-1005.
14. Sabri, N., Ibrahim, Z., Syahlan, S., Jamil, N. and Mangshor, N.N.A. Palm oil fresh fruit bunch ripeness grading identification using color features. *Journal of Fundamental and Applied Sciences*. 2017, **9(4S)**, 563-579.
15. Hambali, A., Siti Hadijah, N. and Rahman, M.A. Application of Integrated AHP and TOPSIS Techniques for Determining the Best Fresh Fruit Bunches (FFB). *Journal of Telecommunincation, Electronic and Computer Engineering* 2017, **9(3)**, 145-149.
16. Junkwon, P., Takigawa, T., Okamoto, H.; Hasegawa, H., Koike, M., Sakai, K., Siruntawinetti, J., Chaeychomsri, W., Vanavichit, A., Tittinuchanon, P. and Bahalayodhin, B. Hyperspectral imaging for nondestructive determination of internal qualities for oil palm (*Elaeis guineensis* Jacq. Var. tenera). *Agricultural Information Research*. 2009, **18**, 130-141.
17. Osama, M.B., Shariff, A.R.M., Shafri, H.Z.M., Mahmud, A.R. and Alfatni, M.S.M. Hyperspectral Technique System for Fruit Quality Determination. Map Asia and ISG. 2010, Kuala Lumpur, Malaysia.
18. Hazir, M.H.M. Ripeness Detection of Oil Palm Fresh Fruit Bunches Using Fluorescence Sensor. Ph.D. Thesis, 2011, University Putra Malaysia, Selangor, Malaysia.
19. Hazir, M.H.M., Shariff, A.R.M. and Amiruddin, M.D. Determination of oil palm fresh fruit bunch ripeness-Based on flavonoids and anthocyanin content. *Industrial Crops and Products* 2012, **36**, 466-475.
20. Alfatni, M.S.M., Shariff, A.R.M., Abdullah, M.Z., Marhaban, M.H., Shafie, S.B., Bamiruddin, M.D. and Saeed, O.M.B. Oil palm fresh fruit bunch ripeness classification based on rule-based expert system of ROI image processing technique results. IOP Conference Series: Earth and Environmental Science 2014.
21. Makky, M., Sony, P. and Salokhe, V.M. Automatic Non-destructive Quality Inspection System for Oil Palm Fruits. *International Agrophysics*. 2014, **28**, 319-329.
22. Harun, N.H., Mirson, N., Sidek, R.M., Aris, I., Wakiwaka, H. and Tashiro, K. Resonant Frequencies Effects on an Induction-Based Oil Palm Fruit Sensor. *Sensors*. 2014, **14(11)**, 21923-21940.
23. Mirson, N., Harun, .N.H., Lee, Y.K., Sidek, R.M., Aris, I., Wakiwaka, H. and Tashiro, K. Improvement in Sensitivity of an Inductive Oil Palm Fruit Sensor. *Sensors*, 2014, **14**, 2431-2448.
24. Silalahi, D.D., Reaño, C.E., Lansigan, F.P., Panopio, R.G., Bantayan, N.C., Caliman, J.P., Davrieux, F., Sudarno, S. and Yuan, Y.Y. Near-infrared spectroscopy: A rapid and non-destructive technique to assess the ripeness of oil palm (*Elaeis guineensis* Jacq) fresh fruit. *Journal of Near Infrared Spectroscopy*. 2016, **24**, 179-190.
25. Shiddiq, M., Salambue, R., Yasmin, N.Z., Lismayeni, F., Fitridhani, S. and Adzani, H. Laser based imaging method to discriminate Riau Province pure honeys. *Journal of Physics: Conference Series*, 2018.
26. Zuhaira, Z.M., Hashim F. H., Raj, T. and Huddin, A. B. A Rapid and Non-Destructive Technique in Determining the Ripeness of Oil Palm Fresh Fruit Bunch (FFB). *Journal Kejuruteraan* 2018, **30**, 93-101.
27. Alfatni, M.S.M., Shariff, A.R.M., Shafri, H.Z.M., Saeed, O.B. and Eshanta, O.M. Oil palm fruit bunch grading system using red, green and blue digital numbers. *Journal of Applied. Sciences*. 2008, **8**, 1444-1452.
28. Wan Ishak, W.I., Mohd Zohadie, B. and Abdul Malik, A.H. Optical Properties for Mechanical Harvesting of Oil Palm FFB. *Journal of Oil Palm Research* 2000, **12(2)**, 38-45.
29. Hong, T.S., Hashim, F.H., Raj, T. and Huddin, A.B. Classification of Oil Palm fruit ripeness Using Artificial Neural Network. IEEE International Conference on Automatic Control and Intelligent Systems (I2CACIS). 2021, 358-363.
30. Tzuan. G.T.H., Hashim, F.H., Raj, T., Baseri Huddin, A. and Sajab, M.S. Oil Palm Fruits Ripe-ness Classification Based on the Characteristics of Protein, Lipid, Carotene, and Guanine/Cytosine from the Raman Spectra. *Plants*. 2022, **11(15)**, 1936.
31. Robi, S.N.A.B.M., Izhar, M.A.B.M. and Ahmad, N.B. Image Detection and Classification of Oil Palm Fruit Bunches. In Proceedings of the 4th International Conference on Smart Sensors and Application (ICSSA), Kuala Lumpur, Malaysia, 2022, **26(28)**, 108-113.
32. Ibn Manzūr, Muhammad ibn Mukarram, Lisān al-‘Arab, ed. Mīrdāmādī J. Beirut: Dār al-Fikr/ Dār Sādir, 1993.
33. Singh, R., Low, E.T.L., Ooi, L.C.L. Ong-Abdullah, M., Nookiah, R., Ting, N.C., Marjuni, M., Chan, P.L., Ithnin, M., Manaf, M.A., Nagappan, J., Chan, K.L., Rosli, R., Halim, M.A., Aziz, N., Budiman, M.A., Lakey, N., Bacher, B., Van Brunt, A., Wang, C., Hogan, M., He, D., MacDonald, J.D., Smith, S.W., Ordway, J.M., Martienssen, R.A. and Sambanthamurthi, R. The oil palm *VIRESCENS* gene controls fruit colour and encodes a R2R3-MYB. *Nature Communications* 2014, **5**, 4106.
34. Jo, K., Lee, M. and Sunwoo, M. Fast GPS-DR Sensor Fusion Framework: Removing the Geodetic Coordinate Conversion Process. *IEEE Transactions on Intelligent Transportation Systems* 2015, **17**, **7**, 2008-2013. doi: 10.1109/TITS.2015.2475620.
35. Badmus, U.O., Crestani, G., Cunningham, N., Havaux, M., Urban, O. and Jansen, M.A. UV Radiation Induces Specific Changes in the Carotenoid Profile of *Arabidopsis thaliana*. *Biomolecules* 2022, **12(2)**, 1879.

36. O'Holohan, D.R. Malaysian Palm Oil: The Story of a Major Edible Vegetable Oil and its Rule in Human Nutrition. Kuala Lumpur: Malaysian Palm Oil Council. 1997, 47-64.
 37. Ooi, C.K., Choo, Y.M., Yap, S.C., Basiron, Y. and Ong, A.S.H. Recovery of carotenoids from palm oil. *Journal of the American Oil Chemists Society*. 1994, **71(4)**, 423-426.
 38. Yi, J., Andersen, M.L. and Skibsted, L.H. Interactions between tocopherols, tocotrienol and carotenoids during autooxidation of mixed palm olein and fish oil. *Food Chemistry*. 2011, **127**, 1792-1797.
 39. Top, A.G., Muhamad, H., Abdullah, A., Sani, H.A. and Dauqan, E. Vitamin, E. and beta, carotene. Composition in four different vegetable oils. *American Journal of Applied Sciences*. 2011, **8**, 407-412.
 40. Alyas, S. A., Abdulah, A. and Idris, N.A. Changes of β -carotene content during heating of red palm olein. *Journal of Oil Palm Research*. 2006, 99- 102.
 41. Nagendran, B., Unnithan, U.R., Choo, Y.M. and Sundram, K. Characteristics of red palm oil, a carotene and vitamin E-rich refined oil for food uses. *Food and Nutrition Bulletin*. 2000, **21(2)**, 189-194.
 42. Choe, E. Interaction of light and temperature on tocopherols during oxidation of sunflower oil. *Journal of the American Oil Chemists Society*. 2013, **90**, 1851-1857.
 43. Rukmini, A. and Raharjo, S. Pattern of peroxide value changes in virgin coconut oil (VCO) due to photo-oxidation sensitized by chlorophyll. *Journal of American Oil Chemists Society*. 2010, **87(12)**, 1407-1412.
 44. Poulli, K.I., Mousdis, G.A. and Georgiou, C.A. Monitoring olive oil oxidation under thermal and UV stress through synchronous fluorescence spectroscopy and classical assays. *Food Chemistry*. 2009, **117**, 499-503.
 45. Kim, N. and Choe, E. Singlet oxygen-related photooxidative stability and antioxidant changes of diacylglycerol-rich oil derived from mixture of olive and perilla oil. *Journal of Food Science*. 2012, **77(11)**, C1185-C1191.
 46. Kim, N. and Choe, E. Contribution of minor compound to the singlet oxygenated photooxidation of olive and perilla oil blend. *Food Science and Biotechnology*. 2013, **22**, 315-321.
 47. Accomasso, D., Arslançan, S., Cupellini, L., Granucci, G. and Mennucci, B. Ultrafast Excited-State Dynamics of Carotenoids and the Role of the SX State. *The Journal of Physical Chemistry Letters*. 2022, **13**, 6762-6769.
 48. Polívka, T. and Sundström, V. Ultrafast Dynamics of Carotenoid Excited States-From Solution to Natural and Artificial Systems. *Chemical Reviews*: 2004, **104**, 2021-2072.
 49. Britton, G., and Helliwell, J. R. Carotenoid-protein interactions. *Carotenoids: Natural Functions*. 2008, **(4)**, 99-118.
 50. Angelé-Martínez, C., Goncalves, L.C.P., Premi, S., Augusto, F.A., Palmatier, M.A., Amar, S.K. and Brash, D.E. Triplet-Energy Quenching Functions of Antioxidant Molecules. *Antioxidants*, 2022, **11(2)**, 357.
 51. Cherry, R.J., Chapman, D. and Langelaar, J. Fluorescence and phosphorescence of β -carotene, *Transaction of the Faraday Society*. 1968, **64**, 2304-2307.
 52. Haley, L.V. and Koningstein, J.A. Space- and time-resolved resonance-enhanced vibrational raman spectroscopy from a femtosecond-lived singlet excited state of β -carotene. *Chemical Physics*, 1983, **77(1)**, 1-9.
 53. Bondarev, S.L., Bachilo, S.M., Dvornikov, S.S. and Tikhomirov, S.A. $S_2 \rightarrow S_0$ fluorescence and transient $S_n \leftarrow S_1$ absorption of all-*trans*- β -carotene in solid and liquid solutions. *Journal of Photochemistry and Photobiology A: Chemistry*. 1989, **46(3)**, 315-322.
 54. Frank, H.A., Chynwat, V., Desamero, R.Z., Farhoosh, R., Erickson, J. and Bautista, J. On the photophysics and photochemical properties of carotenoids and their role as light-harvesting pigments in photosynthesis. *Pure and Applied Chemistry*. 1997, **69(10)**, 2117-2124.
 55. Gillbro, T. and Cogdell, R.J. Carotenoid fluorescence. *Chemical Physics Letters*. 1989, **158 (3-4)**, 312-316.
-

Received 7 April 2023

Accepted 25 July 2023

Impact of Climate Change on Rare Species in Arid Environments

Hamada E. Ali

¹ Department of Biology, College of Science, Sultan Qaboos University, Muscat, Oman.

² Botany and Microbiology Department, Faculty of Science, Suez Canal University, Ismailia 41522, Egypt. Email: h.ibraheem@squ.edu.om.

ABSTRACT: Human development has drastically increased the chances of climate change by burning fossil fuels, including oil, gas and coal, causing disturbances to humans, plants, and animals. Changing climate dynamics has impacted many plants, which are the primary source of life on Earth. Egypt is one of the countries where the temperatures have risen in the past decades due to climate change. In this country, many plants are vulnerable to climate change especially rare plant species. One of the most common tools for determining plant species' biological and conservation activity is the IUCN (International Union for Conservation of Nature) Red list. In this study, two plant species, evaluated *Micromeria serbaliana* and *Veronica kaiseri*, which are identified as critically endangered species. After evaluation, it was seen that *Micromeria serbaliana* falls under the category of B1ab (iii) + 2ab (iii) and is termed an endangered species (EN). The same problem applies to *Veronica kaiseri*, another targeted species which is Endangered (EN) under categories B1ab (iii) + 2ab (iii). Both species are declining and have severely fragmented distributions.

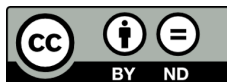
Keywords: *Micromeria serbaliana*; Endangered species; *Veronica kaiseri*.

تأثير التغيرات المناخية على النباتات الأكثر ندرة في البيئات الجافة

حمادة السيد علي

الملخص: حيث أن التغيرات المناخية تناقش الأنماط المترولوجية طويلة المدى. إلى جانب الطبيعة فإن زيادة التنمية البشرية تؤثر بشكل كبير من فرص تغير المناخ عن طريق حرق الوقود الأحفوري، بما في ذلك النفط والغاز والفحم. أدى ذلك إلى اضطراب بين البشر والنباتات والحيوانات. لقد أثرت قابلية التأثر أو ديناميكيات المناخ المتغيرة على النباتات التي تمثل المصدر الأساسي للحياة على الأرض. مصر هي إحدى الدول التي ارتفعت فيها درجات الحرارة في العقود الماضية بسبب تغير المناخ. تتأثر النباتات في هذا البلد بضعف هذا التغير الديناميكي للمناخ، وخاصة الأنواع النباتية النادرة. تعد القائمة الحمراء للاتحاد الدولي لحفظ الطبيعة (IUCN) إحدى أكثر الأدوات أهمية ووفرة لتحديد النشاط البيولوجي وأنشطة الحفظ للأنواع النباتية. لذلك فقد قامت الدراسة بتقييم تأثير التغيرات المناخية على نوعين من الأنواع الأكثر ندرة والمهددة بالانقراض في مصر، وهما *Micromeria serbaliana* و *Veronica kaiseri*. بعد التقييم، لوحظ أن *Micromeria serbaliana* يندرج تحت فئة B1ab (iii) + 2ab (iii) ويطلق عليه نوع من الأنواع المهددة بالانقراض (EN). ينطبق نفس الموقف على الأنواع المستهدفة الأخرى وهي *Veronica kaiseri*، والتي تم تصنيفها على أنها مهددة بالانقراض (EN) ضمن الفئات B1ab (iii) + 2ab (iii). كلا النوعين يتناقضان بشدة في أماكنهما الأصلية بمصر ويجب الحفاظ عليهما في أسرع وقت.

الكلمات المفتاحية: النباتات المهددة بالانقراض؛ مصر؛ البيئات الجافة.



1. Introduction

In the twenty-first century, climate change is the biggest challenge for human society. Many studies have concluded that climate change is real and the dynamics of the physical world are changing considerably [1]. Climate change is not new, but it has recently received more attention. Every country has been affected by this change. Many cases worldwide have been reported on climate vulnerability, including melting glaciers, increasing temperature, volcanic eruptions, and burning forests [2]. Biodiversity is the most affected by this vulnerability of climate. The global temperature has increased by 0.6°C and is predicted to rise quickly [3]. Continuously increasing temperatures will affect biodiversity and ecosystems.

Over the past few hundred years, Egypt's climate has changed dramatically due to its location on earth [2]. Most cities are vulnerable to climate change, including Cairo and the population near the Nile River. Flooding, a decrease in rainfall, and drought have impacted the people in the country [4]. Along with this, plant species are also affected by these climate conditions. Most rainfall happens in the winter season. The Mediterranean and high altitudes of mountains in southern Sinai influence the climate. South Sinai is categorized by a wide range of differences in air temperature. The tropical influence is considerable laterally in the Gulf of Aqaba and the Gulf of Suez [5].

Abdel-Fattah, *et al.* [5] also stated that South Sinai has a range of mountains, including Mousa's Mountain and Catherine Mountain. Mousa's mountain is considered one of the holiest historical mountains and a respectful place in Southern Sinai, Egypt. It is located on the eastern side of Catherine Mountain, and due to its high elevation, Catherine Mountain is considered to have the mildest climate in Southern Sinai and Egypt. Summers are long, arid, and hot, whereas winters are dry and chilly in the areas of Catherine Mountain. It was reported by Kaky and Gilbert [6] that the factors which are influenced by the warming are photosynthesis, and the rate of plant respiration. For instance, carbon emission can increase the photosynthesis mechanism even in warm and dry conditions.

Usually, plants can optimize photosynthesis process at a specific level of temperature. When soil temperature increases, it maximizes the deterioration and decreases the sources of plant mineralization and availability [7]. Plant distribution and spread can be dictated by the soil property, availability of resources, and nutrients availability. Typical plants' responses can be positive or negative depending on the different conditions and variable atmosphere.

Cai [8] supported the argument of Heneidy, *et al.* [9] that fragmentation, disturbance, loss of biodiversity, and habitat destruction are affected by climate vulnerability. Mountain vegetation can suffer as the climate gets warmer and drier. On the other side, higher temperatures lead to higher biodiversity. Due to the environment's vulnerability, some ecologists have noticed that with increasing temperature, the number of Nematodes increases in polyculture plots, whereas their number decline in monoculture plots [10]. Heavy flooding destroys communities and plant species because many species that live in flooded areas have been dislocated. Additionally, its lifespan is decreasing, so preserving those species is very important.

The main objective of this study was to evaluate effects of ongoing climate change on two critically endangered rare species found in Egypt, *Micromeria serbaliana* and *Veronica kaiseri*, and to assess the physicochemical variation in the habitat and between each other.

2. Materials and methods

2.1. Study Area

The study was performed in South Sinai, Egypt. In Egypt, South Sinai has a latitude of 29.3102° N and a longitude of 34.1532° E (Figure. 1A). Precipitation in the study area is characterized by its scantiness, seasonality, and inconsistency [11]. It occurs mainly in winter from October to April, the mean annual precipitation in the study area is 15 mm. The monthly mean temperature varies between 6.8° C in January and 26.1° C in August [10]. The relative humidity is higher in winter than in summer; it attains a minimum average of 32% in May and 62% in February [12].

2.2. Data Collection Process

The data was gained from the "IUCN Red List" for threatened species. The list identifies threats to known plant species [13]. The "IUCN Red List" is divided into many categories according to the severity of climate change. As the name implies, the most affected and at-risk species fall under the categories of endangered, critically endangered, and extinct. The other remaining categories i.e., vulnerable, near threatened, least concerned, and extinct in the wild, have less impact and severity of climate change on them. The categories like data deficient and not evaluated are considered because some species do not have enough information on them [14].

Based on distinct categories, the species collected from the IUCN Red List are classified under the above-mentioned nine groups. These nine groups are shown in Table 1.

The data collection was conducted from July to August 2022. Species selection was based upon the literature review. Literature showed the availability of endangered species in this area of Egypt. *Micromeria serbaliana* and *Veronica kaiseri* were mainly found near and on mountain ranges rather than in other regions. *Veronica kaiseri* was observed at a lower area on the mountain because they are usually found in wet places. In contrast, in patch form, *Micromeria serbaliana* was found in mid and top regions.

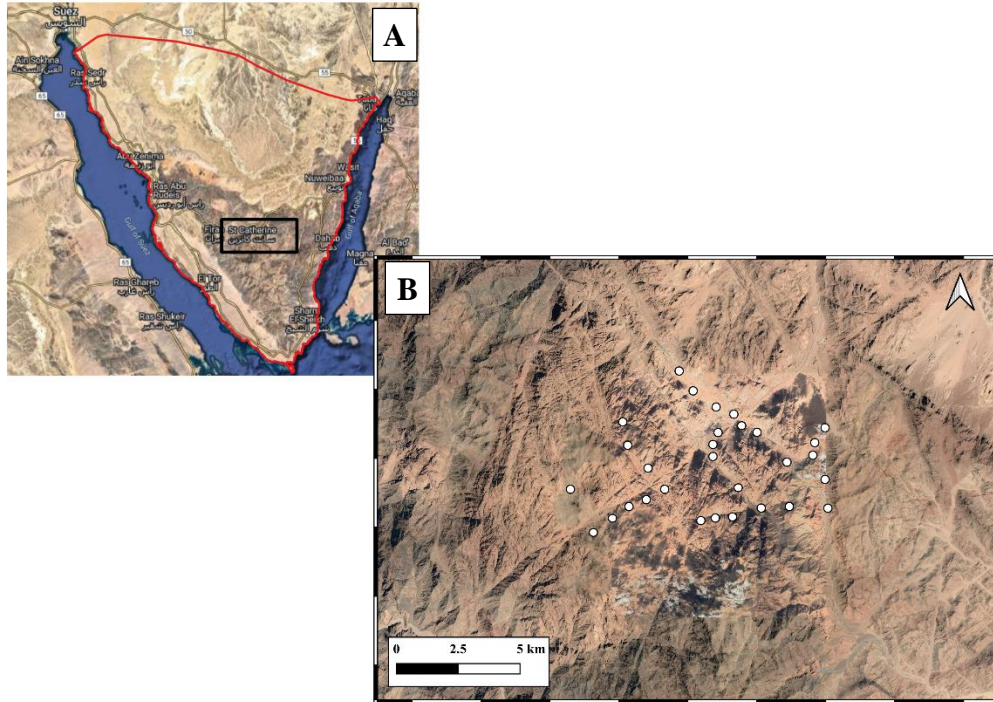


Figure 1. Location map for the study area showing A. South Sinai and B. Sampling sites within the Saint Catherine area.

Table 1. Description of categories according to IUCN.

Categories	The Description based on IUCN
Vulnerable	meets one of the 5 red list criteria and is thus considered to be a high
Near Threatened	close to being at high risk of extinction in the near future
Endangered	very high risk of extinction in the wild meets any of criteria A to E for Endangered.
Critically endangered	in a particular and extremely critical state
Extinct	beyond reasonable doubt that the species is no longer extant
Extinct in wild	survives only in captivity, cultivation, and/or outside the native range, as presumed after exhaustive surveys
Least concerned	unlikely to become extinct in the near future
Data Deficient	Not enough information
Not Evaluated	Not enough information

According to the literature review, 30 plots were investigated (Figure, 1B), in which vegetation data were collected using the quadrat method of a 20 m² size. For geographical and ecological determination, IUCN protocols were followed. Soil was collected at 20 cm depth from each plot using a soil probe. GPS and GeoCAT were used for geographical location. Collected soil samples were further analyzed for soil pH, which were measured using pH meter following Chapman [15] method, soil electric conductivity (EC) and total dissolved salts (TDS) were measured using Wheatstone bridge (TDS and EC meter) as described by Wilde, Voigt [16] in $\mu\text{S}/\text{cm}$ and ppm respectively, the soil organic matter content was determined by loss on ignition method in percentage following Sparks, Page [17], the water content of the soil samples was determined according to Richards [18] in percentage, soil potassium (K) in ppm and Mg (meq/L) were measured using method developed by Mehlich [19], and finally soil SO₄ (meq/L) was measured following Westermann [20].

2.3. Data Analysis

Differences between the vegetation and the physico-chemical parameters of the two studied species were analyzed using Tukey's multiple comparison test in R [21]. The IUCN Red List data were collected through a literature review.

3. Results

Based on data extracted from the IUCN Red list, nine groups of plant species from Egypt that are endangered owing to climatic changes and, thus, are decreasing and becoming rare were reported. After searching for the rare species over the IUCN's category for the Plantae Kingdom, the ones belonging to Egypt are sorted out and depicted in Table 2.

Table 2. Threatened Egyptian Plant Species Listed Under IUCN Red List.

Scientific name	Assessment Year	Category	Criteria
<i>Phlomis aurea</i>	2015	Endangered	B1ab (iii, v) + 2ab (iii, v)
<i>Euphorbia obovata</i>	2015	Endangered	B1ab (iii, v) + 2ab (iii, v)
<i>Silene leucophylla</i>	2020	Endangered	B1ab (i, ii, iii) + 2ab (i, ii, iii)
<i>Bufonia multiceps</i>	2015	Endangered	B1ab (i, ii, iii, v) + 2ab (i, ii, iii, v); C2a (i)
<i>Anarrhinum pubescens</i>	2015	Endangered	B1ab (i, ii, iii, iv, v) + 2ab (i, ii, iii, iv, v); C2a (i)
<i>Medemia argun</i>	2019	Vulnerable	B2ab (iii)
<i>Cyperus papyrus</i>	2008	Vulnerable	B2ab (v)
<i>Stipa tenacissima</i>	2015	Vulnerable	A4acd
<i>Rosa arabica</i>	2015	Critically Endangered	B1ab (i, ii, iii, iv, v); C2a (i)
<i>Primula boveana</i>	2014	Critically Endangered	B1ab (i, ii, iii, iv, v) + 2ab (i, ii, iii, iv, v)
<i>Juncus maroccanus</i>	2013	Critically Endangered	B1ab (iii) + 2ab (iii); D
<i>Veronica kaiseri</i>	2020	Critically Endangered	B1ab (i, ii, iii, iv)
<i>Nymphaea lotus</i>	2007	Critically Endangered	B1ab (i, ii, iv) c (ii, iv) + 2ab (i, ii, iv) c (ii, iv)
<i>Silene oreosinaica</i>	2020	Critically Endangered	B1ab (ii, iii) + 2ab (ii, iii)
<i>Micromeria serbaliana</i>	2020	Critically Endangered	B1ab (ii, iii)
<i>Marsilea strigosa</i>	2007	Endangered	B2ab (ii, iii, iv, v)
<i>Marsilea minuta</i>	2007	Endangered	B2ab (ii, iii, iv, v)
<i>Dracaena ombet</i>	1998	Endangered	A1cd
<i>Silene schimperiana</i>	2020	Endangered	B1ab (ii, iii) + 2ab (ii, iii)

Table 2 depicts plant species that are declining or becoming rare. Two species, namely *Micromeria serbaliana* and *Veronica kaiseri*, are identified as critically endangered species, and are evaluated in this study.

3.1. *Micromeria serbaliana*

One of the most promising plants of the Lamiaceae family is the *Micromeria serbaliana*. This plant has remarkable antimicrobial and anti-inflammatory features that is used efficiently for medical purpose such as "against heart disease, headache, wound skin, infections, colds, as an antispasmodic, and as a stimulant [22]. In Egypt, *Micromeria* is represented by five species, namely *M. serbaliana*, *M. sinaica*, *M. imbricata*, *M. nervosa*, and *M. myrtifolia*" [23].

3.2. *Veronica kaiseri*

The genus of *Veronica*, comprises over 500 species. The species have the adaptability to grow in different climates and different habitats like water land or the elevated mountainous level. Eleven other species of *Veronica* have been identified in the region of Egypt [24].

The current research only targets two species, i.e., *Micromeria serbaliana* and *Veronica kaiseri*, so the focus was only on these species. After evaluation, it was seen that *Micromeria serbaliana* falls under the category of B1ab (iii) + 2ab (iii) and is termed an Endangered (EN) species. The same situation is for another targeted species, *Veronica kaiseri*, which falls under categories B1ab (iii) + 2ab (iii) and is qualified as Endangered (EN). Both species are declining and severely fragmented in their fields.

Some primary threats of the targeted species based on the IUCN list are displayed in Table 3.

IMPACT OF CLIMATE CHANGE ON RARE SPECIES IN ARID ENVIRONMENTS

Table 3. Threats of target species based on the IUCN list.

Threats	Severity
Farming activities	Moderate can cause fluctuation
Disturbances occur by humans	Moderate can cause fluctuation
Climate change (e.g., drought)	Very severe, rapidly increasing
Natural disasters	Rare, slowly increasing

The results indicated that both targeted species are under drought stress. Grazing impact on *M. serbaliana* species can arise from grazing domestic animals. Both targeted species are disturbed through numerous human activities, which includes grazing of animals, collection for medicinal or fuel purposes, and this mis-management of their occurrence.

The results showed a high diversity of *M. serbaliana* than *V. kaiseri* frequency species, while the high total no. of species was observed in *V. kaiseri* (Figure 2).

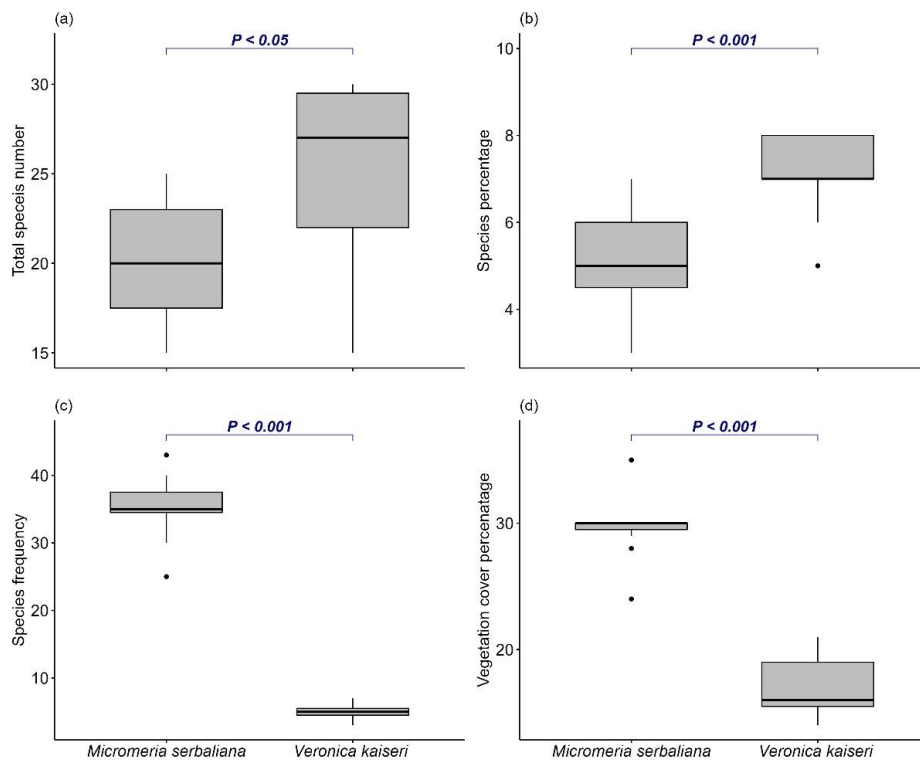


Figure 2. Comparison between the different vegetation parameters of *Micromeria serbaliana* and *Veronica kaiseri* species. Numbers are *P* values of the statistical significant differences between *Micromeria serbaliana* and *Veronica kaiseri* based on pairwise comparisons using Tukey's multiple comparison test (ns: non-significant differences).

The mean maximum value for physicochemical factors in abundant *M. serbaliana* species locations were 1350 ppm Total dissolved solids (TDS), 7.99 (pH), 50.5 meq/L (Mg), 52.9 ppm (potassium), 150 meq/L (sulphate), while 2%, 690 μ S/cm and 16.99% water content, soil EC and organic matter were observed respectively. In comparison, the minimum values were 40 ppm (TDS), 6.85 (pH), 0.49 meq/L (Mg), 11 ppm (potassium), 5 meq/L (sulphate) and 0.5%, 20 μ S/cm and 0.39% water content, soil EC and organic matter were observed, respectively (Figure 3).

The mean maximum value of physico-chemical factors in abundant *Veronica kaiseri* species areas was 402 ppm (TDS), 7.89 (pH) 14 meq/L (Mg), 79.01 ppm (potassium), 79.56 meq/L (sulphate), while 35%, 420 μ S/cm, and 7.23% water content, soil EC and organic matter were observed, respectively. While the minimum values were 65 ppm (TDS), 6.85 (pH), 0.5 meq/L (Mg), 24 ppm (potassium), 26.25 meq/L (sulphate) and 0.5%, 45.63 μ S/cm and 0.32% water content, soil EC and organic matter were observed, respectively (Figure 3).

4. Discussion

As the environment's vulnerability increases, it is essential to predict the risk of extinction, specifically in wild species. By taking the necessary action concerning these extreme environmental conditions, the Egyptian Biodiversity

Strategy and Action Plan has been updated for 2015-2030 to preserve and manage rare, endemic, and endangered plant species with the international community's help [25].

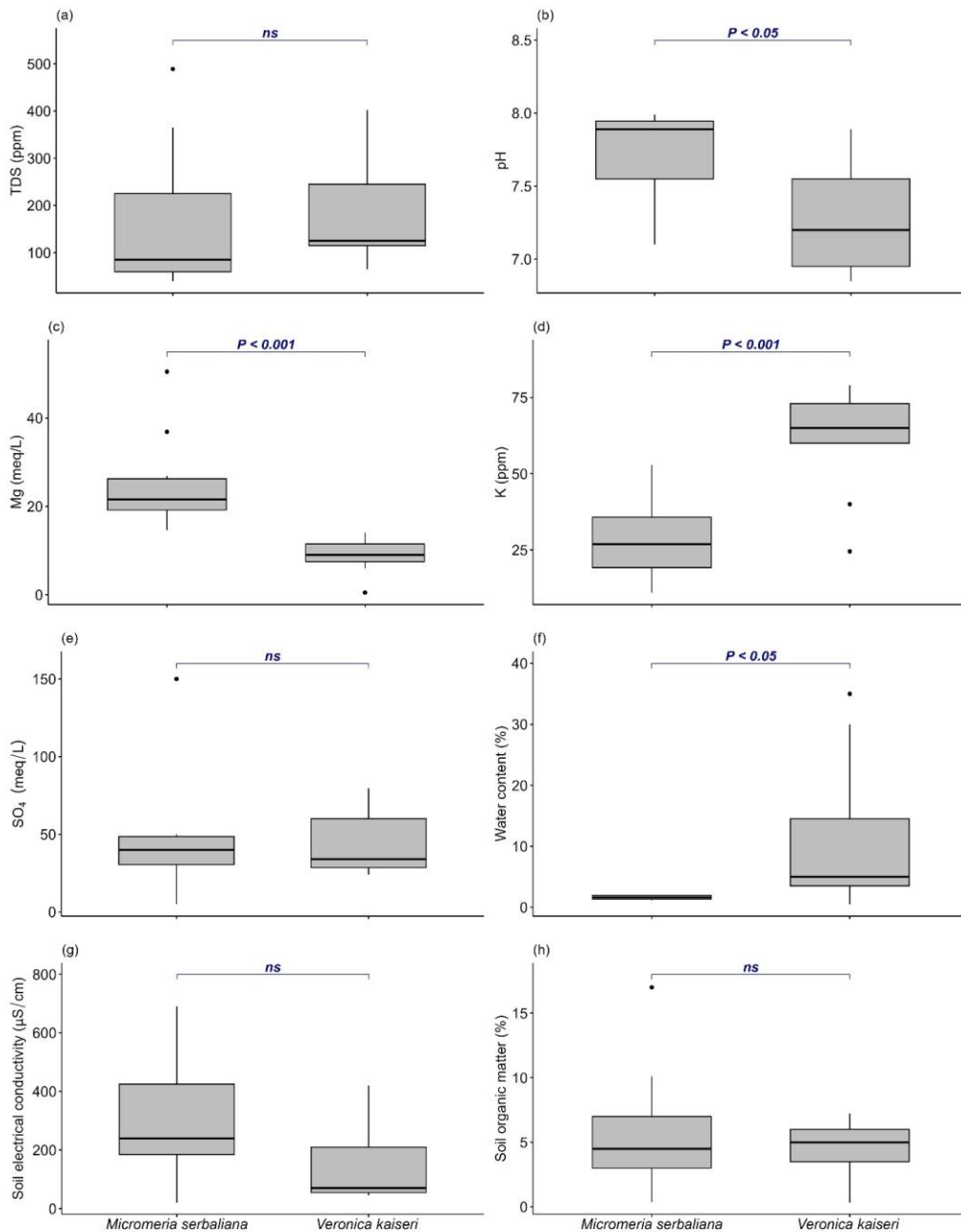


Figure 3. Comparison between the physico-chemical factors in the abundant *Micromeria serbaliana* and *Veronica kaiseri* in the Saint Catherine region's soil. Numbers are *P* values of the statistical significant differences between *Micromeria serbaliana* and *Veronica kaiseri* based on pairwise comparisons using Tukey's multiple comparison test (ns: non-significant differences).

Some researchers, such as Hoveka, *et al.* [26], have offered a number of explanations for the lack of data necessary to safeguard threatened species. He says biases have hindered the data collection processes necessary for effective biodiversity conservation programs in species collection, a lack of funding and research infrastructure, a decrease in the number of taxonomists, the complexity of identifying and describing species, and insufficient training. Therefore, analyzing gaps in the IUCN Red List assessment programs should be a top research priority for any nation that wants to avoid species extinction. As this study and Rodrigues [27] have demonstrated, the distribution, population status, habitats, ecological status, threats, conservation measures, and any other relevant data collected for the IUCN Red List Assessment tool are a significant contribution to filling in gaps in conservation planning programs. The two species that are the focus of this investigation are considered endangered (EN) because they are endemic to a small area and have a severely fragmented population. The quality of their habitat is deteriorating.

Climate change is one of the significant factors responsible for the vulnerable environment. It has impacted all living organisms, including humans, marine creatures, plants, and animals. Every country is affected by climate

IMPACT OF CLIMATE CHANGE ON RARE SPECIES IN ARID ENVIRONMENTS

change, whether they produce low carbon emissions or high [25]. *Micromeria serbaliana* was found in high abundance at the mid and top of mountain areas, but *Veronica kaiseri* was located in lower mountain regions due to its moist habitat (Figure 1-2). Egypt including the Southern Sinai, at higher altitudes have climates that are vulnerable to change. Already some species have disappeared because of flooding, sand storms, and other natural disasters [28].

The findings in this study are in agreement with those of Kaky and Gilbert [6]. The conclusion is that the standard criteria are used to predict a species' distribution and to determine its extinction risk based on the IUCN Red List assessment. The primary objective of combining information and IUCN Red List assessments is to provide the data required to guide decision-makers in determining conservation priorities [29]. However, some *Micromeria serbaliana* and *Veronica kaiseri* species were observed in the endangered species list.

Sadly, since 1998, neither *Veronica kaiseri* nor *Micromeria serbaliana* has been monitored, so there are no conservation programs for these species. In this study, baseline subpopulations were recorded that can be compared to subsequent population inventories. The findings of the present work are in harmony with [30] and support their idea that targeted management, recovery, and reintroduction activities at the species and population levels must be strengthened in addition to conservation programs for threatened species. The successful conservation of plants, the reduction of pressures placed on plants in the wild, and a better understanding of traditional values and practices will benefit from encouraging participatory approaches involving the local community.

5. Conclusion

Based on these study results, it is highly recommended to keep an eye on population or habitat trends and fluctuations. The current study explains the possible features of the targeted species by evaluating the IUCN red list. It was concluded that these targeted species are endangered as categorized by the IUCN red list. The species are decreasing due to sudden climate changes.

Conflict of interest

The author declares no conflict of interest.

Acknowledgment

The author would like to thank Saint Katherine Protectorate staff for their help during the course of the study.

References

1. Erfanian, MB., Sagharyan, M., Memariani, F. and Ejtehadi, H. Predicting range shifts of three endangered endemic plants of the Khorassan-Kopet Dagh floristic province under global change. *Scientific Reports*. 2021, **11(1)**, 9159.
2. Shaltout, KH., Al-Sodany, YM., Eid, EM., Heneidy, SZ. and Taher, MA. Vegetation diversity along the altitudinal and environmental gradients in the main wadi beds in the mountainous region of South Sinai, Egypt. *Journal of Mountain Science*. 2020, **17(10)**, 2447-58.
3. Gentilucci, M., Abdelraouf, A.M., Fagr K.A.G., Samira, R.M., Maria, R.C., Lidia, C., Sara, I., Gilberto, P. and Giulia, G. *Advances in Egyptian Mediterranean Coast Climate Change Monitoring*. Water, 2021, **13(13)**, 1870.
4. Abd El-Azeem, SAE-MM. Impacts of Climate Change on Microbial Activity in Agricultural Egyptian Soils. In: Ewis Omran E-S, Negm AM, editors. *Climate Change Impacts on Agriculture and Food Security in Egypt: Land and Water Resources-Smart Farming-Livestock, Fishery, and Aquaculture*. Cham: Springer International Publishing; 2020. p. 97-114.
5. Abdel-Fattah, S., Negm, AM. and Bek, MA. Summary, Conclusions, and Recommendations for Egyptian Coastal Lakes and Wetlands: Climate Change and Biodiversity. In: Negm AM, Bek MA, Abdel-Fattah S, editors. *Egyptian Coastal Lakes and Wetlands: Part II: Climate Change and Biodiversity*. Cham: Springer International Publishing; 2019. p. 261-70.
6. Kaky, E. and Gilbert, F. Assessment of the extinction risks of medicinal plants in Egypt under climate change by integrating species distribution models and IUCN Red List criteria. *Journal of Arid Environments*. 2019, **170**, 103988.
7. Kamel, M. Impact of hiking trails on the diversity of flower-visiting insects in Wadi Telah, St. Katherine protectorate, Egypt. *The Journal of Basic and Applied Zoology*. 2020, **81(1)**, 52.
8. Cai, C., Zhang, X., Zha, J. and Li, J. Predicting Climate Change Impacts on the Rare and Endangered *Horsfieldia tetrapala* in China. *Forests*. 2022, **13(7)**, 1051.
9. Heneidy, S.Z., Halmy, M.W., Toto, S.M., Hamouda, S.K., Fakhry, A.M., Bidak, L.M. and Al-Sodany, Y.M. *Pattern of Urban Flora in Intra-City Railway Habitats (Alexandria, Egypt): A Conservation Perspective*. *Biology*, 2021, **10(8)**, 698.
10. Moustafa, A.A. and Mansour, S.R. Impact of climate change on the Distribution behavior of *Alkanna orientalis* in Saint Catherine, south Sinai, Egypt. *Catrina: The International Journal of Environmental Sciences*. 2020, **22(1)**, 29-34.

11. Moustafa, A., Helmy, M., Abd-El-Wahab, R. and Batanouny, K. Phenology, germination and propagation of some wild trees and shrubs in South Sinai Egypt. *Egyptian Journal of Botany (Egypt)*. 1996.
 12. Zaghloul, MS., Abdel-Wahab, RH., Moustafa, AA. and Ali, HE. Choosing the right diversity index to apply on mountainous arid environments - a case study from Mt Serbal. *Acta Botanica Hungarica*. 2013, **55(1-2)**, 141-65.
 13. IUCN. IUCN Red List categories and criteria, version 3.1: IUCN Species Survival Commission (SSC); 2012.
 14. Mongabay. List of Critically Endangered species in Egypt 2019 [Available from: <https://rainforests.mongabay.com/biodiversity/en/egypt/CR.html>].
 15. Chapman SB. *Methods in plant ecology*. 1976.
 16. Wilde S, Voigt G, Lyer J. *Soil and Plant analysis for tree culture*. 4th rev. ed. ed. New Delhi: Oxford and IBH Pub. Co.; 1972.
 17. Sparks DL, Page AL, Helmke PA, Loeppert RH. *Methods of soil analysis, part 3: Chemical methods*: John Wiley and Sons; 2020.
 18. Richards L. *Diagnosis and improvement of saline and alkali soils*: US Government Printing Office; 1954.
 19. Mehlich, A. Determination of P, Ca, Mg, K, Na, and NH₄. North Carolina Soil Test Division (Mimeo 1953). 1953, 23-89.
 20. Westermann DT. Indexes of Sulfur Deficiency in Alfalfa. I. Extractable Soil SO₄-S₁. *Agronomy Journal*. 1974, **66(4)**, 578-81.
 21. R Development Core Team. *R: A language and environment for statistical computing*. 4.3.0 ed. Vienna, Austria: R Foundation for Statistical Computing; 2023.
 22. Formisano, C., Oliviero, F., Rigano, D., Saab, AM. and Senatore, F. Chemical composition of essential oils and in vitro antioxidant properties of extracts and essential oils of *Calamintha origanifolia* and *Micromeria myrtifolia*, two Lamiaceae from the Lebanon flora. *Industrial Crops and Products*. 2014, **62**, 405-11.
 23. Bräuchler, C., Ryding, O. and Heubl, G. The genus *Micromeria* (Lamiaceae), a synoptical update. *Willdenowia*. 2008, **38(2)**, 363-410.
 24. Boulos, L. *Flora of Egypt: Volume Three (Verbinaceae-Compositae)*. Al-Hadara Publishing, Cairo, Egypt. 2002, 373.
 25. Osman, MAM. and Shebl, MA. Vulnerability of Crop Pollination Ecosystem Services to Climate Change. In: Ewis Omran E-S, Negm AM, editors. *Climate Change Impacts on Agriculture and Food Security in Egypt: Land and Water Resources-Smart Farming-Livestock, Fishery, and Aquaculture*. Cham: Springer International Publishing; 2020. p. 223-47.
 26. Hoveka, LN., van der Bank, M., Bezeng, BS. and Davies, TJ. Identifying biodiversity knowledge gaps for conserving South Africa's endemic flora. *Biodiversity and Conservation*. 2020, **29(9)**, 2803-19.
 27. Rodrigues, ASL., Pilgrim, JD., Lamoreux, JF., Hoffmann, M. and Brooks, TM. The value of the IUCN Red List for conservation. *Trends in Ecology and Evolution*. 2006, **21(2)**, 71-6.
 28. Pearson, RG. and Dawson, TP. Predicting the impacts of climate change on the distribution of species: are bioclimate envelope models useful? *Global Ecology and Biogeography*. 2003, **12(5)**, 361-71.
 29. Fivaz, FP. and Gonseth, Y. Using species distribution models for IUCN Red Lists of threatened species. *Journal of Insect Conservation*. 2014, **18(3)**, 427-36.
 30. Valderrábano, M. and Gil, T. Heywood V, Montmollin Bd, editors. *Conserving wild plants in the south and east Mediterranean region*. Spain: IUCN Centre for Mediterranean Cooperation; 2018.
-

Received 21 May 2023

Accepted 18 July 2023

An Efficient Sensor Based on Anodic Activation of Graphene Oxide for Sensitive and Selective Determination of Dopamine in Blood Serum

Al-Ghafri L.^a, Al-Hatmi N.^a, Joudi S.A.^b and Khudaish E.A.^{*a}

Department of Chemistry, College of Science, Sultan Qaboos University, Box 36, Al-Khodh 123, Oman; ^bUniversity of Waikato, School of Science, Department of Chemistry, Hamilton, New Zealand. *E-mail:ejoudi@squ.edu.om.

ABSTRACT: A native graphene oxide (NGO) prepared by Hummers modified method was used as the template materials for the fabrication of electrochemically oxidative graphene oxide (OGO) onto a glassy carbon electrode (GCE). The fabrication of OGO-GCE proceeded via reversible anodic cycles of previously coated NGO base surface materials. The development of a new aldehyde/alcoholic functional group on OGO-GCE characterized by X-ray photoelectron spectroscopy (XPS) analysis is a marked signal for surface oxygen richness that provokes the cost of (C-C/C-H) hybridized states. The measurements obtained by an electrochemical impedance spectroscopy (EIS) method demonstrated that the conductivity and the rate of electron transfer process at the OGO-GCE have improved substantially. Quantitatively, the estimated rate constant of OGO was 9 times greater than that of that of NGO. Further evidence on the superiority of OGO over NGO was demonstrated by the outstanding analytical performance on the simultaneous determination of ascorbic acid (AA), dopamine (DA) and uric acid (UA) using the differential pulse voltammetry (DPV) technique. The selectivity of the as-prepared OGO sensor for DA quantification in the presence of high concentrations of both AA and UA was achieved successfully with a detection limit ($DL_{3\sigma}$) lowered to 12 nM in comparison to many electrochemical modified surfaces. The proposed method for the construction of OGO sensors could provide a robust sensing platform for the reliable detection of DA in real biological samples. The OGO-GCE sensor showed excellent stability and performance in serum blood analysis with an acceptable recovery percentage of trace DA quantification ranging between 96% and 102%.

Keywords: Oxidative graphene oxide; Anodic pretreatment; Thin film; Dopamine analysis.

بناء كاشف فعال بواسطة الأوكسدة النشطة لأوكسيد الكرافين لغرض التقدير الإنتقائي والحساس لمادة الدوبامين في الدم

لمياء الغافري ونسيبة الحاتمي وصلاح الدين جوده و عماد خديش

الملخص: إن مادة أوكسيد الكرافين المحضر بطريقة هومرس المعدلة قد اعتمدت كمادة أساسية في تطوير مستشعر حساس بواسطة التنشيط الكهروكيميائي على سطح الكربون الزجاجي. أن عملية التصنيع تتم بواسطة الأوكسدة المتعاقبة لأوكسيد الكرافين المطلي على سطح الكربون الزجاجي، مما يساهم في زيادة تركيز مجموعات الأوكسجين الوظيفية. من خلال قياس التحليل السطحي الذي أثبت وجود مجموعة أوكسجين وظيفية جديدة من الألدهايد / الكحول على سطح المادة المصنعة. كذلك أثبتت طرق الطيف الكهروكيميائي أن سرعة انتقال الإلكترونات إزدادت بمقدار 9 مرات للمستشعر المطور و ذلك يؤيد ان الأوكسدة الفعالة لها دور مهم أيضا في زيادة المسافات البينية بين طبقات أوكسيد الكرافين مما يجعل قدرته التوصيلية على مستويات أعلى وأكبر. لقد أثبتت نتائج التحليل الكهروكيميائي المقدر والانتقائية العالية للمستشعر المطور في تقدير تركيز الدوبامين الى حدود دنيا مقترية من 12 نانو- مولار وبوجود كميات كبيرة من حمض الأسكوربيك وحمض اليوريك كمواد بيولوجية متداخلة ومثبطة. لقد أثبت المستشعر المطور أيضا على تقدير الدوبامين في عينات من مصل الدم وصلت الى مستويات عالية، أن الطريقة المقترحة لتحضير المستشعر من الممكن أن توفر منصة قوية لتقدير الدوبامين في عينات بيولوجية حقيقية. في هذا المضمار فان المستشعر أظهر إستقرارية وقدرة تحليل عالية لعينات من الدم مع نسبة إسترداد مئوية عالية تتراوح بين 96% و 102% لمادة الدوبامين .

الكلمات المفتاحية: أوكسيد الكرافين المتأكسد؛ المعالجة الأنودية؛ الأسطح الرقيقة؛ تحليل الدوبامين.



1. Introduction

Dopamine (DA) is an important catecholamine species that exerts significant influence on the central nerves, memory, hormonal and cardiovascular system [1]. It is composed of an amino group attached to the catechol molecular structure and considered as an electrochemically active constituent. Higher or lower concentrations are associated with neurological disorders such as Schizophrenia and Parkinson's diseases [2,3]. Therefore, accurate and rapid quantification of DA in biological samples is a crucial test that requires a highly sensitive and selective analytical method [4-6].

Recently, several analytical approaches and techniques have been used for the DA detection including spectrophotometric methods such as spectrophotometry, chemiluminescence, electro-chemiluminescence, surface-enhanced Raman spectroscopy and colorimetry [7,8]. These approaches were successfully applied for accurate and sensitive DA quantification but require advanced technical expertise and extreme experimental conditions, are expensive and time-consuming, and suffer from sensitivity and selectivity issues [9]. Electrochemical methods integrate microfluidic systems and are used extensively for DA determination in biological samples with the aim of improving selectivity, sensitivity, feasibility and continuous monitoring ability, fast response times and lower detection limits [10,11]. The coexistence of interfering biomolecules such as ascorbic acid (AA) and uric acid (UA) in biological blood and urine samples gives rise to some challenges due to their close oxidation potential to DA [12,13]. Accordingly, substantial efforts were implemented for construction of modified electrodes with active surface materials capable of overcoming possible overlapping electrochemical signals of the above three biological molecules. Therefore, electrochemical sensors have received considerable interest for biological analysis because of their rapid response, high sensitivity and selectivity [14].

Carbon-based materials including graphene derivatives such as graphene oxide (GO) and reduced graphene oxide (RGO) are the constituents of interest for electrode surface modification for their high reactivity, surface area, stability and simple fabrication [15-17]. They are considered as polymeric-like compounds consisting of various oxygenated functionalities [18]. The structure of GO sheet is characterized by the presence of edge and basal planes defined by the nature of existing oxygen functional groups [19]. The edge plane consists mainly of carbonyl and carboxyl groups, which marks its hydrophilicity along with reaction kinetics facility [20]. The basal plane comprises a combination of both hydrophilic (epoxy and hydroxyl groups) and hydrophobic aromatic domains [21]. Moreover, the oxygenated groups are responsible for ease of solvation and surface functionalization [22]. The above unique structure is acknowledged to strongly influence surface communication and hence the observed electrochemical signal [23,24]. Application of graphene-based materials for construction of active sensors is dominated by combining them with other supportive compounds such as organo-metallic complexes and polymers, metal and metal oxide nanoparticles and other hybrid constituents [25-30]. Application of pristine graphene independently as an active sensing materials is not widely applied because of certain disadvantages attributed to surface passivation and slow electrode kinetics [31,32].

The aim of the present work is to fabricate an active surface materials based on oxidative graphene oxide (OGO) via anodic potential excursion of a previously coated NGO film onto a GCE dipped in the buffer background electrolyte. Herein, we present a full study on the electrochemical properties, elemental structure, surface morphology of the proposed sensor (OGO-GCE) along with its catalytic activity on DA analysis.

2. Experimental

2.1 Chemicals and electrodes

Analytical grade DA, AA, UA, potassium ferrihexacyanate ($K_4[Fe(CN)_6]$), potassium ferrihexacyanate ($K_3[Fe(CN)_6]$), graphite powder, sodium nitrate ($NaNO_3$), sulfuric acid (H_2SO_4), potassium permanganate ($KMnO_4$) and hydrogen peroxide (H_2O_2) were purchased from Sigma-Aldrich Chemie, Germany. Potassium orthophosphate (KH_2PO_4) and dipotassium phosphate (K_2HPO_4) were obtained from BDH, UK. A 0.10 M phosphate buffer solution (PBS) with pH 7.28 was made by mixing certain portions of (KH_2PO_4) and (K_2HPO_4) in distilled water and used for all the present electrochemical measurements unless stated otherwise.

All electrochemical measurements were conducted using BAS 50W workstation (Bioanalytical System, West Lafayette, IN, USA) in a three-electrode cell comprised of glassy carbon working electrode (GCE), a platinum coil and $Ag/AgCl/KCl_{(sat.)}$ as counter and reference electrodes, respectively. Prior to each experiment, the GCE was polished sensibly and evenly with alumina slurry (5.0 and 1.0 μm) at a polishing cloth, rinsed thoroughly with distilled water and sonicated for 5 min using (JAC Ultra Sonic, 1505, LABKOREA INC, Korea) to remove possible adsorbed debris and finally rinsed with distilled water.

2.2 Preparation of graphene oxide

The native blended GO material was synthesized from graphite powder according to the modified Hummers method [31]. Briefly, a mixture of 1.2 g graphite, 1.0 g $NaNO_3$ and 46 mL of H_2SO_4 (98%) were placed in an ice bath and carefully stirred. Then 6.0 g potassium permanganate ($KMnO_4$) was added steadily with continuous stirring. The reaction mixture was then placed in a water bath at 35 °C for 1 h to complete the oxidation reaction.

AN EFFICIENT SENSOR BASED ON ANODIC ACTIVATION OF GRAPHENE OXIDE

The developed reaction mixture was diluted with 100 mL of distilled water and its temperature raised to 95°C for 2 h with gentle stirring when the suspended solution turned brown. The brownish suspension was then treated with 30 mL of 30% H₂O₂ to remove the remaining excess amount of KMnO₄. Finally, the residual material produced in the solution mixture was centrifuged at 6000 rpm for 15 min, separated out and washed with distilled water for several times. The obtained black GO paste was dried under vacuum and a suspended blend of (1 mg GO/1 mL distilled water) was prepared for further surface modification.

2.3 Construction of modified electrodes

A modified GCE was prepared by drop casting of 20 µL GO dispersed solution onto a polished and clean GCE. The modified electrode (NGO-GCE) was placed underneath a warm light projector to dryness. The proposed oxidative OGO-GCE was fabricated by electrochemical pretreatment of (NGO-GCE) in PBS (pH = 7.28) induced by 15 reversible voltammetric cycles between 0.0 mV and 1000 mV at 50 mV/s and terminated in the more anodic potential.

2.4 Equipment and techniques

X-ray Photoelectron Spectroscopy (XPS) was performed to study the relative amounts of elemental groups present in the studied samples (Omicron, Germany). The spectra of individual constituents were estimated by fitting the C 1s curve spectra using Gaussian Lorentzian peak shape after background correction with Shirley function in Casa XPS software (Casa Software Ltd, UK). The binding energies were calibrated with respect to adventitious C 1s feature at 284.6 eV.

Electrochemical Impedance Spectroscopy (EIS) was performed with an open circuit potential using Gamry potentiostat (Interface 1000E, USA) with a frequency range between 100 kHz and 1 Hz at amplitude of 5 mV. The EIS experiments were achieved in electrolytic solution composed of 5 mM of [Fe(CN)₆]^{3-/4-} to study the surface modification influence on the electron transfer kinetics. Fitting of the EIS experimental data were accomplished by selecting the Randle's equivalent simple circuit.

Cyclic voltammetry (CV) was employed for surface modification via reversible potentiodynamic cycles. The differential pulse voltammetry (DPV) was utilized as an active electrochemical method for analytical performance examination of modified electrodes.

2.5 Preparation of the real sample

A serum blood sample collected from Sultan Qaboos University Hospital (SQUH, Muscat, Oman) was diluted three times with the PBS (0.1 M of pH = 7.28) and used directly with no further treatment. An aliquot of 5.0 mM DA was diluted 5 times with the serum buffer solution for the standard addition procedure. The electrochemical measurements of DA were achieved using DPV technique. The regression data obtained from the selective determination of DA in the presence of AA and UA in the prepared artificial sample were used to convert the anodic current response of DA real sample into its equivalent DA concentration. Accordingly, the recovery percentage of DA was estimated to evaluate the performance of the proposed sensor.

3. Results and Discussion

3.1 Characterization methods for identification of surface materials

3.1.1 Surface elemental composition using XPS method

The C 1s XPS experimental data are shown in Figure 1, which identifies the chemical structure of NGO (A) and OGO (B) samples, respectively. The binding energy profiles of carbon functional groups with their different atomic percentage in both samples are evidences of composition alteration. The C 1s core level XPS spectrum of NGO illustrated in Figure 1(A) displays five different chemically shifted components of carbon-carbon and carbon-oxygen functionalities. The characteristic bands at 284.0 and 284.6 eV are attributed to the sp² and sp³ hybridized carbon, respectively, with a total concentration of 47.6%. These are followed by a three smaller peaks centered at 287.0 eV (22.7%), 288.5 eV (21.0%) and 290.4 eV (11.4%) emitted from the carbon-oxygen bonding atoms corresponding to epoxy (C-O-C), carbonyl (C=O), and carboxylate (O-C=O) groups, respectively.

On the other hand, the C 1s spectra for the OGO sample presented in Figure 1(B) is fitted with five peaks obtained at 284.6 eV (26.5%), 285.4 eV (22.4%), 286.4 eV (14.6%), 288.7 eV (28.3%) and 290.1 eV (8.2%) corresponding to (C-C/C-H), (C-O/C-OH), (C-O-C), (C=O) and (O-C=O), respectively.

Variation of the full-width half-maximum (FWHM) values corresponding to the functional groups in both surface materials are quite evident. For instance, the (C-H) hybridized peak in the OGO dropped by 40% while the (C-O-C) and (O-C=O) functionalities are larger by two times as all compared to the NGO.

A close inspection of the data demonstrates the appearance of a new oxygenated peak obtained at 285.4 eV belonging to the aldehyde/alcoholic functional group [34]. The generated peak of (C-O/C-OH) in the OGO configuration with 22.4% is a noticeable evidence for a progressive surface modification achieved by anodic pretreatment of NGO. Increasing the surface concentration of oxygenated groups at the cost of sp² and sp³ hybridized components is another evidence of successful fabrication of OGO.

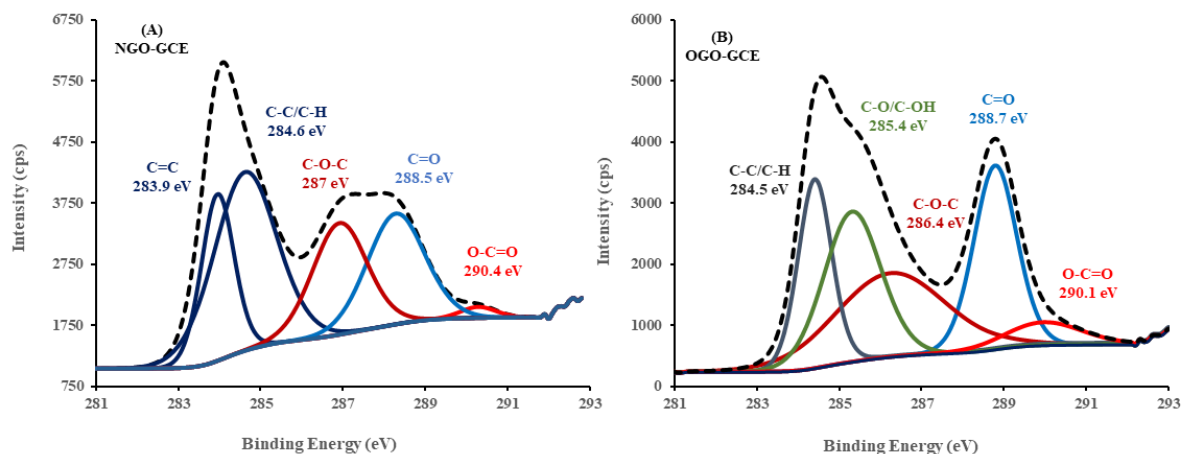


Figure 1. High resolution and curve fitting of C 1s XPS spectra for NGO-GCE (A) and OGO-GCE (B).

3.1.2 Surface interfacial analysis by EIS method

The EIS data for the present two surface modified electrodes were gained under open circuit potential (V_{oc}) in the presence of 5 mM $[\text{Fe}(\text{CN})_6]^{3-/4-}$ solution. A Nyquist plot is a fundamental electrochemical instructive method used to inspect kinetic limitations due to surface modification. As shown in Figure 2, the plot consists of a semicircle curve at high frequency corresponding to the charge transport resistance (R_{ct}) at the electrode/electrolyte interface. The data line at low frequency aligned with the semicircle curve indicates the diffusion-limited process at the active surface materials. Moreover, the non-faradaic process due to uncompensated solution resistance (R_s) is induced by charging of the double layer capacitance (C_{dl}) via the electrostatic attraction of ions at the electrode/electrolyte interface.

Apparently, the gained R_{ct} fitting data for NGO (3250 Ω) is relatively high indicating a surface material of low conductivity that hinders the electron transfer kinetics. At the same time, the Nyquist curve of OGO (inset of Figure 2) is incomparable where the obtained R_{ct} value has dropped markedly to (375 Ω).

The plot suggests a substantial improvement on the surface conductivity and hence the electron transfer kinetics. The electrochemical behavior of NGO before and after anodic treatment shows a major change in the physical properties of doped surface materials, which is influenced by the interlayer distance between graphene layers. The above experimental data demonstrates strong stacking attractions among NGO layers. Nevertheless, the interlayer spacing in OGO were increased by increasing the surface oxygen functionalities during anodic treatment that improves its intrinsic conductivity.

The apparent electron transfer rate constant (k_{app}) evaluated theoretically using equation (1) [35], correspond to OGO and NGO results with values of (2.1×10^{-3} cm/s) and (2.3×10^{-4} cm/s), respectively.

$$R_{ct} = \frac{RT}{F^2 A k_{app} C^*} \quad (1)$$

Obviously, the estimated (k_{app}) value for the OGO-GCE is close to nine times greater than that of NGO indicating remarkable electrode kinetics, surface adsorption capacity and electron shuttling processes.

3.1.3 Surface reactivity using DPV method

Figure 3 shows the reactivity of both surface modified electrodes for the simultaneous determination of AA (500 μM), DA (2 μM) and UA (25 μM) in PBS (pH = 7.28). The characteristic and well-defined three peaks corresponding to the all oxidation species determine the reactivity of both surface materials. The recorded current responses of the three biological molecules with the OGO-GCE are much pronounced and greater than those obtained with NGO-GCE. The remarkable reactivity exhibited by OGO-GCE is apparently associated with the large adsorption capacity offered by the presence of surface-active components that enhance the bonding process [36]. The NGO with large passive surface limits the number of binding sites available for adsorption processes, which results in lower electrochemical responses. The presented data describe the powerful properties of OGO surface materials that facilitates the electrochemical measurements.

In addition, there is evidence relating the reactivity of OGO to the anodic exfoliation of NGO at which the abundance surface oxygen functionalities play a role on enhancement of electrode kinetics. The anodic exfoliation is believed to extend to the interlayer spacing among the NGO sheets, which makes electron shuttling more efficient.

3.2 The analytical performance of OGO-GCE

Selective determination of DA in biological samples is vital for diagnosis of a number of diseases. In addition, DA is biologically present at very low concentration compared to the interfering electroactive species such as AA and UA. Therefore, the analytical performance of the proposed sensor (OGO-GCE) was tested for the quantification of DA in the presence of certain amounts of AA or/and UA in PBS (pH = 7.28) using DPV technique.

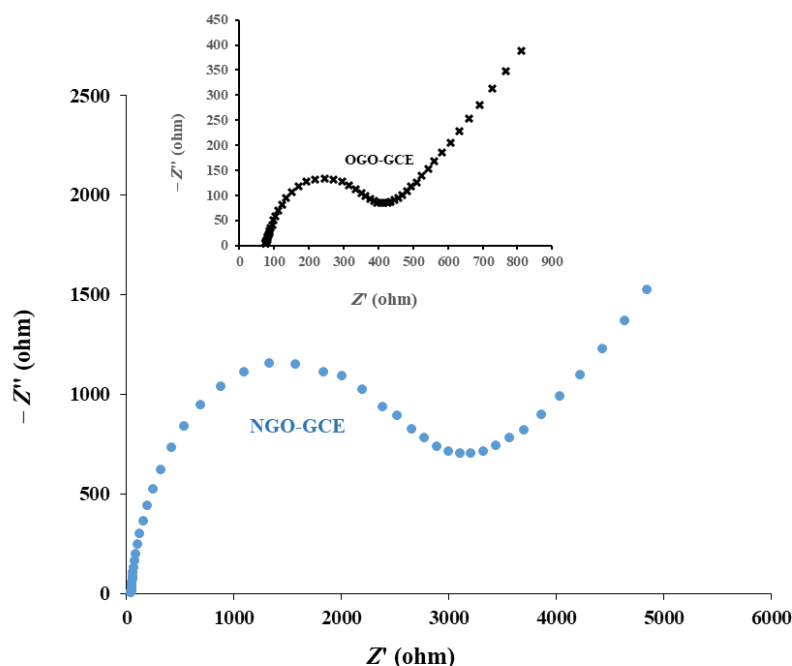


Figure 2. EIS experimental data presented by the Nyquist plot for NGO-GCE. The inset is the data for OGO-GCE.

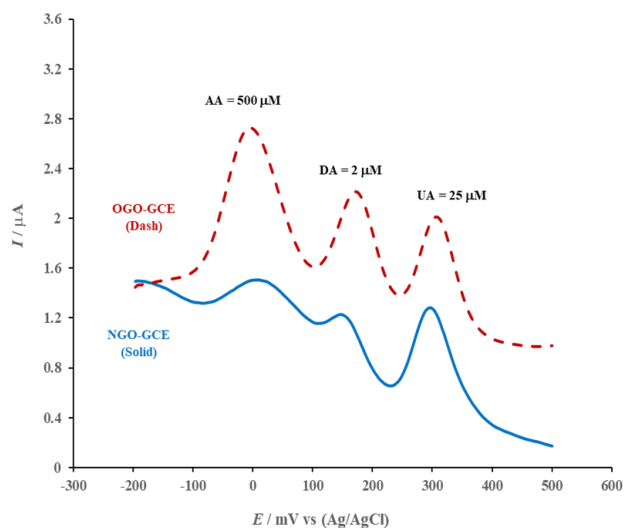


Figure 3. DPV curves of NGO-GCE (blue, solid) and OGO-GCE (red, dashed) towards the simultaneous determination of AA (500 μM), DA (2 μM) and UA (25 μM).

3.2.1 Selectivity test in a binary solution

Figure 4(A) shows the DPV curves for the determination of DA in the presence of 500 μM AA. The dotted line is the current response in the absence of DA where a single anodic peak obtained at 10 mV is characteristic of AA oxidation. With subsequent addition of DA, a new anodic peak arises at 196 mV corresponding to DA oxidation, which increases linearly with each increment of DA concentration. The potential gap (186 mV) between both peak responses is quite reasonable to avoid possible overlap occurring in bare electrodes.

Apparently, the high concentration of AA has no major effect on DA adsorption or electron transfer processes accounted for the electrochemical measurements of DA oxidation. The correlation of peak current (I_p) of DA oxidation to the DA concentration ([DA]) taken from the experimental data given in Figure 4(A) was set up and presented in Figure 4(B).

The regression data of the linear relationship were; $I_p(\mu\text{A}) = 0.5099 (\mu\text{M}) [\text{DA}] + 0.9134 (\mu\text{A})$, which produces a detection limit ($\text{DL}_{3\sigma}$) of 10 nM (DA), where σ is the standard deviation of the background response ($n = 3$) divided by the slope of the linear regression data.

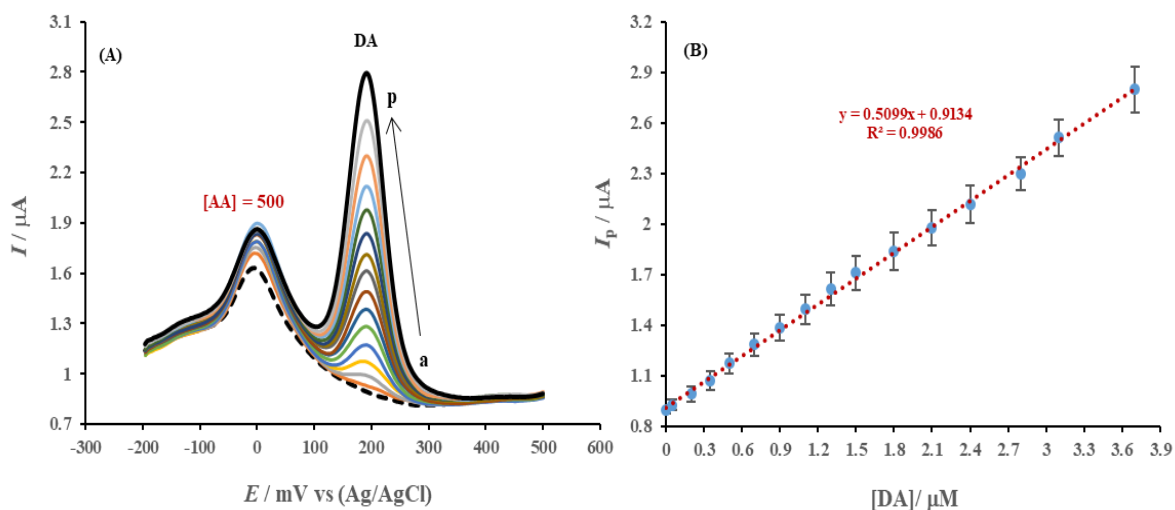


Figure 4. (A) Selective determination of DA in the presence of 500 μM of AA at OGO-GCE in 0.10 M PBS (pH 7.28) using DPV method for a range of [DA] between 0.0 (dotted line, a) and 3.7 μM (solid black, p). (B) The calibration curve plotted as I_p vs [DA] for the data presented in (A) with corresponding error bars.

Figure 5(A) shows the selective determination of DA in the presence of 50 μM UA where the DPV curve in the absence of DA (dotted line) demonstrates the rise of a single anodic peak obtained at 325 mV corresponding to UA oxidation. A new anodic peak current arises by successive addition of small amount of DA obtained at 195 mV due to DA oxidation and increases steadily regardless of the presence of large [UA]. The peak potential separation is 130 mV which is adequate for good identification and assures accurate quantification. The experimental data given in Figure 5(A) were utilized to construct the calibration curve by plotting on the (I_p) of DA versus [DA] as shown in Figure 5(B). The regression data of the linear relationship were; $I_p(\mu\text{A}) = 0.5045 (\mu\text{M}) [\text{DA}] + 1.0054 (\mu\text{A})$, at which the calculated detection limit of DA ($\text{DL}_{3\sigma}$) was 14 nM.

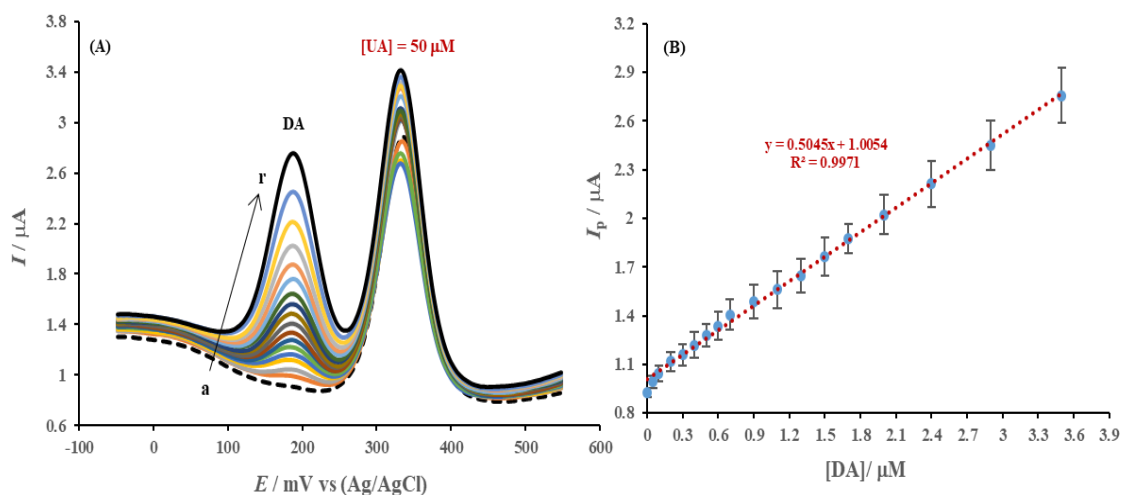


Figure 5. (A) Selective determination of DA in the presence of 50 μM of UA at OGO-GCE in 0.10 M PBS (pH 7.28) using DPV method for a range of [DA] between 0.0 (dotted line, a) and 3.7 μM (solid black, r). (B) The calibration curve plotted as I_p vs [DA] for the data presented in (A) with corresponding error bars.

3.2.2 Selectivity test in a ternary solution

The analytical performance of the proposed sensor for DA detection was examined in an aliquot composed of 500 μM AA and 100 μM UA as shown in Figure 6(A). The dotted line represents the electrode activity in the absence of DA, which results with the appearance of a couple anodic peaks obtained at 15 mV and 335 mV corresponding to AA and UA oxidation, respectively. The addition of DA in small increments produces a well-defined third anodic peak obtained at 195 mV corresponding to DA oxidation, which increases linearly and constantly regardless of the presence of large concentration of the couple interference species. The potential peak-to-peak separation among above studied species exceeds 140 mV, which demonstrates features of merits, robustness and steadiness of the surface materials for sensitive analysis. Figure 6(B) demonstrates the linear (I_p) versus [DA] relationship for the experimental data collected from Figure 6(A). The regression data of the linear relationship were: $I_p(\mu\text{A}) = 0.5056 (\mu\text{M}) [\text{DA}] + 0.8224 (\mu\text{A})$, and the calculated detection limit of DA ($\text{DL}_{3\sigma}$) is 12 nM.

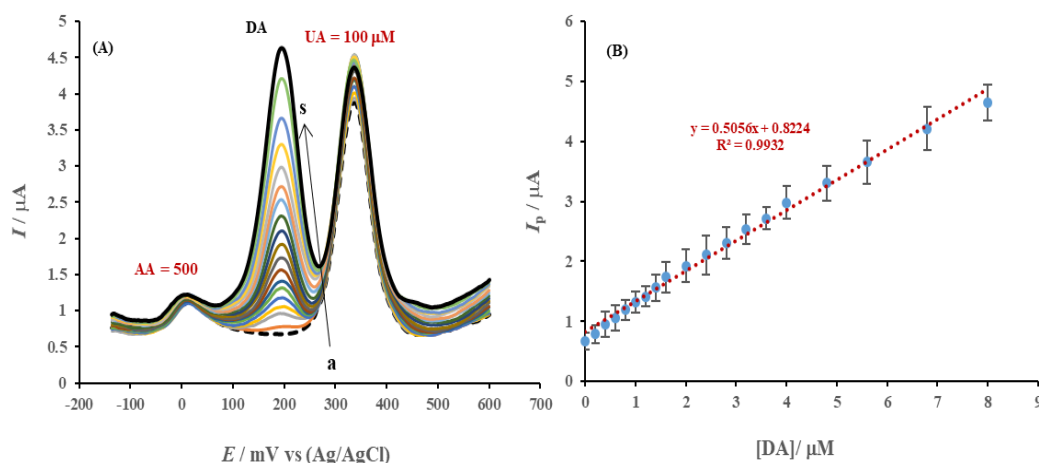


Figure 6. (A) Selective determination of DA in the presence of a binary mixture composed of 500 μM AA and 100 μM UA determined at OGO-GCE in PBS (pH 7.28) using DPV method for a range of [DA] between 0.0 (dotted line, a) and 8.0 μM (solid black, s). (B) The calibration curve plotted as I_p vs [DA] for the data presented in (A) with corresponding error bars.

It is important to note that the standard deviation illustrated by error bars for all data sets presented in the construction of calibration curves shown above were less than 5%. In addition, the slopes of these curves on average have the same value indicating excellent stability and selectivity. Therefore, the overall performance of the present sensor was compared with other applied modified electrodes to summarize its catalytic efficiency as listed in Table 1. The reported detection limit and the sensitivity of the proposed sensor is comparable to or better than the results reported by other relevant surface modified electrodes [37-44]. The above reported results show the importance of the new intended approach on the fabrication of a highly active electrochemical surface characterized by a large surface area and adsorption capacity.

Table 1. The analytical performance of the proposed sensor for DA detection compared to other modified electrodes.

Modified Electrode	DL (μM)	Sensitivity ($\mu\text{A}/\mu\text{M}$)	Reference
PIlox-GO-GCE	0.630	0.211	[37]
ERGO-GCE	0.500	0.482	[38]
PdNPs/GR/CS/GCE	0.100	0.223	[39]
ERGO-P(lysine)-GCE	0.100	0.560	[40]
CNH-P(glycine)-GCE	0.030	0.160	[41]
Ag(hcf)-GR-GCE	0.030	0.133	[42]
Cdots-rGONS-CF	0.020	0.006	[43]
P(glycine)-GO-GCE	0.015	0.534	[44]
OGO-GCE	0.012	0.506	This work

3.3. The stability of the OGO sensor

The reactivity and hence the stability of the proposed sensor was tested by 10 repetitive DPV scans in the presence of 500 μM (AA), 8 μM (DA) and 100 μM (UA). Figure 7 exhibits a negligible drop in the anodic current magnitude of all species. Moreover, the obtained anodic peak potential of the three biological species were consistent and maintained the same peak potential separation. The percent drop of peak current (I_p)% was calculated using equation (2), where $(I_p)_n$ is the peak current at run (n) and $(I_p)_i$ is the initial peak current value at run 1.

$$(I_p)\% = \frac{(I_p)_n}{(I_p)_i} \times 100\% \quad (2)$$

The percent drop in the last run approaches a value of 6%, 4% and 12% of its maxima for AA, DA and UA, respectively, indicating robustness of the solid-state sensor that maintains its reactivity and surface structure environment. The experimental results confirm that the sensor resists poisoning or passivation due to adsorption process of original electroactive molecules and their oxidation byproducts. These unwanted activities are known to deactivate the electrode kinetics associated with weak electrochemical responses.

3.4 Quantification of DA in serum blood

The developed (OGO-GCE) sensor was tested for the determination of DA in serum sample (prepared as described above in the experimental section) using the standard addition method. Figure 8(A) shows a nil current response of serum blood sample as indicated by the dashed line. With subsequent addition of serum-DA aliquot, a well-defined anodic peak was obtained at 192 mV corresponding to DA oxidation, which noticeably increased with each increment. A calibration curve correlates the anodic peak current as a function of [DA] in the range of 0.10 to 2.5 μM as shown in Figure 8(B).

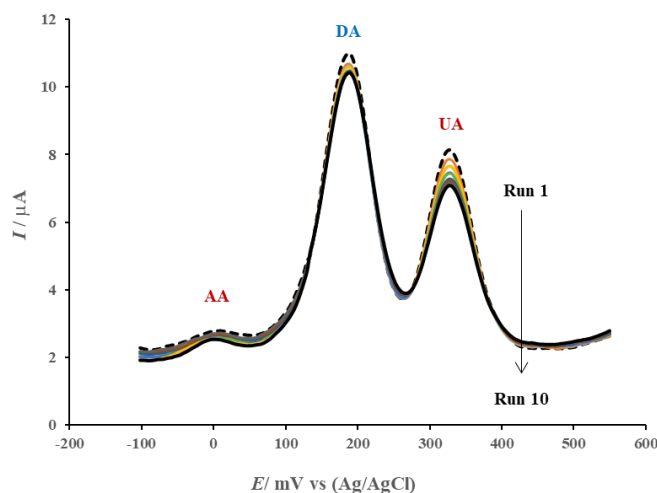


Figure 7. The stability test of the OGO-GCE by repeating the DPV runs from 1 (dotted) to 10 (solid black) in the presence of 500 μM (AA), 8 μM (DA) and 100 μM (UA).

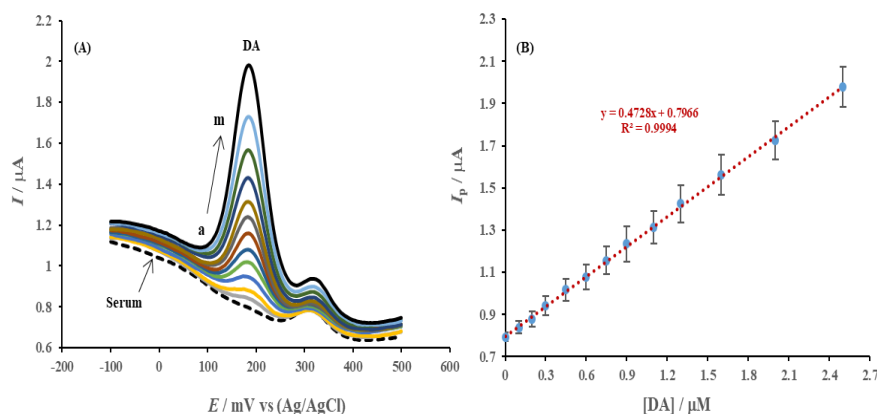


Figure 8. (A) The analytical performance OGO-GCE in the determination of DA in serum blood using standard addition method in PBS (pH 7.28) using DPV method. The [DA] ranged between 0.0 μM (dash black, a) to 2.5 μM (solid black, m). (B) The calibration curve plotted as I_p vs [DA] for the data presented in (A) with corresponding error bars.

3.5 Progress in Neuro-Psychopharmacology and Biological Psychiatry

The regression data are interestingly matching those evaluated above in the sections of selectivity tests. The estimated peak current response in (μA) obtained at 192 mV corresponding to each DA increment was converted into its equivalent concentration in (μM) using the regression data of the calibration curve. Accordingly, the recovery percentages for DA concentrations were calculated ($n = 3$) and summarized in Table 2 along with the relative standard deviation (RSD). The reported recovery values are analytically acceptable which attests to the reliability, stability and robustness of the proposed sensor for accurate DA analysis.

Table 2. The recovery percentage of DA in serum blood sample using standard addition method.

Samples	[Add] (μM)	[Found] \pm RSD ^(a) (μM)	Recovery (%)
(1)	0.00	Not Detected	NA
(2)	0.10	0.097 ± 0.028	96.5
(3)	0.30	0.296 ± 0.027	98.8
(4)	0.60	0.594 ± 0.025	99.0
(5)	0.90	0.915 ± 0.032	101.7
(6)	1.30	1.330 ± 0.027	102.3
(7)	2.50	2.495 ± 0.038	99.8

(a) Relative Standard Deviation ($n = 3$).

7. Conclusion

A steady and simple fabrication approach based on electrochemical oxidative pretreatment of NGO was used to prepare the developed OGO sensor. The exfoliation process of NGO via the anodic activation is expected to increase the interlayer spacing distance between the resultant OGO materials. The conductivity and the rate of electron transfer were substantially increased improving the electrochemical activity of the prepared sensor and hence extending its sensing potential applications. The structure and the catalytic activity of the prepared surface materials were characterized employing various analytical techniques such as XPS, EIS and DPV, all of which have proven the supremacy of OGO over NGO modified electrode. The OGO-GCE sensor showed an outstanding reactivity and stability to the simultaneous and selective determination of DA while lowering the detection limit to 12 nM. The proposed sensor was applied successfully for DA detection in real blood sample with satisfactory results at which the minimum recovery percentage was close to 96.5%.

Conflict of interest

The authors declare no conflict of interest.

Acknowledgment

We would like to thank Sultan Qaboos University (SQU), Sultanate of Oman for supporting this work by the research grant number (IG/SCI/CHEM/18/01). We thank Sultan Qaboos University Hospital (SQUH) for providing serum blood sample.

References

1. Wightman, R.M., May, L.J. and Michael, A.C. Detection of dopamine dynamics in the brain. *Analytical Chemistry* 1988, 60, 769A-779A.
2. Franco, R., Reyes-Resina, I. and Navarro, G. Dopamine in health and disease: Much more than a neurotransmitter. *Biomedicines* 2021, 9, 109 (13 pages).
3. Napier, T.C., Kirby, A. and Persons, A.L. The role of dopamine pharmacotherapy and addiction-like behaviors in Parkinson's disease. *Progress in Neuro-Psycho-pharmacology and Biological Psychiatry* 2020, 102, 109942.
4. Guo, Z., Seol, M-L., Kim, M-S., Ahn, J-H., Choi, Y-K., Liu, J-H. and Huang, X-J., Sensitive and selective electrochemical detection of dopamine using an electrode modified with carboxylated carbonaceous spheres. *Analyst* 2013, 138, 2683-2690.

5. Khudaish, E.A., Al-Nofli, F., Rather, J.A., Al-Hinaai, M., Laxman, K., Kyaw, H.H. and Al-Harthy, S. Sensitive and selective dopamine sensor based on novel conjugated polymer decorated with gold nanoparticles. *Journal of Electroanalytical Chemistry* 2016, **761**, 80-88.
6. Joshi, A., Schuhmann, W. and Nagaiah, T.C. Mesoporous nitrogen containing carbon materials for the simultaneous detection of ascorbic acid, dopamine and uric acid. *Sensors and Actuators B*: 2016, **230**, 544-555.
7. Wang, C., Qi, L. and Liang, R. A molecularly imprinted polymer-based potentiometric sensor based on covalent recognition for the determination of dopamine. *Analytical Methods* 2021, **13**, 620-625.
8. Rostami, A., Hadjizadeh, A. and Mahshid, S. Colorimetric determination of dopamine using an electrospun nanofibrous membrane decorated with gold nanoparticles. *Journal of Materials Science* 2020, **55**, 7969-7980.
9. Ye, F., Feng, C., Jiang, J. and Han, S. Simultaneous determination of dopamine, uric acid and nitrite using carboxylated graphene oxide/lanthanum modified electrode. *Electrochimica Acta* 2015, **182**, 935-945.
10. Kamel, A.H., Amr, A.E., Ashmawy, N.H., Galal, H.R., Al-Omar, M.A. and Sayed, A.Y. Solid-Contact Potentiometric Sensors Based on Stimulus-Responsive Imprinted Polymers for Reversible Detection of Neutral Dopamine. *Polymers* 2020, **12**, 1406(13 pages).
11. Huang, Y., Tang, Y., Xu, S., Feng, M., Yu, Y., Yang, W. and Li, H. A highly sensitive sensor based on ordered mesoporous ZnFe₂O₄ for electrochemical detection of dopamine. *Analytica Chimica Acta* 2020, **1096**, 26-33.
12. Khudaish, E.A., Al-Ajmi, K. and Al-Harthy, S. A solid-state sensor based on ruthenium (II) complex immobilized on polytyramine film for the simultaneous determination of dopamine, ascorbic acid and uric acid. *Thin Solid Films* 2014, **564**, 390 -396.
13. Dey, M.K. and Satpati, A.K. Functionalised carbon nanospheres modified electrode for simultaneous determination of dopamine and uric acid. *Journal of Electroanalytical Chemistry* 2017, **787**, 95-101.
14. Zhang, X., Zhang, Y.C. and Ma, L.X. One-pot facile fabrication of graphene-zinc oxide composite and its enhanced sensitivity for simultaneous electrochemical detection of ascorbic acid, dopamine and uric acid. *Sensors and Actuators B*: 2016, **227**, 488-496.
15. Lee, J., Kim, J., Kim, S. and Min, D.H. Biosensors based on graphene oxide and its biomedical application. *Advanced Drug Delivery Reviews* 2016, **105**, 275-287.
16. Sadak, O. One-pot scalable synthesis of rGO/AuNPs nanocomposite and its application in enzymatic glucose biosensor. *Nanocomposites* 2021, **7**, 44-52.
17. Sireesha, M., Babu, V.J., Kiran, A.S.K. and Ramakrishna, S. A review on carbon nanotubes in biosensor devices and their applications in medicine. *Nanocomposites* 2018, **4**, 36-57.
18. Ye, Z.B., Xu, Y., Chen, H., Cheng, C., Han, L.J. and Xiao, L. A novel micro-nano-structure profile control agent: Graphene oxide dispersion. *Journal of Nanomaterials* 2014, Article ID 582089 (9 pages).
19. Compton, O.C. and Nguyen, S.B. Graphene oxide, highly reduced graphene oxide, and graphene: Versatile building blocks for carbon-based materials. *Small* 2010, **6**, 711-723.
20. Davies, T.J., Moore, R.R., Banks, C.E. and Compton, R.G. The cyclic voltammetric response of electrochemically heterogeneous surfaces. *Journal of Electroanalytical Chemistry* 2004, **574**, 123-152.
21. Brownson, D.A.C., Kampouris, D.K. and Banks, C.E. Graphene electrochemistry: fundamental concepts through to prominent applications, *Chemical Society Reviews* 2012, **41**, 6944-6976.
22. Kuilla, T., Bhadra, S., Yao, D., Kim, N.H., Bose, S. and Lee, J.H. Recent advances in graphene based polymer composites. *Progress in Polymer Science* 2010, **35**, 1350-1375.
23. Power, A.C., Gorey, B., Chandra, S. and Chapman, J. Carbon nanomaterials and their application to electrochemical sensors: a review. *Nanotechnology Reviews* 2018, **7**, 19-41.
24. Silva, A.D., Paschoalino, W.J., Damasceno, J.P.V. and Kubota, L.T. Structure, properties, and electrochemical sensing applications of graphene-based materials. *ChemElectroChem* 2020, **7**, 4508-4525.
25. Vinodh, Kumar, G., Ramya, R., Potheher, I.V., Vimalan, M. and Peter, A.C. Synthesis of reduced graphene oxide/Co₃O₄ nanocomposite electrode material for sensor application. *Research on Chemical Intermediates* 2019, **45**, 3033-3051.
26. Li, G., Zhong, P., Ye, Y., Wan, X., Cai, Z., Yang, S., Xia, Y., Li, Q., Liu, J. and He, Q. A highly sensitive and stable dopamine sensor using shuttle-like α -Fe₂O₃ nanoparticles/electro-reduced graphene oxide composites. *Journal of Electrochemical Society* 2019, **166**, B1552-B1561.
27. Al-Graiti, W., Foroughi, J., Liu, Y. and Chen, J. Hybrid graphene/conducting polymer strip sensors for sensitive and selective electrochemical detection of serotonin. *American Chemical Society Omega* 2019, **4**, 22169-22177.
28. Khudaish, E.A., Myint, M.T.Z. and Rather, J.A. A solid-state sensor based on poly(2,4,6-triaminopyrimidine) grafted with electrochemically reduced graphene oxide: Fabrication, characterization, kinetics and potential analysis on ephedrine. *Microchemical Journal* 2019, **147**, 444-453.
29. Gorle, D.B. and Kulandainathan, M.A. Electrochemical sensing of dopamine at the surface of a dopamine grafted graphene oxide/poly(methylene blue) composite modified electrode. *Royal Society of Chemistry Advances* 2016, **6**, 19982-19991.
30. Li, J., Wang, Y., Sun, Y., Ding, C., Lin, Y., Sun, W. and Luo, C. A novel ionic liquid functionalized graphene oxide supported gold nanoparticle composite film for sensitive electrochemical detection of dopamine. *Royal Society of Chemistry Advances* 2017, **7**, 2315-2322.

31. Liu, Q., Ma, R., Du, A., Zhang, X., Fan, Y., Zhao, X., Zhang, S. and Cao, X. Investigation on structure and corrosion resistance of complex inorganic passive film based on graphene oxide. *Corrosion Science* 2019, **150**, 64-75.
 32. Su, Y., Kravets, V.G., Wong, S.L., Waters, J., Geim, A.K. and Nair, R.R. Impermeable barrier films and protective coatings based on reduced graphene oxide. *Nature Communications* 2014, **5**, 4843-4845.
 33. Khudaish, E.A. and Al-Khodouri, A. A surface network based on reduced graphene oxide/gold nanoparticles for selective determination of norepinephrine in real samples. *Journal of Electrochemical Society* 2020, **167**, 146516.
 34. Gengenbach, T.R., Major, G.H., Linford, M.R. and Easton, C.D. Practical guides for x-ray photoelectron spectroscopy (XPS): Interpreting the carbon 1s spectrum. *Journal of Vacuum Science and Technology A*: 2021, **39**, 013204.
 35. Bard, A.J. and Faulkner, L.R. *Electrochemical Methods: Fundamentals and Applications*, Wiley, New York, Second Edition, 2001.
 36. Brownson D.A.C., Gómez-Mingot M. and Banks C.E., CVD graphene electrochemistry: biologically relevant molecules. *Physical Chemistry Chemical Physics* 2011, **13**, 20284-20288.
 37. Liu, X.F., Zhang, L., Wei, S.P., Chen, S.H., Ou, X. and Lu, Q.Y. Over-oxidized polyimidazole-graphene oxide copolymer modified electrode for the simultaneous determination of ascorbic acid, dopamine, uric acid, guanine and adenine. *Biosensors and Bioelectronics* 2014, **57**, 232-238.
 38. Yang, L., Liu, D., Huang, J. and You, T. Simultaneous determination of dopamine, ascorbic acid and uric acid at electrochemically reduced graphene oxide modified electrode. *Sensors and Actuators B*: 2014, **193**, 166-172.
 39. Wang, X., Wu, M., Tang, W., Zhu, Y., Wang, L., Wang, Q., He, P. and Fang, Y. Simultaneous electrochemical determination of ascorbic acid, dopamine and uric acid using a palladium nanoparticle/graphene/chitosan modified electrode. *Journal of Electroanalytical Chemistry* 2013, **695**, 10-16.
 40. Zhang, D., Li, L., Ma, W., Chen, X. and Zhang, Y. Electrodeposited reduced graphene oxide incorporating polymerization of l-lysine on electrode surface and its application in simultaneous electrochemical determination of ascorbic acid, dopamine and uric acid. *Materials Science and Engineering C*: 2017, **70**, 241-249.
 41. Zhang, G., He, P., Feng, W., Ding, S., Chen, J., Li, L., He, H., Zhang, S. and Dong, F. Carbon nanohorns/poly(glycine) modified glassy carbon electrode: Preparation, characterization and simultaneous electrochemical determination of uric acid, dopamine and ascorbic acid. *Journal of Electroanalytical Chemistry* 2016, **760**, 24-31.
 42. Zhang, F., Li, S., Zhang, H. and Li, H. A Silver Hexacyanoferrate-Graphene Modified Glassy Carbon Electrode in Electrochemical Sensing of Uric Acid and Dopamine. *International Journal of Electrochemical Science* 2017, **12**, 11181-11194.
 43. Fang, J., Xie, Z., Wallace, G. and X. Wang. Co-deposition of carbon dots and reduced graphene oxide nanosheets on carbon-fiber microelectrode surface for selective detection of dopamine. *Applied Surface Science* 2017, **412**, 131-138.
 44. He, S., He, P., Zhang, X., Zhang, X., Liu, K., Jia, L. and Dong, F. Poly(glycine)/graphene oxide modified glassy carbon electrode: Preparation, characterization and simultaneous electrochemical determination of dopamine, uric acid, guanine and adenine. *Analytica Chimica Acta* 2018, **1031**, 75-82.
-

Received 4 April 2023

Accepted 28 May 2023

Preparation and Characterization of Iron Oxide Nano-adsorbent by *Enteromorpha Flexuosa* Algae obtained from Yanbu Red Sea, Saudi Arabia

Alaa Elmi¹, Rafat Afifi Khattab², Omar M.L. Alharbi³, Gunel Imanova⁴ and Imran Ali^{*1,5}

¹Department of Chemistry, School of Sciences, Taibah University, Medina 41477, Saudi Arabia, ²Marine Science Department, Suez Canal University, Ismailia 41522, Egypt ³Department of Biology, School of Sciences, Taibah University, Medina 41477, Saudi Arabia¹, ⁴Institute of Radiation Problems, Ministry of Science and Education Republic of Azerbaijan, Baku AZ-1143, Azerbaijan, ⁵Department of Chemistry, Jamia Millia Islamia, New Delhi 110025, India. *Email: drimran.chiral@gmail.com.

ABSTRACT: Water contamination caused by toxic cadmium metal ions is a worldwide problem. There is a need to explore new methods of cadmium removal from water. The green algae *Enteromorpha flexuosa*, obtained from the Red Sea in Yanbu, Saudi Arabia, was used to prepare iron nanoparticles. TEM, FT-IR, XRD, and SEM techniques were used to characterize the prepared nanoparticles. The prepared nanoparticle's surface was rough, with nanoparticle sizes ranging from 10 to 50 nm. The developed nanoparticles were used to adsorb cadmium ions from water in batch mode. With a 25.0 µg/L concentration, a temperature of 25°C, 7.0 pH, 60 minutes contact time and 0.5 g/L dose, the maximum removal of cadmium was 48.2 µg/g. The sorption efficiency was measured using the Dubinin-Radushkevich, Temkin, Langmuir and Freundlich models. The amounts of ΔG° were -8.0, -9.93 and -12.24 kJ/mol while the values of ΔS° and ΔH° were -30.96×10^{-3} kJ/mol and 37.79×10^{-2} kJ/mol. These data confirmed the endothermic nature of cadmium metal ions removal. Along with the liquid film diffusion process, the adsorption adopted the kinetics of pseudo-second-order type. The recorded adsorption method is fast, cost-effective, and environmentally friendly and can be applied for testing the elimination of cadmium metal ions in natural waters.

Keywords: Green synthesis; Nanoparticles; Adsorption; Water treatment; Modeling; Kinetics and thermodynamics.

تحضير وتوصيف الممتز النانوي لأكسيد الحديد بواسطة طحلب *Enteromorpha Flexuosa* المستخرج من ينبع البحر الأحمر، المملكة العربية السعودية

علاء علمي، رأفت عفيفي خطاب، عمر محمد الحربي، جونيل إيمانوفا و*عمران علي

المخلص: يعد تلوث المياه بسبب أيونات معدن الكاديوم السامة مشكلة عالمية، ولا تزال هناك حاجة لإستكشاف طرق جديدة لإزالة الكاديوم من الماء. تم استخدام الطحالب الخضراء *Enteromorpha flexuosa*، التي تم الحصول عليها من البحر الأحمر في ينبع بالمملكة العربية السعودية، لتحضير جزيئات الحديد النانوية. تم استخدام تقنيات TEM، FT-IR، XRD، SEM لتوصيف الجسيمات النانوية المحضرة. كان سطح الجسيمات النانوية المحضرة خشناً، وتتراوح أحجام الجسيمات النانوية من 10 إلى 50 نانومتر. تم استخدام الجسيمات النانوية المطورة لإمتصاص أيونات معدن الكاديوم من الماء في وضع الدفعة. مع تركيز 25.0 ميكروغرام/لتر، ودرجة حرارة 25 درجة مئوية، ودرجة حموضة 7.0، ووقت تلامس 60 دقيقة وجرعة 0.5 غرام/لتر، كان الحد الأقصى لإزالة الكاديوم 48.2 ميكروغرام/لتر. تم قياس كفاءة الإمتصاص بإستخدام نماذج Dubinin-Radushkevich و Temkin و Freundlich. كانت كمية ΔG° -8.0، -9.93، -12.24 كيلو جول/مول بينما كانت قيم ΔS° و ΔH° -30.96×10^{-3} كيلو جول/مول و 37.79×10^{-2} كيلو جول/مول. أكدت هذه البيانات الطبيعة الماصة للحرارة لإزالة أيونات معدن الكاديوم. جنباً إلى جنب مع عملية إنتشار الغشاء السائل، إعتمدت عملية الإمتزاز حركية النوع من الدرجة الثانية الزائفة. تتميز طريقة الإمتزاز المسجلة بأنها سريعة وفعالة من حيث التكلفة وصديقة للبيئة ويمكن تطبيقها لإختبار التخلص من أيونات معدن الكاديوم في المياه الطبيعية.

الكلمات المفتاحية: التخليق الأخضر؛ الجسيمات النانوية؛ الإمتزاز؛ معالجة المياه؛ النمذجة؛ الحركية والديناميكا الحرارية.



1. Introduction

Throughout the last few decades, water safety has been a big concern. [1-7]. Toxic trace metal ions are among the numerous water contaminants that are extremely harmful due to their serious toxicity and side effects, which include cancer [8]. These ions have tendency for interacting with proteins and enzymes and are not biodegradable [9-11]. These metal ions appear to accumulate in tissues, causing a variety of diseases and health problems. Humans are thought to be at risk from exposure to these metals, even at trace levels [12-15]. As a result, scientists, academics, and government officials are all concerned about metal contamination. Nanotechnology's goals are to develop eco-friendly designs in order to reduce health and environmental risks by finding ways to substitute current applications with green nanotechnology products. Nanotechnology is the production of components in particular by a number of material processes and/or ingredients, ultimately to be applied in a range of applications [17]. A nanoparticle is well-defined as a minute element with a minimum of at least one dimension in the range of 10 to 100 nm. They have unique electrochemical, thermal, and optical properties making them useful in numerous applications in the areas of energy, environment, medicine, chemistry, agriculture, communication, information, consumer goods, and heavy industry.

To remove toxic metal ions from aqueous media, some researchers have used nanoparticles as adsorbents. Because of their catalytic strength, small size, large number of active sites, high reactivity, and ease of separation for interacting with various contaminants, nanomaterials make excellent adsorbents. These features are related to the great adsorption capabilities, as determined by the adsorption power. Zhang [18] investigated the characterization, synthesis, and use of Fe⁰/Ni⁰, Fe⁰/Ag⁰, Fe⁰/Pt⁰, Fe⁰/Co⁰ and Fe⁰/Pd⁰ nanoscale Fe⁰ particles, as well as Fe⁰/Co⁰ Fe⁰/Ni⁰, Fe⁰/Ag⁰ and Fe⁰/Pt⁰ nanoscale Fe⁰ particles. Cr(VI) was efficiently reduced to mobile and less toxic Cr(III) type using Fe⁰ and bimetallic Fe⁰ nanoparticles. Deliyanni and Matis [19] extracted cadmium using akaganeite (-FeOOH) nanoparticles with a 17.1 mg/g adsorption potential. Furthermore, since the adsorption potential increased from 30% to 90% as the temperature rises from 25 to 65 °C; the whole process was exothermic. In order to remove Cr(VI) from groundwater, it was discovered that starch-stabilized Fe⁰ nanoparticles were more adsorbent than native zero-valent metal particles. As pH and dosage were increased, adsorption ability was found to decrease. Lazaridis, *et al.* [20] synthesized nanocrystalline akaganeite rod-like nanoparticles (3-6 nm diameter) with a comprehensive removal rate of 80.0 mg/g to extract Cr(VI). According to Hu, *et al.* [21] Cr(VI) elimination from wastewater using maghemite nanoparticles was 19.2 mg/g. The nanoparticles had an established diameter of 10 nm, and the maximum adsorption occurred within 15 minutes at pH 2.5. Di, *et al.* [22] used carbon nanotubes to strip Cr(VI) from drinking water. The strongest Cr(VI) adsorption, according to the researchers, occurred at a pH range of 3.0-7.4, with a power of 30.2 mg g⁻¹. The use of chitosan-Fe(0) nanoparticles to purify water from Cr(VI) was recorded by Geng, *et al.* [23].

Recently, scientists started to prepare nanoparticles using plant extracts. This is a green and environmentally friendly process. Some reviews have been presented on the synthesis of various nanoparticles using the green approach [24-26]. Only a few authors exploited these nanoparticles for water treatment. Ehrampoush, *et al.* [27] used the extract of tangerine peel and prepared nanoparticles of iron oxides for the decontamination of cadmium in water. Biosynthesis of stable iron nanoparticles was carried out using Phoenix dactylifera L. extract which was able to reduce iron ions to iron nanoparticles [28]. Iron oxide nanoparticles (IONPs) were synthesized using a cost-effective and eco-friendly method, taking *Moringa oleifera* leaves extract as a bio-reducer [29]. The influence of different parameters on removal efficiency, such as metal concentration, adsorbent dosage, pH and contact time was studied. Ehrampoush, *et al.* [30] prepared iron oxide nanoparticles by green synthesis for the removal of cadmium from aqueous solution. The authors used plant extract to make nanoparticles. Zhu, *et al.* [31] synthesized nanoscale zero-valent iron/Cu prepared by green synthesis. The exclusion effectiveness of Cr (VI) was 94.7 percent at a pH of 5 and a temperature of 303 K with observable rate constant K_{obs} values of 0.07430, 0.09650, 0.1183, and 0.1473 min⁻¹ at 298, 303, 308, and 313 K. Ali and co-workers prepared complex and functionalized iron nano particles using a black tea extract. The nanoparticles were used for the removal of azorubine dye [32], tetracycline and chlortetracycline antibiotics [33], actinides and rare earth elements [34], dioxidine [35], samarium ions [36], ketoprofen [37], and tetracycline antibiotics [38]. The authors tested their data with various models. The removal of these pollutants was in the range of 80-90 %. The objectives of this study are to prepare a new generation nano-adsorbent by green methods as well as the removal of cadmium using batch mode.

2. Experimental

2.1 Materials

The chemicals were purchased from Merck, Darmstadt, Germany, included cadmium nitrate, iron chloride, iron sulphate, sodium hydroxide, hydrochloric acid, and others. Purified water was obtained by using Heal Force water purification system, China. The pH of the solutions was evaluated using a Control Dynamics pH meter (Model APX175 E/C). The nanoparticles were removed by a powerful magnet. FT-IR Nicolet380 was used to record FT-IR spectra. Powdered X-ray diffraction was conducted on a Philips PX-1830 diffractometer with a proportional counter detector, a Cu filter on secondary optics, 30 mA current, Cu-K_α radiation ($\lambda = 1.54$ nm), and 25 kV voltage. Images

were captured using scanning electron and transmission microscopes. ICP-MS Agilent Technologies 7500 Series was used to assess the residual content of Cd(II), as per the normal procedure.

2.2 Iron nanoparticle preparation

Preparation of iron nanoparticles (NPs) using Green technology was done using a standardized protocol [39,40]. The Red Sea alga (*Enteromorpha flexuosa*, 10.0 g/L) was rinsed numerous times using deionized water before being blended for 30 minutes with 500 mL of deionized water. The paste was heated at 80 °C for about 2-3 hrs. It was then cooled before being filtered through Whatman filter paper (No. 24). The solutions of FeCl₃ and FeSO₄ (0.1 M) were prepared in 250 and 125 mL, separately and respectively. Both solutions were mixed together. Now, 500 ml extract of alga was mixed slowly with constant string. 0.1 N sodium hydroxide was used to keep the pH of the solution at 10. For 24 hours, the solution was stirred. A strong magnet was used to isolate the settled nanoparticles. The nanoparticles were splashed with deionized water numerous times before being immersed in 70% ethanol. The nanoparticles were dried at 100 °C in an oven for 5 hrs. These were cooled and prepared for later use in a vacuum desiccator. The green approach to the synthesis of iron oxide nanoparticles is depicted schematically in Figure 1.

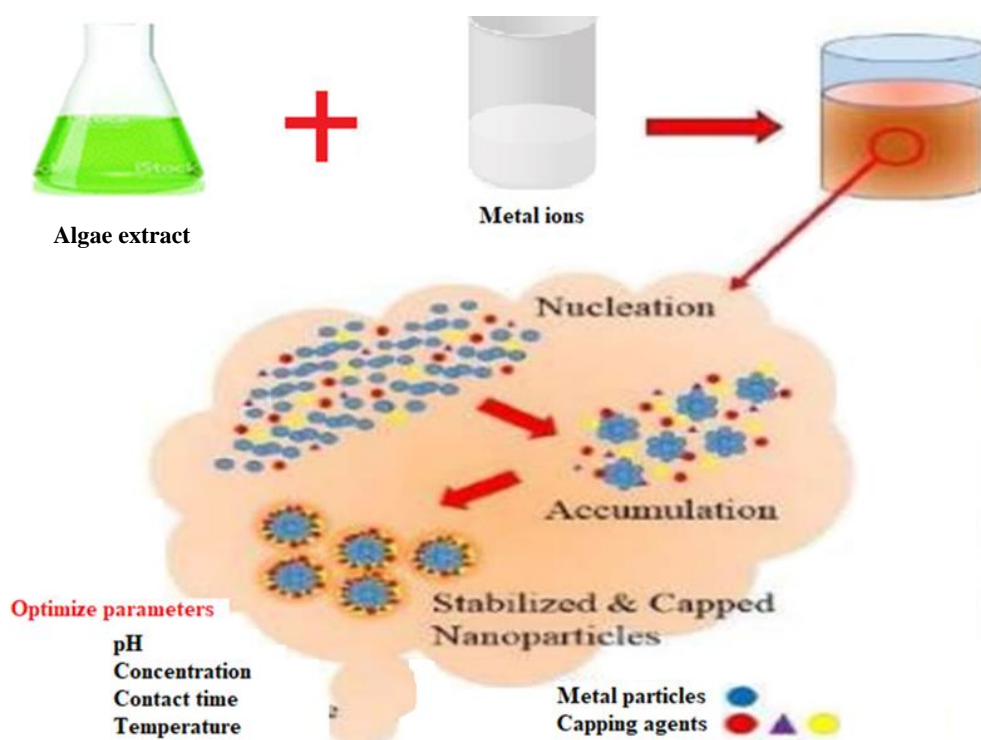


Figure 1. The green method used to synthesize iron nanoparticles.

2.3 Characterization of iron nanoparticles

The synthesized iron nanoparticles were classified using FT-IR, XRD, TEM and SEM approaches. At a voltage of 10 kV, photographs of samples were taken at various magnifications. Using a Philips PX-1830 diffractometer, Cu-K_α radiation ($\lambda = 1.54$ nm) was used to obtain X-ray diffraction (XRD) patterns of native and iron nano-impregnated particles using a proportional counter detector, a secondary optics Cu filter, 25 kV voltage and 30 mA current. At a rate of 3 °C per minute, the temperature from 10 to 80 °C for the iron nano-impregnated particles were scanned.

2.4 Adsorption studies

All of the adsorption tests were performed in a thermostatic water bath shaker at a specific temperature and duration. Following adsorption, the liquid and solid materials were separated using centrifugation. The concentrations of Cd(II) in solution samples were measured using an ICP-MS system. Adsorption isotherms were investigated using a concentration range of 5-30 µg/L, a pH range of 2-9.0, a contact time of 10-90 minutes, a dosage of 0.1-0.50 g/L, and temperatures of 15-35 °C. Isothermal and kinetic parameters were determined using various mathematical simulations. Data from batch studies were used to measure the equilibrium Cd(II) uptake potential. It was calculated using the equation below.

$$Q_e = (C_0 - C_e)/m.$$

3. Results and Discussion

3.1 Iron nanoparticles characterization

Changes in the color of algae extract were used to assess the development of iron nanoparticles. The green color of the algae extracts changed from brown to black after mixing in iron salt solution. The color change is an indication of the chemical reaction and formation of nanoparticles. The physical appearance of iron oxide nanoparticles is shown in Figure 2. The FT-IR spectra of nanoparticles showed peaks at 574 cm^{-1} indicating the presence of Fe-O. A Bruker D8 fitted with monochromatic copper radiation (K_{α} , $\lambda = 0.154\text{ nm}$) was used to record the nanoparticles' X-ray diffraction (XRD) pattern at room temperature. XRD patterns of Fe_3O_4 NPs confirmed the formation of a pure phase of Fe_3O_4 NPs. The peaks were obtained at the 2θ of 30, 40, 60, and 70 indicating the presence of iron oxide, iron(III) oxide-hydroxide, and free Fe^0 (zero-valent iron), respectively. The XRD pattern indicates the amorphous nature of nanoparticles. A TOPCON 002B transmission electron microscope (TEM) with a GATAN GIF 200 electron imaging filter and a 200 kV operating voltage (point resolution 0.18 nm) was used to study the morphology and crystalline structure of the nanoparticles. Figures 3 and 4 display SEM and TEM images of the prepared nanoparticles, respectively. An evaluation of SEM images indicates the rough and crystalline surface. The evaluation of TEM images shows nanoparticle sizes ranging from 10 to 50 nm.

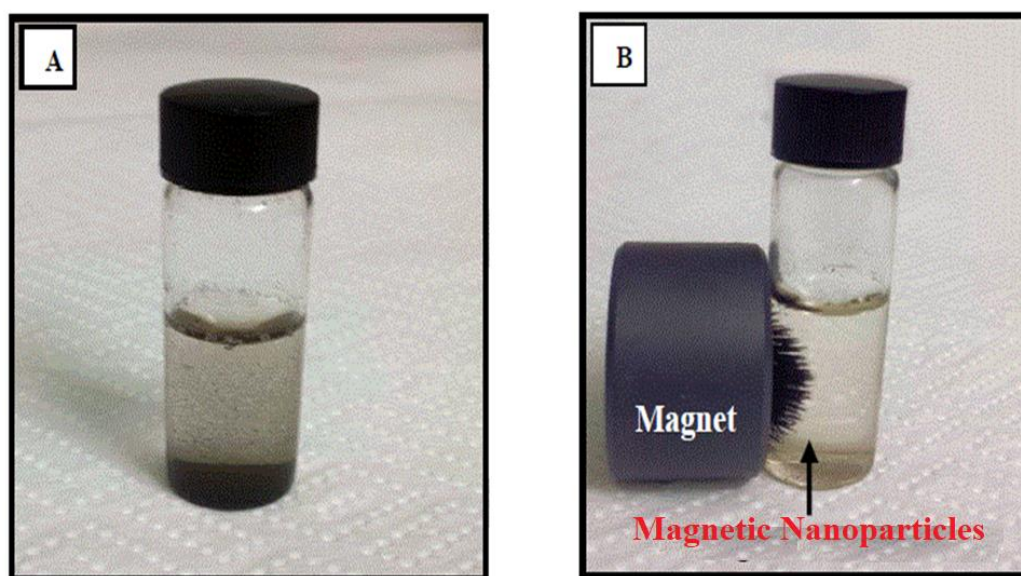


Figure 2. Iron oxide magnetic nanoparticle (A): before and (B): after magnetic property.

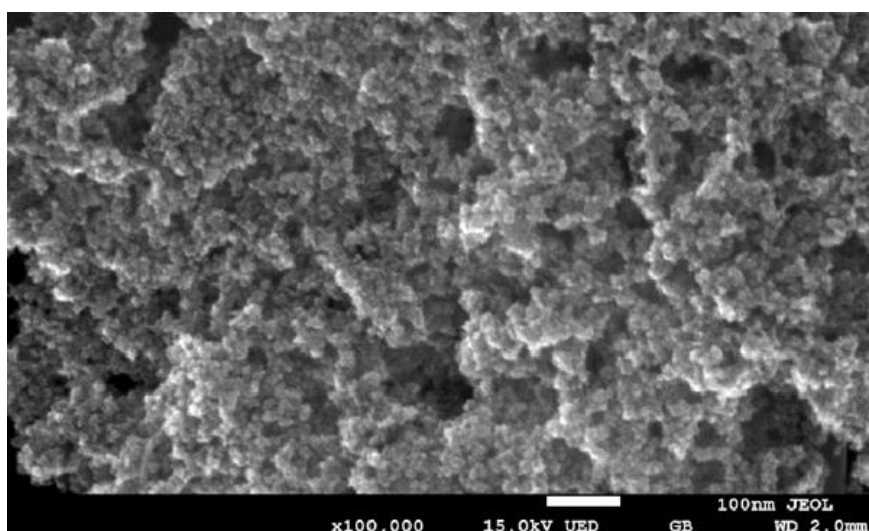
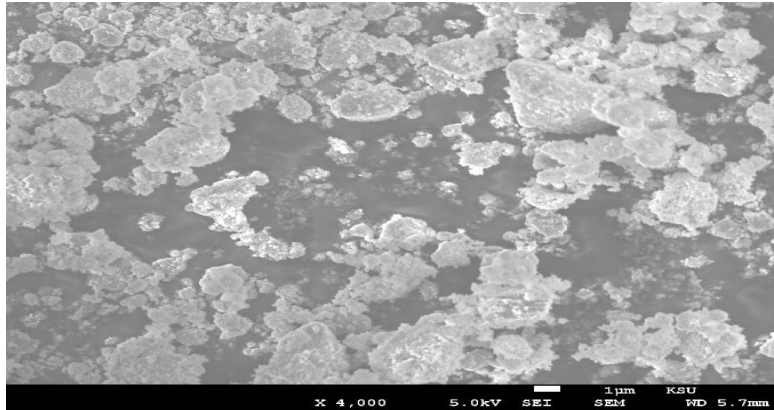
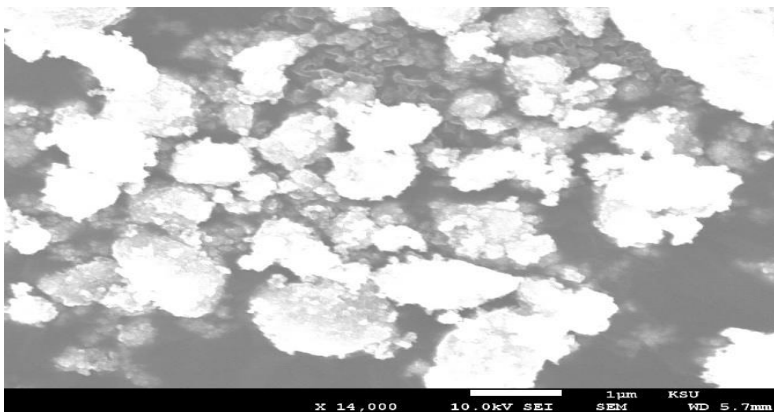


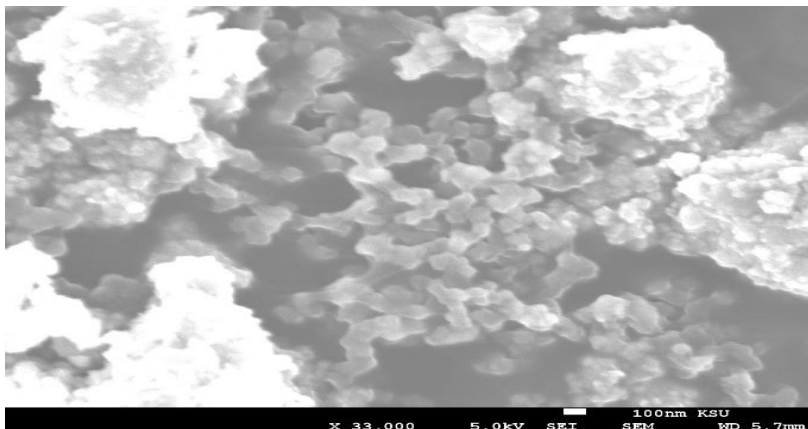
Figure 3. SEM of iron nanoparticles.



(a)



(b)



(c)

Figure 4. TEM images of iron nanoparticles at different magnifications, (a): 4,000, (b): 14,000 and (c): 33,000.

3.2 Adsorption studies

3.2.1 Effect of concentration

The concentration was optimized by varying the concentration between 5 and 30 g/L. The temperature was 25°C, the pH was 7.0, the dose was 0.5 g/L, and the contact time was 25 minutes. As previously mentioned, the residual concentration of Cd(II) was determined. Figure 5 depicts this effect, with the maximum uptake of Cd(II) at 25.0 g/L. Adsorption increased rapidly from 9.5 µg/g at 5.0 g/L to 48.2 µg/g at 25.0 g/L concentration (as seen in this graph). After a concentration of 25.0 g/L, the adsorption became constant. At higher concentrations, adsorption capacities did not increase. As a result, the optimum concentration was determined to be 25.0 g/L.

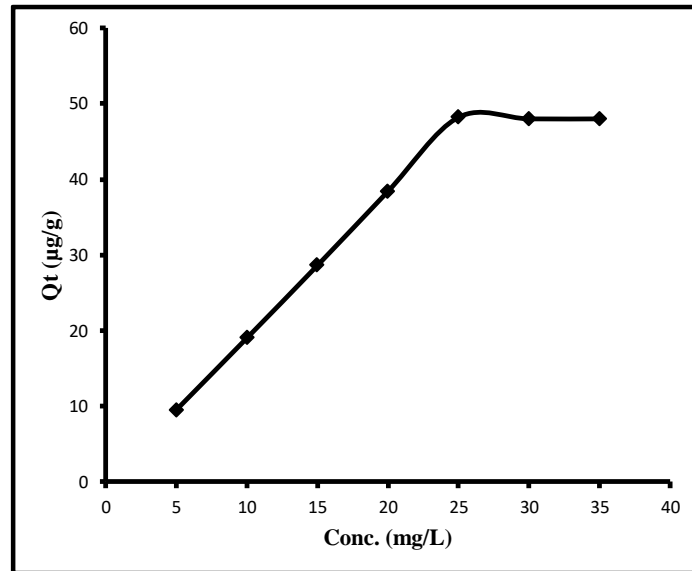


Figure 5. The initial concentration effect on cadmium removal.

3.2.2 Effect of contact time:

Experiments ranging from 10 to 90 minutes were used to maximize the impact of contact time. Contact time was tested against the other variables of 25 g/L concentration, pH 7.0, dosage 0.5 g/L, and temperature 25 °C. Figure 6 depicts the outcome of this effect. The adsorption capacities increased from 10 (43.0 g/g) to 60 minutes (48.0 g/g) as seen in this graph. More contact time did not improve adsorption. Therefore, it was concluded that 60 minutes was the optimized time.

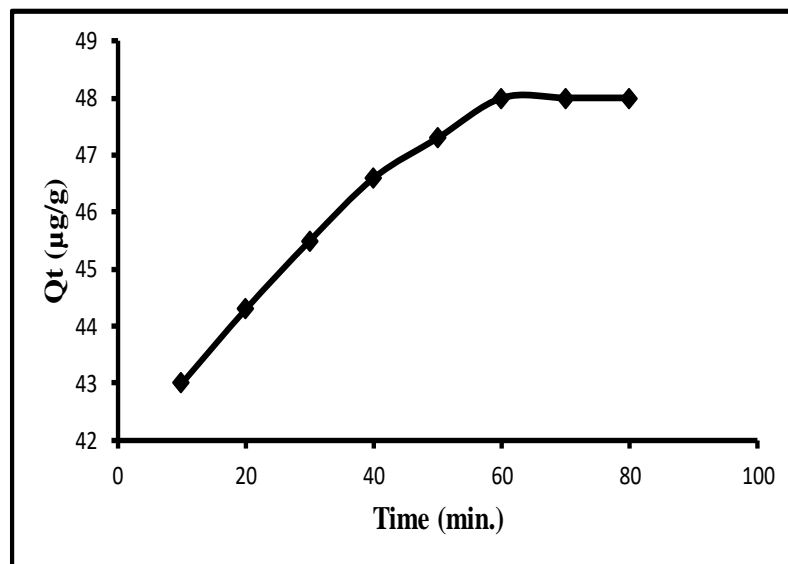


Figure 6. The contact time effect on cadmium removal.

3.2.3 Effect of pH

Experiments at various pHs were used to maximize the pH of adsorption (2-9). Contact time was 60 minutes, concentration was 25 g/L, the dosage was 0.5 g/L, and the temperature was 25 °C. Figure 7 depicts the outcome of this effect. The adsorption capacities increased from 4.5 µg/g at pH 2.0 to 48.5 µg/g at pH 7.0 as seen in this graph. More adsorption would be difficult to accomplish with a higher pH. As a result, it was concluded that pH 7.0 was the best.

3.2.4 Effect of dosage

The effect was investigated using a dosage range of 0.1-0.8 g/L. Contact time was 60 minutes, concentration was 25 g/L, pH was 7.0, and the temperature was 25 °C. Figure 8 depicts the outcome of this effect. The adsorption

capacities increased from 4.28 $\mu\text{g/g}$ at 0.1 g/L dose to 48.0 $\mu\text{g/g}$ at 0.5 g/L dose as seen in this graph. Higher dosage did not improve adsorption. As a result, the 0.5 g/L dose was determined to be the best.

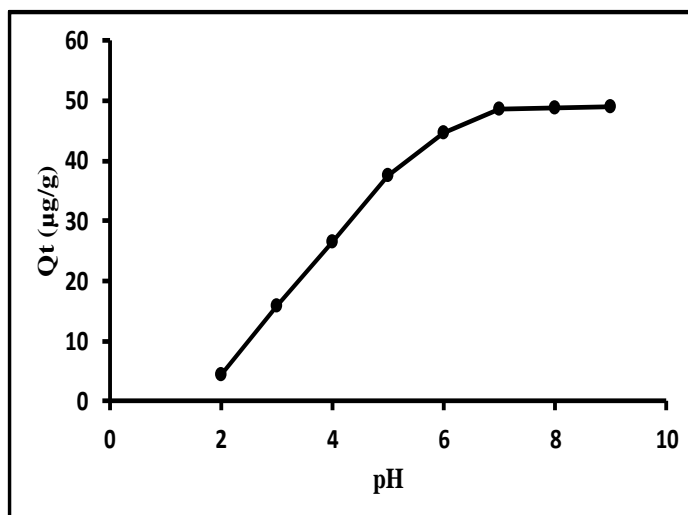


Figure 7. pH effect on cadmium removal.

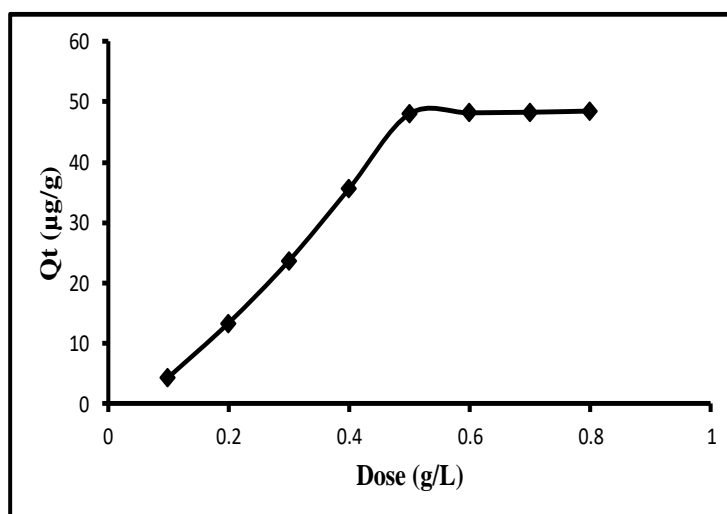


Figure 8: Effect of dose on cadmium removal.

3.2.5 Effect of temperature

Temperature effects on adsorption were investigated at 15, 25, and 35°C. Contact time was 60 minutes, concentration was 25 $\mu\text{g/L}$, pH was 7.0, and the dosage was 0.5 g/L. Figure 9 depicts the results of this parameter. The sorption of Cd(II) decreased as the temperature increased, suggesting an exothermic adsorption process. The order of Cd(II) removal was 15 > 25 > 35 °C. Of course, since most water sources have a temperature range of 15-35 °C, the adsorption process was deemed environmentally friendly. All the experiments were carried out 3 times ($n = 3$) and the standard deviation ranged from 0.45 to 0.67%.

3.3 Adsorption models

Well-known models illustrate the elimination of the cadmium metal ion. These are listed in more detail below.

3.3.1 Langmuir model

The most commonly used method for measuring the amount of adsorbate on an adsorbent as a function of a given temperature at partial pressure or concentration is the Langmuir adsorption model. It reflects a molecule's adsorption on an idealized surface. The molecule is thought to bind to several different locations on the solid's surface.

In the most basic case this model makes the following assumptions: the adsorption of a single adsorbate onto several identical sites on the surface of a solid

1. There are no corrugations on the surface containing the adsorbing sites (assuming the surface is homogeneous).
2. The adsorbing gas becomes immobile as a result of the adsorption process.

PREPARATION AND CHARACTERIZATION OF IRON OXIDE NANO-ADSORBENT

3. Every location is the same.
 4. Each molecule can only be stored in one site at a time (mono-layer coverage only).
 5. Adsorbate molecules on neighboring sites have no interactions with one another.
- With mono-layer sorption, the secret to the Langmuir model is the assumption of even sorption energy on the adsorbent surface. Equation 1 is the model's linear form. [41].

$$\frac{1}{q_e} = \frac{1}{q_0} + \frac{1}{q_0 b C_e} \quad (1)$$

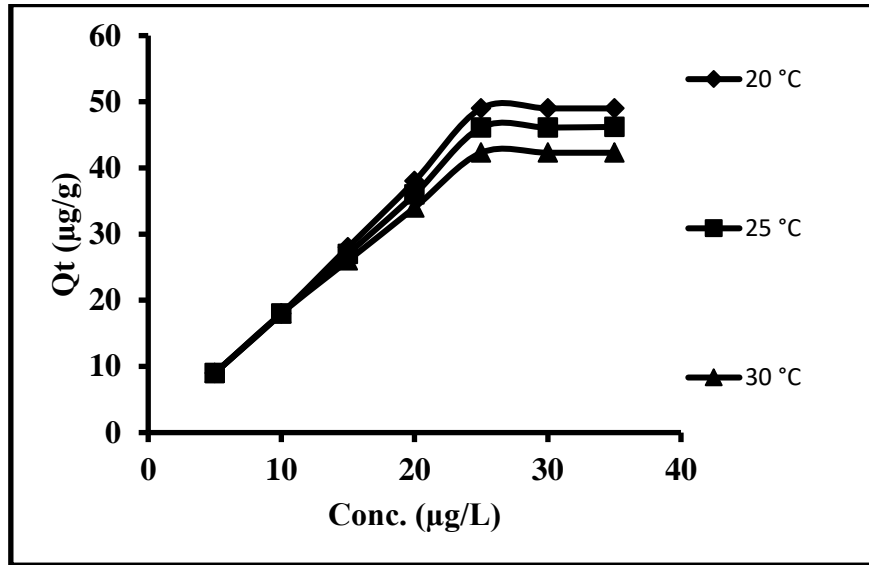


Figure 9. Effect of temperature on the removal of cadmium.

Table 1. Models parameter values for cadmium metal ion.

Models	Parameters	Numerical Values		
		15 °C	25 °C	35 °C
Langmuir	Q_0 (µg/g)	28.99	54.95	119.05
	b (L/µg)	0.80	0.51	0.27
	R_L	0.61	0.69	0.80
	R^2	0.980	0.992	0.947
Freundlich	k_F (µg/g)	76.95	54.29	44.72
	n (µg/L)	0.50	0.64	0.77
	R^2	0.995	0.978	0.899
Temkin	K_T (L/µg)	1.58	1.59	1.64
	B_T (kJ/mol)	0.018	0.023	0.029
	R^2	0.996	0.927	0.807
Dubinin-Radushkevich	Q_e (µg/g)	213.80	157.32	123.87
	E (kJ/mol)	0.78	0.83	0.88
	R^2	0.948	0.954	0.916

A straight line is obtained when $1/q_t$ is plotted against $1/C_e$ (Figure 10), demonstrating the Langmuir model's usefulness. The intercept and slope of the graphs determine the values of the constants (b and Q_0) (Table 1). For Cd(II), the values of q_0 and b ranged from 28.99 to 119.05 g/g. R_L values ranged between 0.61 and 0.80. At all temperatures, the regression constants' magnitudes ranged from 0.947 to 0.992. This is where the model's applicability is proven.

3.3.2 Freundlich model

For rough surfaces, the most powerful multisite adsorption isotherm is the Freundlich isotherm. Freundlich isotherm adsorption, as opposed to monolayer adsorption, is multilayer adsorption on a heterogeneous surface with a non-uniform distribution of adsorption heat and affinities. The total number of adsorbates adsorbed on the adsorbent's surface is called the total number of all sites. As the adsorption process continues, the adsorption energies decrease exponentially. This is how the Freundlich adsorption isotherm is calculated:

$$\log Q_e = \log k_F + \frac{1}{n} \log C_e \quad (2)$$

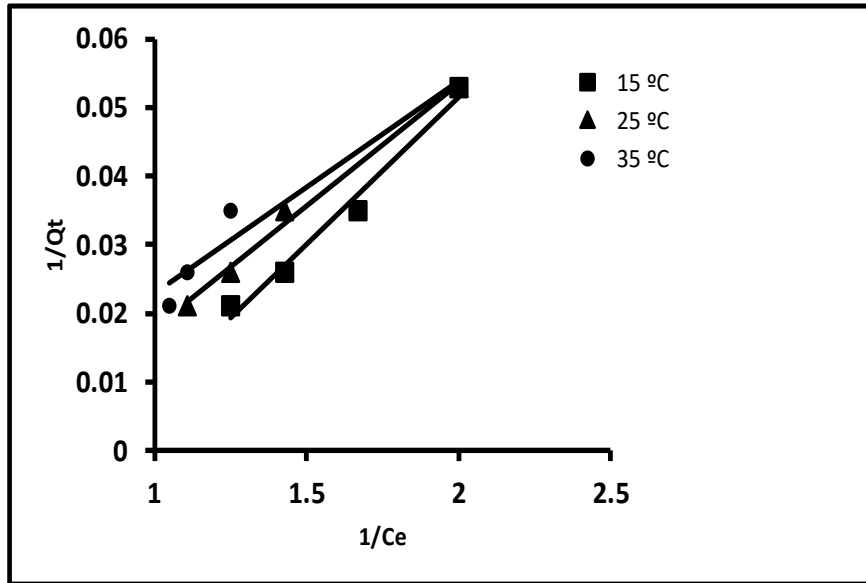


Figure 10. Langmuir plots showing cadmium adsorption.

Freundlich constants, K_f ($\mu\text{g/g}$) and n ($\mu\text{g/L}$) are empirical constants. The exponent is denoted by n , and the relative adsorption potential of the adsorbent is denoted by k_f . (1-10 for a successful adsorption process). The plot of $\log Q_t$ vs $\log C_e$ should be a straight line, and the intercept on the $\log Q_t$ -axis should give the value of $\log k_F$, according to equation 2. (Figure 11). The adsorption strength is determined by the slope (equal to $1/n$). The lower the $1/n$ value, the more heterogeneous the adsorption process. Chemisorption was suggested by $1/n$ values less than unity. Above unity values, on the other hand, indicate cooperative adsorption, which is characterized by intense interactions between adsorbate molecules on the adsorbent's surface. At three temperatures, the values of K_F for Cd(II) ranged from 44.72 to 76.95. (Table 1). K_F values increased, indicating an improvement in sorption capacity on the adsorbent and a boost in sorption efficiency. At different temperatures, the values of n for Cd(II) ranged from 0.899 to 0.995 1.79, indicating that the adsorbent has a desirable sorption. The model's applicability was verified at this point.

3.3.3 Temkin model

This model accounts for the adsorbate's indirect interactions with the adsorbent on the adsorbent surface. Temkin discovered that the heat of adsorption begins to decrease as the amount of coverage increases. It can be determined using the equation below [42].

$$q_e = \left(\frac{RT}{B_T}\right) \ln K_T + \left(\frac{RT}{B_T}\right) \ln C_e \quad (3)$$

The equilibrium binding constant and sorption heat are expressed by the constants K_T and B_T , respectively. As Q_t is plotted against $\log C_e$ (Figure 12), the intercept and slope correspond to the constants K_T and B_T . Table 1 summarizes the B_T and K_T values that were predicted. Cd(II) had B_T values ranged from 0.018 to 0.029 kJ/mol. The modified B_T values revealed a loose interface between the adsorbent and the Cd(II). As a result, it was believed that adsorption occurred via an ion exchange process. The K_T values for Cd(II) ranged from 1.58 to 1.64 L/ μg . These results indicated that Cd(II) was well bound to the adsorbent.

3.3.4 Dubinin-Kaganer-Radushkevich (DKR) model

The key to the Dubinin-Radushkevich model is the presumption of different physical and chemical adsorption rates. This model also explains a Gaussian energy delivery on an irregular surface [43]. The linear forms of the model are Equations 4 and 5.

$$\ln q_e = \ln q_m - \beta \varepsilon^2 \quad (4)$$

$$\varepsilon = RT \ln\left(1 + \frac{1}{C_e}\right)$$

The [saturation ability ($\text{mol}^2 \text{J}^{-2}$)] is used to evaluate the likelihood of sorption through a physical or chemical process. Equation 7 is used to measure [Polanyi potential ($\mu\text{g g}^{-1}$)]. [44].

$$\varepsilon = 1/\sqrt{\beta} \quad (5)$$

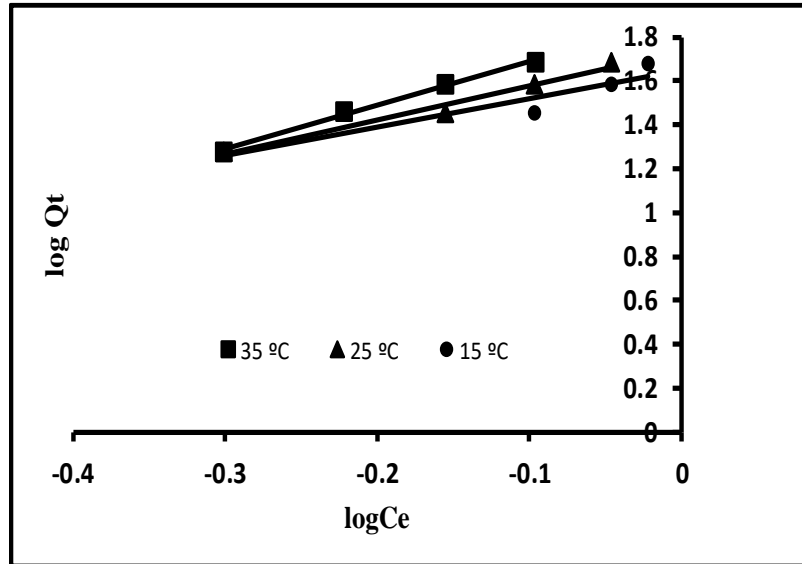


Figure 11. Freundlich plots showing cadmium adsorption.

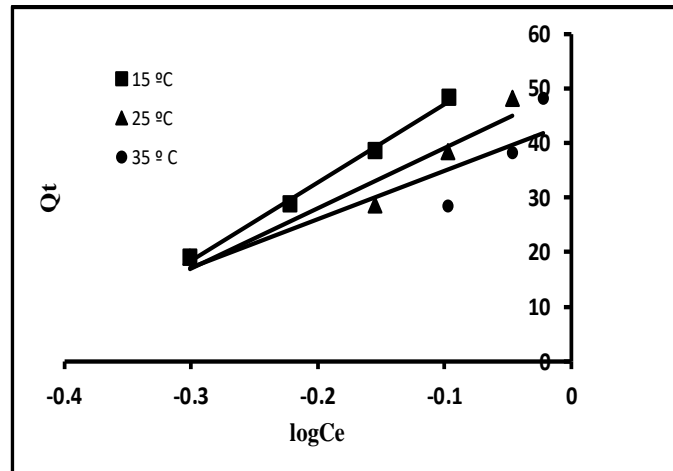


Figure 12. Temkin plots showing cadmium adsorption.

A straight line is formed when $\ln Q_t$ is plotted against E_2 (Figure 13), with intercept and slope corresponding to ϵ and q_e , respectively. Table 1 shows the values of q_e for the average sorption free energy per mole of Cd. These q_e and kJ/mol values ranged from 123.87 to 213.8 $\mu\text{g/g}$ and 0.78 and 0.88 kJ/mol , respectively. Positive and lower values than 8.0 kJ/mol values confirm ion exchange and physical sorption of Cd(II) onto the sorbate. Lower BT values in the Temkin segment confirm these scenarios.

3.4 Thermodynamics study

The thermodynamic process is defined by energy, enthalpy, and entropy. As shown below, Vant Hoff's equation connects the equilibrium constant to the Gibbs free energy transition of adsorption.

$$\Delta G^\circ = -RT \ln K \quad (6)$$

ΔG° , T, R, and K stand for free energy change (kJ/mol), absolute temperature (K), uniform gas constant ($0.008314 \text{ kJ mol}^{-1} \text{ K}^{-1}$), and equilibrium constant, respectively. When K is replaced with X_m , the equation becomes as follows (Langmuir constant).

$$\Delta G^\circ = -RT \ln Q_0 \quad (7)$$

ΔG° values at 15, 25, and 35 °C were determined and found to be -8.0, -9.93, and -12.24 kJmol^{-1} , respectively (Table 2). The negative ΔG° values indicate favorable and spontaneous adsorption. The following equations relate changes in entropy (S°) and enthalpy (H°) to Gibb's free energy of adsorption (ΔG°).

$$\Delta G^\circ = \Delta H^\circ - T\Delta S^\circ \quad (8)$$

The following equation can be substituted for the one above.

$$\ln(Q^\circ) = \Delta S^\circ/R - \Delta H^\circ/RT \quad (9)$$

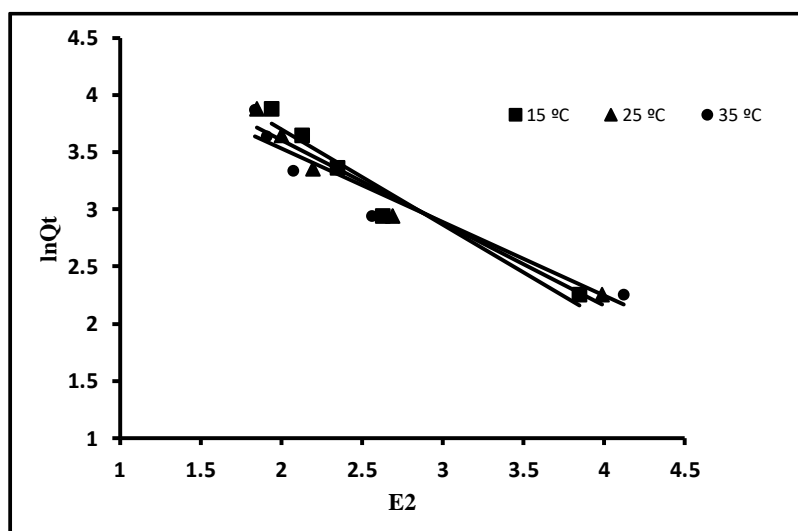


Figure 13. Dubinin-Radushkevich plots showing cadmium adsorption.

A straight line was drawn while plotting $\ln Q_0$ vs $1/T$. (graph not shown). ΔS° was assigned to the intercept, while ΔH° was assigned to the slope. ΔH° and ΔS° had values of -37.79×10^{-2} and -30.96×10^{-3} , respectively. Exothermic adsorption was demonstrated by the negative value of enthalpy shift. The entropy of the adsorption mechanism decreases as the negative value of ΔS° decreases. As a result, Cd(II) adsorption was related to a reduction in Cd mobility freedom (II).

Table 2. Values of cadmium metal ion thermodynamic parameters.

ΔG° (kJ/mol)			ΔH° (kJ/mol)	ΔS° (kJ/mol K)
T= 288 K	T=298 K	T=308 K		
-8.0	-9.93	-12.24	-37.79×10^{-2}	-30.96×10^{-3}

3.5 Modeling of Kinetics

The mechanism of adsorption was determined using kinetic simulation. It was defined by the adsorbent's and adsorbate's physical and chemical characteristics. As a result, adsorption data was used to evaluate different models. The following sub-sections go over each of these.

Table 3. Kinetic parameters for cadmium metal ion.

Kinetic models	Kinetic parameters	Numerical values
Model of pseudo-first-order kinetics	k_1 (min^{-1})	0.421
	Experimental q_e ($\mu\text{g g}^{-1}$)	48.2
	Theoretical q_e ($\mu\text{g g}^{-1}$)	7.94
	R^2	0.978
Model of pseudo-second-order kinetics	k_2 ($\mu\text{g g}^{-1}\text{min}^{-1}$)	0.010
	Experimental q_e ($\mu\text{g g}^{-1}$)	48.20
	Theoretical q_e ($\mu\text{g g}^{-1}$)	49.26
	h ($\mu\text{g g}^{-1}\text{min}^{-1}$)	10.0
	R^2	0.999
Kinetic model of Elovich	α ($\mu\text{g g}^{-1}\text{min}^{-1}$)	30.20
	β ($\mu\text{g g}^{-1}\text{min}^{-1}$)	0.022
	R^2	0.999

3.5.1 Model of pseudo-first-order kinetics.

This is the first mechanism assessment model. The following equation is used to calculate it.

$$dQ_t/dt = k_1 (Q_e - Q_t) \tag{10}$$

To obtain a linearized equation, the boundary conditions of $t = 0$ with $Q_t = 0$ and $t = t$ with $Q_t = Q_t$ were combined with the above equation.

$$\ln(Q_e - Q_t) = \ln_e - k_1 t \tag{11}$$

The solute number (mg/g) adsorbed at equilibrium and the equilibrium rate constant, respectively, are Q_e , Q_t , and k_1 (min⁻¹). Table 3 shows the results of the calculations. At a temperature of 25 °C, plotting $\ln(Q_e - Q_t)$ vs. t yielded the rate constant (Figure 14). With a regression coefficient of 0.978, the pseudo-first-order rate constant was 0.421 (min⁻¹) (R^2). Q_e was 48.2 gg⁻¹ in the experiment and 7.94 gg⁻¹ in the theory, respectively. This model cannot be used since the difference between these values is 83.53 percent.

As a consequence, the pseudo-second-order kinetic model was examined.

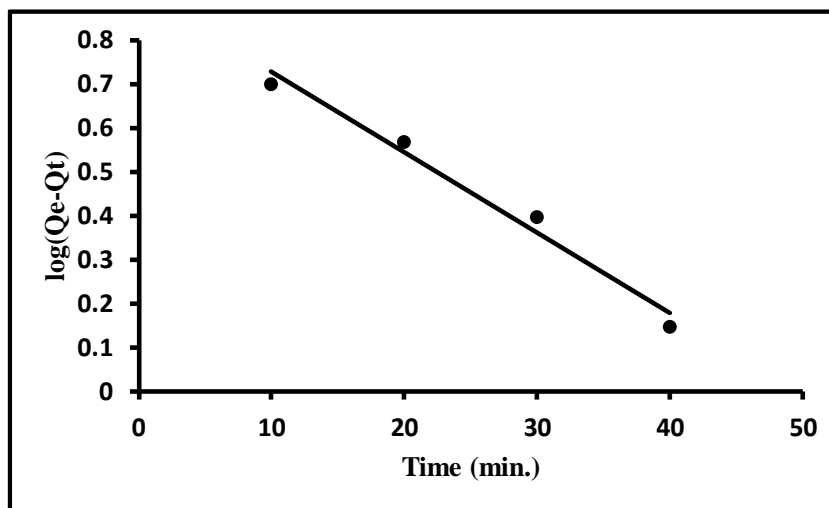


Figure 14. The adsorption elimination kinetic plot in pseudo-first order.

3.5.2 Model of pseudo-second-order kinetics

An attempt was also made to test a pseudo-second-order kinetic model using the experimental results. For the adsorption phenomenon, the following equation describes a pseudo-second-order kinetic model.

$$dQ_t/dt = k_2 (Q_e - Q_t)^2 \tag{12}$$

The definitions of Q_e , Q_t , and t are the same as before. With boundary conditions of $t = 0$ with $Q_t = 0$ and $t = t$ with $Q_t = Q_t$, the above equation was integrated. The equation that results is as follows:

$$t/Q_t = 1/k_2 Q_e^2 + t/Q_e \tag{13}$$

h was substituted for $k_2 Q_e^2$ in the previous equation, yielding the following equation.

$$t/Q_t = 1/h + t/Q_e \tag{14}$$

where h is the adsorption rate constant at the start. It was figured out using a pseudo-second-order plot. As the time reached zero, Q_t/t became $h k_2$ is the pseudo-second-order adsorption rate constant (g/mg/min). The slope and intercept of the plot t/Q_t vs t were used to measure Q_e and k_2 (Figure 15). Table 3 displays the measured parameters. k_2 and h were 0.010 $\mu\text{g g}^{-1}\text{min}^{-1}$ and 10.0 $\mu\text{g g}^{-1}\text{min}^{-1}$, respectively. These results showed a rapid rate of adsorption at first, followed by a sluggish rate as time passed. The regression coefficient (R^2) was 0.999, suggesting that the pseudo-second-order model of the adsorption mechanism was suitable. The experimental and theoretical Q_e values were 48.2 and 49.26 $\mu\text{g/g}$, respectively. It was just a difference of 2.21 %. The validity of the pseudo-second-order kinetic model was confirmed by both of these values. As a result, this model was deemed appropriate.

3.5.3 Elovich's kinetic model

Elovich's kinetic model can be used to quantify adsorption and desorption rates. Elovich's equation was created to represent the kinetics of gaseous chemo-adsorption on solid surfaces. Chien and Clayton [45] changed it after that, taking into account a linear increase in adsorption activation energy with surface coverage. The following equation describes this model.

$$dQ_t/dt = \alpha \exp(-\beta Q_t) \quad (15)$$

The initial adsorption rate is correlated by α ($\mu\text{g/g}\cdot\text{min}$). β ($\mu\text{g/mg}$) is the desorption constant. To integrate the above equation, the boundary conditions $t = 0$ with $Q_t = 0$ and $t = t$ with $Q_t = Q_t$ were used. If it is greater than one, equation 15 becomes the following.

$$Q_t = \beta \ln(\alpha\beta) + \beta \ln t \quad (16)$$

The experimental findings were applied using Elovich's model. In Table 3, the values of α , β and R^2 are listed, 0.022 $\text{mg}\cdot\text{g}^{-1}$ and 0.999, respectively, were 30.20, $\text{mg}\cdot\text{g}^{-1}\cdot\text{min}^{-1}$, 0.022 $\text{mg}\cdot\text{g}^{-1}$, and 0.999. The adsorption rate was found to be higher than the desorption rate. Furthermore, the regression constant's value was close to one, suggesting that the model was suitable.

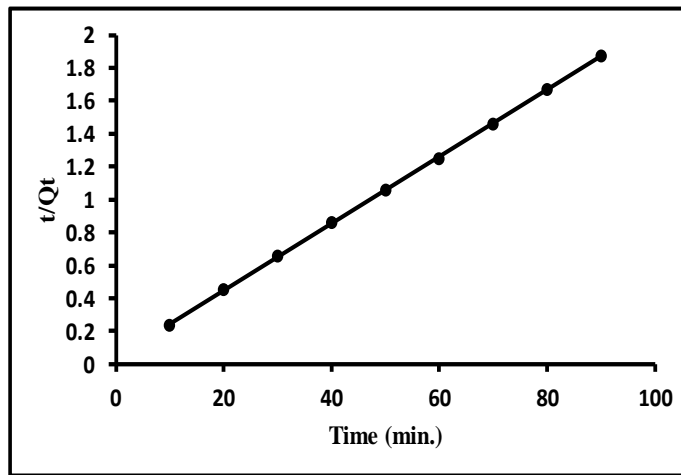


Figure 15. The adsorption removal pseudo-second-order kinetic plot.

3.6 Adsorption mechanism

Film diffusion, pore diffusion, and intra-particle diffusion are the most common pathways for adsorption. The adsorption phenomenon is controlled by the rate-determining process, which is the slowest. Intraparticle and film diffusion models were used to match the experimental results to figure out how Cd(II) sorption on the observed adsorbent works.

3.6.1 Kinetic model of intraparticle diffusion

There are several methods for adsorbate adsorption on adsorbent surfaces, including i) a liquid film is used to transport adsorbate from a bulk solution to an adsorbent surface, ii) adsorbate sorption onto an adsorbent surface, and iii) adsorbate movement within an adsorbent's pores. As a result, either surface adsorption kinetics or transport phenomena (film and intraparticle diffusions) or both control the adsorption process. The second step is very fast and cannot be used to calculate a value. The first and third measures could be used to calculate the rate. As a result, two models were used to investigate these changes. The sum of adsorbed Cd(II) and the square root of contact time may be used to measure the transfer of Cd(II) from solution to adsorption sites. The formula for this can be found below.

$$Q_t = k_{ipt} t^{0.5} \quad (17)$$

Adsorption is caused by intra-particle diffusion (kipd) if a graph of Q_t vs $t^{0.5}$ is a straight line passing through the origin and the slope of the line corresponds to the rate constant. This graph was generated by Q_t vs $t^{0.5}$ (Figure not given). The rate constant was found to be 1.11 $\mu\text{g}\cdot\text{g}^{-1}$. The intercept and regression coefficients were 36.0 and 0.998. (Table 4). The graph did not move through the origin, indicating that the intra-particle diffusion model was not applicable.

3.6.2 Kinetic model of liquid film diffusion

Boyd, *et al.* [46] developed a liquid film diffusion kinetics model. The adsorption mechanism is regulated by the boundary in this model. The liquid film diffusion model is represented by the equation below.

PREPARATION AND CHARACTERIZATION OF IRON OXIDE NANO-ADSORBENT

$$\text{Or } \ln(1-Q/Q_e) = -k_{fd}t \quad (18)$$

$$\ln(1-F) = -k_{fd}t \quad (19)$$

Table 4. Modeling of adsorption mechanism of cadmium metal ion.

Kinetic models	Kinetic parameters	Numerical values
Intraparticle diffusion kinetic model	k_{ipdl} ($\mu\text{g g}^{-1}\text{min}^{-0.5}$)	1.11
	Intercept	36.0
	R^2	0.998
Film diffusion kinetic model	k_{fd} ($\mu\text{g g}^{-1}\text{min}^{-1}$)	0.047
	Intercept	1.5
	R^2	0.981

The fractional attainment of equilibrium is denoted by F (Q_t / Q_e). k_{fd} is the film diffusion rate constant. Adsorption is thought to occur via the film diffusion process if the graph of $\ln(1-F)$ vs t is a straight line with zero intercepts. The film diffusion rate constant, intercept, and regression constant (R^2) were 0.047 ($\mu\text{g g}^{-1}\text{min}^{-1}$), 1.5, and 0.981, respectively (Table 4). The straight line passes through the origin with a minor deviation from the zero intercept (-1.5). This deviation from zero may be attributed to the kinetic experiments' high rate of agitation. Furthermore, the small deviation from zero may be explained by a difference in mass transfer rates between the preliminary and final stages of the adsorption process. Comparable findings have been published in the literature [47-49]. The liquid film diffusion mechanism thus regulated Cd(II) adsorption on the adsorbent. The developed method was applied in real water samples and found to be effective.

4. Conclusion

The yield of nanoparticles obtained was 92%. FT-IR, XRD, SEM, and TEM techniques were used to classify the prepared nanoparticles. The surface of the nanoparticles was rough, with iron nanoparticles ranging in size from 10 to 50 nanometers. In batch mode, the formed nanoparticles were used to extract cadmium metal ions from water. With a 25.0 $\mu\text{g/L}$ concentration, 60 minutes contact time, 7.0 pH, 0.5 g/L dose, and a temperature of 25 °C, the maximum removal of cadmium was 48.2 $\mu\text{g/g}$. The Langmuir, Freundlich, Temkin, and Dubinin-Radushkevich models all predicted the sorption performance. At 15, 25, and 35 °C, the thermodynamic parameters ΔG° , ΔH° and ΔS° were -8.0, -9.93, and -12.24, respectively, with -37.79×10^2 kJ/mol and -30.96×10^{-3} kJ/mol K. The endothermic existence of cadmium metal ion removal was verified by these findings. Along with the liquid film diffusion process, the adsorption adopted pseudo-second-order kinetics. The documented adsorption method is fast, environmentally friendly, and inexpensive, and it can be used to test for the removal of cadmium metal ions in natural water samples.

Conflict of interest

The authors declare no conflict of interest.

Acknowledgment

The authors are thankful to the Department of Chemistry, Taibah University, Al-Madinah Al-Munawwarah, Saudi Arabi for providing all necessary facilities.

References

- Imran, A., Alexandr, E. Burakov, A.V., Melezhib, A.V., Babkin, I.V., Burakova, E.A., Neskomornaya, E.V., Galunin, A.G., Tkachev, D.V. and Kuznetsov, K. Thermodynamics and mechanism of copper and zinc metal ions removal in water on newly synthesized polyhydroquinone/graphene nanocomposite material, *ChemSelect*, 2019, **4**, 12708-12718.
- Imran, A., Kon'kova, T., Than, Z., Htay, Hein Thu Aung., Mishenko, E., Mohammad, N.S., Abdulraheem, S.A., Almalki, A., Alhadhrami, A., Alsubaie, A.M., Alharbi, H.A. Economic and fast electro-flotation extraction of heavy metals from wastewater, *Environ. Technol.*, 43, 4019-4028 (2022).
- Imran, A., Omar, M.L., Alharbi, Z., Alothman, A. and Ahmad, Y.B. Kinetics, thermodynamics and modeling of amido black dye photo-degradation in water using Co/TiO₂ nanoparticles, *Photochem. and Photobiol.*, 2018, **94**, 935-941.
- Imran, A., Tatiana, S., Kuznetsova, A.E., Burakov, I.V., Burakova, T.V., Pasko, T.P., Dyachkova, E.S., Mkrtychyan, A.V., Babkin, A.G., Tkachev, H.M., Albishri, W.H., Alshitari, A.M.H and Alharbi, A. Polyaniline modified CNTs

- and graphene nanocomposite for removal of lead and zinc metal ions: Kinetics, thermodynamics and desorption studies, *Molecules*, *27*, 5623 (2022).
5. Imran, A., Gunel, T., Imanova, H.M., Albishri, W.H., Alshitari, A.M.H., Marcello, L., Mohammad, N.S. and Ahmed, M.H. An ionic-liquid-imprinted nanocomposite adsorbent: simulation, kinetics and thermodynamic studies of triclosan endocrine disturbing water contaminant removal, *Molecules*, *7*, 5358 (2022).
 6. Imran, A., Omar, M.L., Alharbi, Z.A., ALOthman, A.A., Amal, M. Al-Mohaimeed. Preparation of a carboxymethylcellulose-iron composite for the uptake of atorvastatin in water, *Int. J. Biol. Macromol.* 2019, **132**, 244-253.
 7. Nora, H. Al-Shaalan, Imran, A., Zeid, A. ALOthman., Lamy, H. Al-Wahaibi and Hadeel, A. High-performance removal and simulation studies of diuron pesticide in the water on MWCNTs, *J. Mol. Liq.*, *289*, 111039 (2019).
 8. Imran, A., Neskornaya, E.A., Melezhik, A.V., Babkin, A.V., Kulnitskiy, B.A., Burakov, A.E., Burakova, I.V., Tkachev, A.G., Abdulraheem, S.A., Almalki, A. Alsubaie. Magnetically active nanocomposite aerogels: preparation, characterization and application for water treatment, *J. Pour. Mat.*, 2022, **29**, 545-557.
 9. Hu, Jun, Donglin Zhao, and Xiangke Wang. Removal of Pb (II) and Cu (II) from aqueous solution using multiwalled carbon nanotubes/iron oxide magnetic composites. *Water Sci. Technol.* 2006, **63(5)**, 917-923.
 10. Srivastava, S.K., Bhattacharjee, G., Tyagi, R., Pant, N. and Pal, N. Studies on the removal of some toxic metal ions from aqueous solutions and industrial waste. Part I (Removal of lead and cadmium by hydrous iron and aluminum oxide). *Environ. Technol.* 1988, **9(10)**, 1173-1185.
 11. Ozay, O., Ekici, O., Baran, Y., Aktas, N. and Sahiner, N. Removal of toxic metal ions with magnetic hydrogels. *Water Res.* 2009, **43(17)**, 4403-4411.
 12. Jamil, M., Muhammad S.Z. and Muhammad, Q. Contamination of agro-ecosystem and human health hazards from wastewater used for irrigation. *J. Chem. Soc. Pak.* 2010, **32(3)**, 370-378.
 13. Khan, S., Cao, Q., Zheng, Y.M., Huang, Y.Z. and Zhu, Y.G. Health risks of heavy metals in contaminated soils and food crops irrigated with wastewater in Beijing, China. *Environ. Pollut.* 2008, **152(3)**, 686-692.
 14. Singh, A., Sharma, R.K., Agrawal, M. and Marshall, F.M. Health risk assessment of heavy metals via dietary intake of foodstuffs from the wastewater irrigated site of a dry tropical area of India. *Food Chem. Toxicol.* 2010, **48(2)**, 611-619.
 15. Peng, S.-H., Wang, W.-X., Li, X. and Yen, Y.-F. Metal partitioning in river sediments measured by sequential extraction and biomimetic approaches. *Chemosphere.* 2004, **57(8)**, 839-851.
 16. Kuppasamy, P., Yusoff, M.M., Maniam, G.P. and Govindan, N. (2016). Biosynthesis of metallic nanoparticles using plant derivatives and their new avenues in pharmacological applications-An updated report. *Saudi Pharm J.* 2016, **24(4)**, 473-484.
 17. Zhang, Wei-xian. Nanoscale iron particles for environmental remediation: an overview. *J Nanopart Res.* 2003, **5(3)**, 323-332.
 18. Deliyanni, E.A. and Matis, K.A. Sorption of Cd ions onto akaganeite-type nanocrystals. *Sep. Purif. Technol.* 2005, **45(2)**, 96-102.
 19. Niu, S.-f., Liu, Y., Xin-hua, Xu, X.-h. and Lou, Z.H. Removal of hexavalent chromium from aqueous solution by iron nanoparticles. *Journal of Zhejiang University-Science B.* 2005, **6(10)**, 1022-1027.
 20. Lazaridis, N.K., Bakoyannakis, D.N. and Deliyanni, E.A. Chromium (VI) sorptive removal from aqueous solutions by nanocrystalline akaganeite. *Chemosphere.* 2005, **58(1)**, 65-73.
 21. Hu, J., Guohua, C. and Irene, MC, Lo. Removal and recovery of Cr (VI) from wastewater by maghemite nanoparticles. *Water Res.* 2005, **39(18)**, 4528-4536.
 22. Di, Z.C., Ding, J., Peng, X.J., Li, Y.H., Luan, Z.K. and Liang, J. Chromium adsorption by aligned carbon nanotubes supported ceria nanoparticles. *Chemosphere.* 2006, **62(5)**, 861-865.
 23. Bing, G., Zhaohui, J., Tielong, L. and Xinhua, Q. Kinetics of hexavalent chromium removal from water by chitosan-Fe₀ nanoparticles. *Chemosphere.* 2009, **75(6)**, 825-830.
 24. Agarwal, H., Venkat, K.S. and Rajeshkumar, S. A review on green synthesis of zinc oxide nanoparticles—An eco-friendly approach. *Resource-Efficient Technologies.* 2017, **3(4)**, 406-413.
 25. Mohammadlou, M., Maghsoudi, H. and Jafarizadeh-Malmiri, H. A review on green silver nanoparticles based on plants: Synthesis, potential applications and eco-friendly approach. *International Food Research Journal.* 2016; **23(2)**.
 26. Imran, A., Mohd, S., Eva, C., López, R., Khattab, A., Hassan, M. and Albishri, W.H. Advances in graphene-based materials for the treatment of water, *Arabian Journal of Geosciences.* *15*, 521(2022).
 27. Ehrampoush, M.H., Miria, M., Salmani, M.H. and Mahvi, A.H. Cadmium removal from aqueous solution by green synthesis iron oxide nanoparticles with tangerine peel extract. *Journal of Environmental Health Science and Engineering.* 2015, **13(1)**, 1-7.
 28. Abdullah, J.A.A., Eddine, L.S., Abderrhmane, B., Alonso-González, M., Guerrero, A. and Romero, A. Green synthesis and characterization of iron oxide nanoparticles by pheonix dactylifera leaf extract and evaluation of their antioxidant activity. *Sustain. Chem. Pharm.* 2020, **17**, 100280.
 29. Laid, T.M., Abdelhamid, K., Eddine, L.S. and Abderrhmane, B. Optimizing the biosynthesis parameters of iron oxide nanoparticles using central composite design. *Journal of Molecular Structure.* 2021, 1229, 129497.

PREPARATION AND CHARACTERIZATION OF IRON OXIDE NANO-ADSORBENT

30. Ehrampoush, M.H., Miria, M., Salmani, M.H. and Mahvi, A.H. Cadmium removal from aqueous solution by green synthesis iron oxide nanoparticles with tangerine peel extract. *Journal of Environmental Health Science and Engineering*, 2015, **13**(1), 1-7.
31. Zhu, F., Ma, S., Liu, T. and Deng, X. Green synthesis of nano zero-valent iron/Cu by green tea to remove hexavalent chromium from groundwater. *J. Clean.* 2018, **174**, 184-190.
32. Imran, A., Tatiana, K., Elena, L., Ekaterina, S., Zeid, A., ALOthman, A., Taghrid, S., Alomar, M. and Ataul, I. Preparation and characterization of SnO₂-CeO₂ nanocomposites: Sorption, modeling and kinetics for azorubine dye removal in water, *Journal of Molecular Liquid.* 346, 117119 (2022).
33. Zeid, A., ALOthman, A., AlMasoud, N., Mbianda, X.Y. and Imran A. Synthesis and characterization of γ -cyclodextrin-graphene oxide nanocomposite: Sorption, kinetics, thermodynamics and simulation studies of tetracycline and chlortetracycline antibiotics removal in water, *Journal of Molecular Liquid.* 345, 116993 (2022).
34. Imran, A., Zakharchenko, E.A., Myasoedova, G.V., Molochnikova, N.P., Rodionova, A.A., Baulin, V.E., Burakov, A.E., Burakova, I.V., Babkin, A.V., Neskromnaya, E.A., Melezhik, A.V., Tkachev, A.G., Mohamed A.H., Adel El-Marghany, M.S. and Ayman, G. Preparation and characterization of oxidized graphene for actinides and rare earth elements removal in nitric acid solutions from nuclear wastes, *Journal of Molecular Liquid.*, 335, 116260 (2021).
35. Imran, A., Tatiana, K., Vitalii, K., Anton, R., Stefan, P., Mbianda. X.Y., Mohamed, A.H. and AlMasoud, N. Preparation and characterization of nano-structured modified montmorillonite for dioxidine antibacterial drug removal in water, *Journal of Molecular Liquid.* 331, 115770 (2021).
36. Imran, A., Alexander, V., Babkin, I.V., Burakova, A.E., Burakov, E.A., Neskromnaya, A.G., Tkachev, S.P., AlMasoud, N., Taghrid, S. Alomar. Fast removal of samarium ions in water on highly efficient nanocomposite-based graphene oxide modified with polyhydroquinone: Isotherms, kinetics, thermodynamics and desorption, *J. Mol. Liq.*, 329, 115584 (2021).
37. Zeid, A., ALOthman, A., Yacine, B., Osamah, M., Alduhaish, K., Rathinam, S.P. and Imran, A. Synthesis, characterization, kinetics and modeling studies of new generation pollutant ketoprofen removal in water using copper nanoparticles, *Journal of Molecular Liquid.* 323, 115075 (2021).
38. Zeid, A., ALOthman, Ahmad., Yacine, Badjah., Omar, M.L., Alharbi. and Imran, A. Copper carboxymethyl cellulose nanoparticles for efficient removal of tetracycline antibiotics in water, *Environmental Science and Pollution Research.* 2020, **27**, 42960-42968.
39. Imran, A., Shirin, A., Yousef, P., Ali, A., Yousef, R., Abolfazl, F., Asghar, H. and Mehdi, F. Green preparation of activated carbon from pomegranate peel coated with zero-valent iron nanoparticles (nZVI) and isotherm and kinetic studies of amoxicillin removal in water, *Environmental Science and Pollution Research.* 2020, **27**, 36732-36743.
40. Panwar, V., Kumar, P., Bansal, A., Ray, S.S. and Jain, S. Gylated magnetic nanoparticles (PEG@ Fe₃O₄) as cost effective alternative for oxidative cyanation of tertiary amines via CH activation. *Applied Catalysis A: General.* 2015, **498**, 25-31.
41. Langmuir, Irving. The adsorption of gases on plane surfaces of glass, mica and platinum. *Journal of American Chemical Society.* 1918, **40**(9), 1361-1403.
42. Temkin, M.I. Kinetics of ammonia synthesis on promoted iron catalysts. *Acta Physiochim. URSS.* 1940, **12**, 327-356.
43. Dabrowski, A. Adsorption-from theory to practice, *Adv. Colloid Interface. Sci.* 2001, **93**, 135-224.
44. Hobson, John P. Physical adsorption isotherms extending from ultrahigh vacuum to vapor pressure. *Journal of Physical Chemistry. C.* 1969, **73**(8), 2720-2727.
45. Chien, S.H. and W.R. Clayton. Application of Elovich equation to the kinetics of phosphate release and sorption in soils 1. *Soil Science Society of American Journal.* 1980, **44**(2), 265-268.
46. Boyd, G.E., Adamson, A.W. and Myers, L.S. The Exchange Adsorption of Ions from Aqueous Solutions by Organic Zeolites. II. Kinetics, *Journal of American Chemical Society.* 1947, **69**, 2836-2848.
47. Zeid, A., ALOthman, A., Yacine, B., Omar, M.L. Alharbi. and Imran, A. Synthesis of chitosan composite iron nanoparticles for removal of diclofenac sodium drug residue in water, *International Journal of Biological Sciences. Macromol.*, 2020, **159**, 870-876.
48. Imran, A., Omar, M.L. Alharbi., Zeid, A., ALOthman, A., Amal, Mohammed., Al-Mohaimed., Abdulrahman, Alwarthan. Modeling of fenuron pesticide adsorption on CNTs for mechanistic insight and removal in water, *Environ. Res.*, 2019, **170**, 389-397.
49. Zeid, A., ALOthman, A., Yacine, B. and Imran, A. Facile synthesis and characterization of multi-walled carbon nanotubes for fast and effective removal of 4-tert-octylphenol endocrine disruptor in water, *Journal of Molecular Liquid.* 2019, **275**, 41-48.

Received 25 May 2023

Accepted 25 June 2023

Analysis of Fractional Linear Multi-Step Methods of Order Four from Super-convergence

Khadija Al-Hassani and H.M. Nasir*

Department of Mathematics, Sultan Qaboos University, P.O.Box: 36, Al Khod, Muscat, Sultanate of Oman. *Email: nasirh@squ.edu.om

ABSTRACT: We analyzed two implicit fractional linear multi-step methods of order four for solving fractional initial value problems. The methods are derived from the Grünwald-Letnikov approximation of fractional derivative at a non-integer shift point with super-convergence. The weight coefficients of the methods are computed from fundamental Grünwald weights, making them computationally efficient when compared with other known methods of order four. We also show that the stability regions are larger than those of the fractional Adams-Moulton and fractional backward difference formula methods. We present numerical results and illustrations to verify that the theoretical results obtained are indeed satisfied.

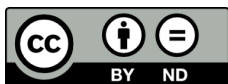
Keywords: Fractional initial value problem; Generating function; Super-convergence; Grünwald-Letnikov approximation; Fractional linear multi-step method; stability region.

تحليل طرق كسرية خطية متعددة الخطوات ذات الرتبة الرابعة من التقارب الفائق

خديجة الحسني وحنيفة محمد ناصر

المخلص: في هذا البحث نقوم بتحليل طريقتين ضمنييتين كسريتين خطيتين ومتعدديتي الخطوات ذات الرتبة الرابعة لحل مسائل القيم الأولية الكسرية، تم اشتقاق الطرق من تقريب جرنوالد للمشتقة الكسرية عند نقطة تحول عدد غير صحيح باستخدام التقارب الفائق، حيث يتم حساب معاملات الوزن للطرق من أوزان جرنوالد لكتوف الأساسية مما يجعلها فعالة من الناحية الحسابية عند مقارنتها بالطرق الأخرى المعروفة من الترتيب الرابع، كما وضحنا أيضا أن مناطق الاستقرار لهذه الطرق أكبر من مناطق أدمز مولتن الكسرية وكذلك طرق صيغة الفرق العكسي الجزئي، تم أيضا تقديم النتائج العددية والرسوم التوضيحية للتحقق من أن النتائج النظرية التي تم الحصول عليها مرضية بالفعل.

الكلمات المفتاحية: مسائل القيم الأولية الكسرية؛ الدالة المولدة؛ التقارب الفائق؛ تقريب جرنوالد لكتوف؛ طرق أدمز مولتن الكسرية؛ مناطق الاستقرار.



1. Introduction

Consider the fractional initial value problem (FIVP)

$$D_{t_0}^{\beta} y(t) = f(t, y(t)), \quad t \geq t_0, \quad 0 < \beta \leq 1, \quad (1)$$

$$y(t_0) = y_0, \quad (2)$$

where $D_{t_0}^{\beta}$ is the left Caputo fractional derivative operator defined in Section 2, $f(t, y)$ is a function satisfying the Lipschitz condition in the second argument y which guarantees a unique solution to the problem [1,2]. When $\beta = 1$, problem (1) with (2) becomes the classical initial value problem (IVP) with first order derivative.

Many numerical schemes for approximately solving the FIVP (1) have been proposed in the recent past. The numerical methods referred to as fractional linear multi-step methods (FLMMs) are of particular interest.

The simplest and most highly investigated FLMM is the fractional Euler method (also known as the Grünwald-Letnikov method) obtained by approximating the fractional derivative $D_{t_0}^\beta y(t)$ in (1), after some modifications, by the Grünwald-Letnikov (GL) approximation (See Section 2).

Converting the FIVP (1) in the form of Volterra integral equation (VIE) of the second kind, Lubich [3–5] proposed a class of higher-order FLMMs for the VIE as convolution quadrature rules. The quadrature coefficients of the FLMMs are obtained from the fractional order power of some rational polynomials from the linear multistep methods (LMMs) for classical IVPs. Moreover, Lubich [5], suggested a set of implicit fractional backward difference formula (FBDF) methods as a subclass of these FLMMs.

Galeone and Garrappa [6] investigated another subclass of implicit FLMMs and called them fractional Adams-Moulton methods (FAM), also suggested by Lubich in [5]. They also constructed in [7,8] some explicit FLMMs of this subclass and called fractional Adams-Bashforth methods (FAB). Another set of explicit FLMMs was constructed by Bonab and Javidi [9].

Aceto [10] constructed another subclass of FLMMs by approximating Lubich's generating functions of the FBDFs by Pade approximations. However, in this class, the orders of the FLMMs are reduced compared to the source FLMMs.

The present authors proposed two new implicit FLMMs of order 4 with preliminary properties and tests presented in [11]. The methods use the super convergence of the GL approximation. Earlier, the authors used super convergence to derive an FLMM of order 2 in [12].

This paper analyzes the two implicit FLMMs of order 4 presented in [11]. As FLMMs of orders higher than two are not A-stable according to Dahlquist's second barrier for FIVPs [13], we analyze the stability of the methods through $A(\pi/2)$ -stability and unconditional stability. We also show that the methods are better in stability than the FAM4 of order 4 and one of the methods is better than FBDF4 of order 4.

The computational costs of these methods have also been compared with other order 4 methods and show that the new FLMMs are computationally competitive with the FAM and simpler than that the FBDF4.

This paper is organized as follows. Section 2 gathers the necessary definitions, theories, and results on fractional calculus and numerical solutions of FIVPs. In Section 3, we give the main results by constructing the new FLMMs along with an algorithm to compute approximate solutions using these methods. In Section 4, we analyze the stability of the methods. Section 5 compares our methods with other known methods of order 4. In Section 6, we draw conclusions.

2. Preliminaries

The fundamental definitions of fractional derivatives in fractional calculus are typically presented as follows:

Definition 2.1 Let $y(t)$ be a function defined in the interval domain $[t_0, T]$ and is sufficiently smooth to hold the following:

1. When $y \in L_1([t_0, T])$, the Riemann-Liouville (RL) fractional integral of order $\beta > 0$ of $y(t)$ is defined as

$$J_{t_0}^\beta y(t) = \frac{1}{\Gamma(\beta)} \int_{t_0}^t (t-s)^{\beta-1} y(s) ds. \quad (3)$$

2. The RL fractional derivative of order $\beta > 0$ is defined by

$$\tilde{D}_{t_0}^\beta y(t) = \frac{1}{\Gamma(m-\beta)} \frac{d^m}{dt^m} \int_{t_0}^t (t-s)^{m-\beta-1} y(s) ds, \quad m-1 \leq \beta < m. \quad (4)$$

where $m = \lceil \beta \rceil$ is the integer ceiling of β , and $\Gamma(\cdot)$ denotes Euler's gamma function. $D^m = \frac{d^m}{dt^m}$ is the m -th order differential operator.

3. The Caputo derivative of order $\beta > 0$ is defined by

$$D_{t_0}^\beta y(t) = \frac{1}{\Gamma(m-\beta)} \int_{t_0}^t (t-s)^{m-\beta-1} y^{(m)}(s) ds, \quad m-1 \leq \beta < m. \quad (5)$$

4. The Grünwald-Letnikov definition of fractional derivative is given by

$$\tilde{D}_{t_0}^\beta y(t) = \lim_{\tau \rightarrow 0} \frac{1}{\tau^\beta} \sum_{k=0}^{\infty} g_k^{(\beta)} y(t-k\tau), \quad (6)$$

where $g_k^{(\beta)} = (-1)^k \frac{\Gamma(\beta+1)}{\Gamma(\beta-k+1)k!}$ are called the *Grünwald weights*.

5. A shifted form of GL fractional derivative is also available [14]:

$$\tilde{D}_{t_0, r}^\beta y(t) = \lim_{\tau \rightarrow 0} \frac{1}{\tau^\beta} \sum_{k=0}^{\infty} g_k^{(\beta)} y(t-(k-r)\tau), \quad (7)$$

where r is the shift which is often taken to be an integer, but any real shift is valid.

Remark: The fractional derivatives given above are called the *left* fractional derivatives as there are also their *right* counterparts. For details see [15,16] and the references therein.

The fractional integrals and derivatives are related such that the RL and Caputo derivatives are two left inverses of the RL integral [1]:

$$\widehat{D}_{t_0}^\beta J_{t_0}^\beta y(t) = D_{t_0}^\beta J_{t_0}^\beta y(t) = y(t). \quad (8)$$

However, the two fractional derivatives in (4) and (5) are related by

$$D_{t_0}^\beta y(t) = \widehat{D}_{t_0}^\beta [y(t) - T_{m-1}(t - t_0)], \quad y \in C^{m-1}[t_0, T], \quad y^{(m)} \in L^1[t_0, T],$$

where

$$T_{m-1}(t) = \sum_{k=0}^{m-1} \frac{t^k}{k!} y^{(k)}(t_0).$$

Hence, the RL and Caputo fractional derivatives are equal under the homogeneous initial conditions $y^{(k)}(t_0) = 0, k = 0, 1, \dots, m-1$ [1, 2]. The GL fractional derivative in (6) and its shifted counterpart in (7) are also equivalent to the Caputo derivative under homogeneous conditions and are often utilized as tools for numerical approximations of fractional derivatives.

2.1 Approximation of fractional integrals and derivatives

To approximate the fractional integrals and derivatives, the involving domain $[t_0, T]$ is discretized into a computational domain with uniformly spaced discrete points $t_k = t_0 + k\tau, k = 0, 1, \dots, N$ with a fixed step size $\tau = (T - t_0)/N$. The fractional integral can be approximated by using a quadrature rule as the sum of weighted function values at the discrete points of the involved integrating domain. Common quadrature rules used in this sense are the rectangular and trapezoid rules [17-19]. Lubich [5] introduced a convolution quadrature approximation formula for the fractional integral

$$J_\tau^\beta y(t) = \tau^\beta \sum_{k=0}^n \omega_k y(t - k\tau),$$

where the weights ω_k are obtained from the power series expansion of the generating function $\omega(\xi) = \left(\frac{\sigma(1/\xi)}{\rho(1/\xi)}\right)^\beta$ with (ρ, σ) being the pair of generating polynomials of the LMM for classical IVPs [1]. The order of consistency for the FLMM is the same as that of the underlying LMM. As for the approximation of fractional derivatives, the fundamental approximation for the RL fractional derivative is obtained from the GL (or generally the shifted GL) definition by simply dropping the limit for a fixed step size τ . This gives an order one approximation $\delta_{\tau,r}^\beta y(t)$ with an integer shift r [5,21].

$$\delta_{\tau,r}^\beta y(t) = \frac{1}{\tau^\beta} \sum_{k=0}^\infty g_k^{(\beta)} y(t - (k-r)\tau) = D_{t_0}^\beta y(t) + O(\tau),$$

where the initial value y_0 has been subtracted from $y(t)$ to satisfy the homogeneous initial condition so that the different definitions coincide.

However, for the particular non-integer shift $r = \beta/2$, the above Grünwald approximation gives order 2 displaying super convergence [22].

$$\delta_{\tau,\beta/2}^\beta y(t) = D_{t_0}^\beta y(t) + O(\tau^2).$$

Analogous to the convolution quadrature approximation for fractional integral, fractional derivatives can also be approximated by convolution quadrature formula in a similar form

$$\Omega_{\tau,r}^\beta y(t) = \tau^{-\beta} \sum_{k=0}^\infty w_k y(t - k\tau),$$

where w_k are the coefficients of a generating function $W(\xi)$.

The order of consistency of an FLMM can be obtained from its generating function through the following theorem.

Theorem 2.2 [14,23,24] *Let $W(\xi)$ be the generating function of an approximation in the shifted form of the fractional derivative $D_{t_0}^\beta y(t)$,*

$$\Omega_{\tau,r}^\beta y(t) = \frac{1}{\tau^\beta} \sum_{k=0}^\infty w_k y(t - (k-r)\tau),$$

where $y(t)$ is sufficiently smooth. The order of the shifted approximation with shift r is m if and only if

$$G(x) = \frac{1}{x^\beta} W(e^{-x}) e^{rs} = 1 + O(x^m). \quad (9)$$

Moreover, we have

$$\Omega_{\tau,r}^\beta y(t) = D_{t_0}^\beta y(t) + \tau^m a_p D_{t_0}^{\beta+m} y(t) + \tau^{m+1} a_{p+1} D_{t_0}^{\beta+m+1} y(t) + \dots, \quad (10)$$

where $\mathbf{a}_k \equiv \mathbf{a}_k(\beta, r)$ are the coefficients of the series expansion of $\mathbf{G}(x)$:

$$\mathbf{G}(x) = \mathbf{1} + \sum_{k=p}^\infty \mathbf{a}_k x^k.$$

2.2 FLMM scheme

The general form of an FLMM scheme for the FIVP in (1) and (2) is given by

$$\sum_{k=0}^n p_k y_{n-k} = \tau^\beta \sum_{k=0}^n q_k f_{n-k}, \quad (11)$$

where p_k and q_k are the coefficients of the generating functions

$$p(\xi) = \sum_{k=0}^{\infty} p_k \xi^k \quad \text{and} \quad q(\xi) = \sum_{k=0}^n \sigma_k \xi^k.$$

and y_k and f_k denote

$$y_k \approx y(t_k) \quad \text{and} \quad f_k = f(t_k, y_k). \quad (12)$$

In numerical computations using the FLMMs of order more than one, the intended order m is achieved only for a certain class of functions, specifically for functions of the form $y(t) = t^\alpha g(t)$, $\alpha \geq m$, with $g(t)$ analytic [5]. However, for $\alpha < m$, the order is reduced to $O(h^\alpha)$ only. To remedy this order reduction, an additional sum is introduced in (11) to have the approximation scheme

$$\sum_{k=0}^s w_{n,k} y_k + \sum_{k=0}^n w_k^{(\beta)} y_{n-k} = \tau^\beta \sum_{k=0}^n \sigma_k f_{n-k}. \quad (13)$$

The starting weights $w_{n,k}$ in (13) are to compensate for the reduced order of convergence.

However, computing the starting weights poses many difficulties in practice. Since the starting weights do not affect the stability or convergence of the solution, we do not include them in the computation and analysis in the subsequent sections. For some developments on the starting weights, we refer to [20, 26, 27].

2.3 Stability

For the analysis of the stability of an FLMM, consider the linear test problem

$$D_{t_0}^\beta y(t) = \lambda y(t), \quad y(t_0) = y_0, \quad \lambda \in \mathbb{C}, \quad 0 < \beta < 1 \quad (14)$$

for which the analytical solution is $y(t) = E_\beta(\lambda t^\beta) y_0$, where $E_\beta(t) = \sum_{k=0}^{\infty} \frac{t^k}{\Gamma(\beta k + 1)}$ is the Mittag-Leffler function. For analytical stability, the solution $y(t)$ of the test problem (14) is stable in the sense that the series of $y(t)$ converges in the region

$$\Sigma_\beta = \{\xi \in \mathbb{C} : |\arg(\xi)| > \beta\pi/2\}.$$

The unstable region is then the infinite wedge with angle $\beta\pi$. (See Figure 1).

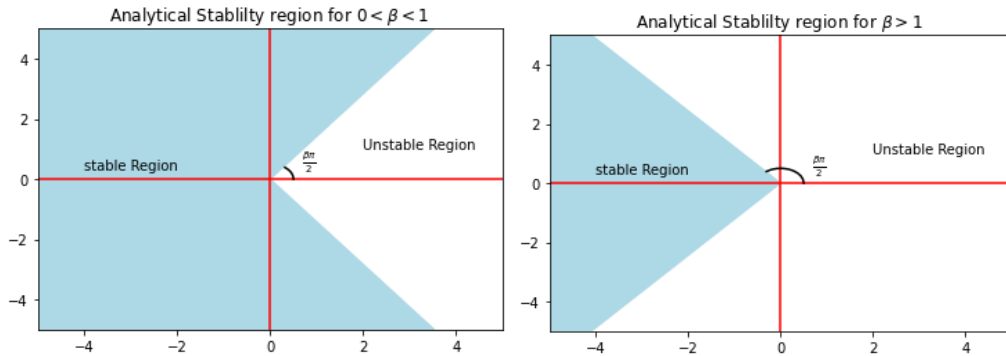


Figure 1. Analytical Stability regions.

For the numerical stability of FLMM, we have the following criteria:

Definition 2.3 Let S be the numerical stability region of an FLMM. For an angle α , measured from the negative real axis, define the wedge $S(\alpha) = \{z : |\arg(z) - \pi| \leq \alpha\}$. The FLMM is said to be

1. $A(\alpha)$ -stable if $S(\alpha) \subseteq S$
2. A -stable if it is $A(\pi - \beta\pi/2)$ stable. That is, $\Sigma_\beta \subseteq S$.
3. $A(\pi/2)$ -stable when the entire left half of the complex plane is included in S .
4. Unconditionally stable if it is $A(0)$ -stable. That is, the negative real line is included in S .

The stability region of an FLMM is also characterized by its generating function:

Theorem 2.4 [5] The stability region of an FLMM with generating function $w(\xi)$ is given by

$$S = \{W(\xi) : |\xi| > 1\} = \mathbb{C} \setminus S^c,$$

where $S^c = \{W(\xi): |\xi| \leq 1\}$ is the unstable region.

3. New FLMMs of order 4

In this section, we give the construction of these methods. Denote by $C^n(\mathbb{R})$ the class of functions having continuous n^{th} derivatives.

3.1 Necessary Approximations

We need the following preparations.

Lemma 3.1 *Let $y(t) \in C^4(\mathbb{R})$ and $h > 0$. For $\mu \in \mathbb{R}$, $y(t + \mu h)$ can be interpolated with order 4 as*

$$y(t + \mu h) = p_0 y(t) + p_1 y(t - h) + p_2 y(t - 2h) + p_3 y(t - 3h) + O(h^4), \quad (15)$$

where $p_i, i = 0, 1, 2, 3$ are the coefficients of the Lagrange interpolation polynomial approximation for a function of μ at the points $\mu_i = 0, -1, -2, -3$ given by

$$p_0 = \frac{(\mu+1)(\mu+2)(\mu+3)}{6}, \quad p_1 = -\frac{\mu(\mu+2)(\mu+3)}{2}, \quad p_2 = \frac{\mu(\mu+1)(\mu+3)}{2}, \quad p_3 = -\frac{\mu(\mu+1)(\mu+2)}{6}. \quad (16)$$

Proof. Consider $y(t + \mu h)$ as a function of μh interpolated at points $\mu_i h = 0, -h, -2h$ and $-3h$. Then the coefficients p_i are the Lagrange interpolation basis functions $L_i(\mu h) = \prod_{j=0, j \neq i}^3 \frac{\mu h - \mu_j h}{\mu_i h - \mu_j h}$ which reduce to $p_i, i = 0, 1, 2, 3$. The error of the interpolation is given by $E = \frac{1}{4!} \prod_{j=0}^3 (\mu h - jh) y^{(4)}(t + \xi h) = O(h^4)$, where $\xi \in (-3, 0)$. ■

Lemma 3.2 *The second derivative of a function $f(x)$ can be approximated by the backward difference forms of order 2 as*

$$\frac{d^2}{dx^2} f(x) = \frac{1}{h^2} (2f(x) - 5f(x - h) + 4f(x - 2h) - f(x - 3h)) + O(h^2) \quad (17)$$

$$\frac{d^2}{dx^2} f(x) = \frac{1}{h^2} (3f(x - h) - 8f(x - 2h) + 7f(x - 3h) - 2f(x - 4h)) + O(h^2). \quad (18)$$

Proof. Taylor series expansions. ■

Lemma 3.3 *The shifted GL approximation (7) with shift $r = \frac{\beta}{2}$ has order 2 super convergence in (10) with the coefficients of the odd order terms $a_{2k+1} = 0$ for $k = 0, 1, 2, \dots$. Moreover, we have $a_2 = \frac{\beta}{24}$.*

Proof. The generating function of the GL approximations in (6) and (7) is $W(z) = (1 - z)^\beta$.

The function $G(x) = \frac{1}{x^\beta} (1 - e^{-x})^\beta e^{\frac{\beta}{2}x}$ in (9) is an even function since

$$G(-x) = \frac{1}{(-x)^\beta} (1 - e^x)^\beta e^{-\frac{\beta}{2}x} = \frac{1}{(-x)^\beta} (-1)^\beta e^{\beta x} (1 - e^{-x})^\beta e^{-\beta x} e^{\frac{\beta}{2}x} = G(x).$$

Hence, the odd order terms of the series expansion of $G(x)$ are zero. Moreover, expanding for the first few terms reveals $a_0 = 1, a_2 = \frac{\beta}{24}$. ■

From Theorem 2.2 again, we have from (10),

$$\delta_{\tau, \frac{\beta}{2}}^\beta y(t_n) = \frac{1}{\tau^\beta} \sum_{k=0}^{\infty} g_k^{(\beta)} y\left(t_n - \left(k - \frac{\beta}{2}\right)\tau\right) = D_{t_0}^\beta y(t_n) + a_2 \tau^2 D_{t_0}^{\beta+2} y(t_n) + O(\tau^4). \quad (19)$$

Writing $D_{t_0}^{\beta+2} = D^2 D_{t_0}^\beta$, we replace the fractional derivative $D_{t_0}^\beta y(t_n)$ in (19) by $f(t_n, y(t_n))$:

$$\sum_{k=0}^{\infty} g_k^{(\beta)} y\left(t_{n-k} + \frac{\beta\tau}{2}\right) = \tau^\beta f(t_n, y(t_n)) + a_2 \tau^{2+\beta} D^2 f(t_n, y(t_n)) + O(\tau^{4+\beta}). \quad (20)$$

We approximate $y(t_{n-k} + \beta\tau/2)$ by (15) in Lemma 3.1 with $\mu = \beta/2$ and $t = t_{n-k}$. Moreover, approximate the second derivative in (20) by (17) in Lemma 3.2. Then, we have from (16) with

$$p_0 = \frac{(\beta+2)(\beta+4)(\beta+6)}{48}, \quad p_1 = -\frac{\beta(\beta+4)(\beta+6)}{16}, \quad p_2 = \frac{\beta(\beta+2)(\beta+6)}{16}, \quad p_3 = -\frac{\beta(\beta+2)(\beta+4)}{48}. \quad (21)$$

$$\begin{aligned} & \sum_{k=0}^{\infty} g_k^{(\beta)} [p_0 y(t_{n-k}) + p_1 y(t_{n-k-1}) + p_2 y(t_{n-k-2}) + p_3 y(t_{n-k-3})] \\ &= \tau^\beta [f(t_n, y(t_n)) + a_2 (2f(t_n, y(t_n)) - 5f(t_{n-1}, y(t_{n-1})) + 4f(t_{n-2}, y(t_{n-2})) \\ & \quad - f(t_{n-3}, y(t_{n-3}))) + O(\tau^{4+\beta})]. \end{aligned} \quad (22)$$

Dropping the error term, with the notations in (12), equation (22) gives an implicit FLMM scheme

$$\begin{aligned} & \sum_{k=0}^{\infty} g_k^{(\beta)} (p_0 y_{n-k} + p_1 y_{n-1-k} + p_2 y_{n-2-k} + p_3 y_{n-3-k}) \\ & = \tau^\beta [f_n + a_2(2f_n - 5f_{n-1} + 4f_{n-2} - f_{n-3})]. \end{aligned} \quad (23)$$

Again, approximating the second derivative in (20) by (18) in Lemma 3.2, with the same operations and notations, we get another implicit FLMM:

$$\begin{aligned} & \sum_{k=0}^{\infty} g_k^{(\beta)} (p_0 y_{n-k} + p_1 y_{n-1-k} + p_2 y_{n-2-k} + p_3 y_{n-3-k}) \\ & = \tau^\beta [f_n + a_2(3f_{n-1} - 8f_{n-2} + 7f_{n-3} - 2f_{n-4})] \end{aligned} \quad (24)$$

For brevity of presentation, we call these FLMMs in (23) and (24) as NFLMM4.1 and NFLMM4.2 respectively.

3.2 Implementation

We use the following notations:

For a sequence $a = \{a_k\}$, we denote the finite vector $[a_i, a_{i+1}, \dots, a_j]$ as $a_{i:j}$. For given two sequences a, b , the convolution of two equal sized vectors $a_{i:j}, b_{l:m}$, with $j - i + 1 = m - l + 1$, as $(a_{i:j} * b_{l:m}) = \sum_{k=i}^j a_k b_{n-k}$, where $n = m + i = l + j$.

Using these notations, the two proposed NFLMMs can be written as

$$(w_{0:n} * y_{0:n}) = \tau^\beta (q_{0:m} * f_{n-m:n}), \quad (25)$$

where $y = \{y_k\}$, $f = \{f_k\}$, $g = \{g_k\}$ and $w = \{w_k\}$ with w_k given by

$$w_k = p_0 g_k + p_1 g_{k-1} + p_2 g_{k-2} + p_3 g_{k-3} = p * g_{k-3:k}, \quad k = 0, 1, \dots,$$

where we have assumed $g_{-1} = g_{-2} = g_{-3} = 0$. The coefficient vectors p, q are given by

$$p = [p_0, p_1, p_2, p_3] \text{ with } \mu = \beta/2, \quad (26)$$

$$\text{for NFLMM4.1: } q = [1 + 2a_2, -5a_2, 4a_2, -a_2], \quad m = 3, \quad (27)$$

$$\text{for NFLMM4.2: } q = [1, 3a_2, -8a_2, 7a_2, -2a_2], \quad m = 4. \quad (28)$$

Extracting terms of y_n , we write (25) as

$$w_0 y_n + (w_{1:n} * y_{0:n-1}) = q_0 \tau^\beta f_n + \tau^\beta (q_{1:m} * f_{n-m:n-1}). \quad (29)$$

First, we consider linear FIVP with $f(t, y) = \lambda y(t) + F(t)$. Then, equation (29) becomes, after solving for y_n ,

$$y_n = \frac{1}{w_0 - q_0 \lambda \tau^\beta} [q_0 \tau^\beta F_n - s_{n-1}],$$

where $F_n = F(t_n)$ and $s_{n-1} = (w_{1:n} * y_{0:n-1}) - \tau^\beta (q_{1:m} * f_{n-m:n-1})$ which is independent of y_n .

Algorithm 1: Linear FIVP Solver

1. Input β, τ, y_0 , function $f(t)$
2. Compute $g = \{g_k\}$, using $g_0 = 1, g_k = (1 - \frac{\beta+1}{k})g_{k-1}, k = 1, 2, \dots, N$.
3. Compute the convolution $w = p * g = [(p * g_{k-m:k}): k = 0, 1, \dots, N]$.
4. For $n = 1, 2, \dots, N$,
5. $s_{n-1} = (w_{1:n} * y_{0:n-1}) - \tau^\beta (q_{1:m} * f_{n-m:n-1})$
6. $y_n = \frac{1}{w_0 - q_0 \lambda \tau^\beta} [q_0 \tau^\beta F_n - s_{n-1}]$.

Next, for the nonlinear FIVP, we write equation (29) in the unknown $y = y_n$:

$$H(t_n, y_n) + s_{n-1} = 0, \quad (30)$$

where $H(t, y) = w_0 y - q_0 \tau^\beta f(t, y)$.

We use Newton-Raphson iteration to solve (30) for y_n using the initial seed $y_{n,0} = y_{n-1}$.

The derivative of $H(t, y)$ with respect to y is $H_y(t, y) = w_0 - q_0 \tau^\beta f_y(t, y)$,

where $f_y = \frac{\partial}{\partial y} f(t, y)$. Then, the algorithm for non-linear FIVP is given by

Algorithm 2: Non-linear FIVP Solver

1. Input β, τ, y_0 , functions $f(t, y), f_y(t, y)$
2. compute $g = \{g_k\}$, using $g_0 = 1, g_k = (1 - \frac{\beta+1}{k})g_{k-1}, k = 1, 2, \dots, N$.
3. Compute $w = p * g = [p * g_{k-3:k}: k = 0, 1, \dots, N]$.
4. Define functions $H(t, y) = w_0 y - q_0 \tau^\beta f(t, y), H_y(t, y) = w_0 - q_0 \tau^\beta f_y(t, y)$
5. For $n = 1, 2, \dots, N$,
6. $s_{n-1} = (w_{1:n} * y_{0:n-1}) - \tau^\beta (q_{1:m} * f_{n-m:n-1})$
7. $y_n = \text{Newton}(H(t_n, y) + s_{n-1}, H_y(t_n, y), y_{n-1})$

where the function $\text{Newton}(h(y), h'(y), y^{(0)})$ performs the Newton-Raphson iterations to compute the root of $h(y) = 0$ with initial seed $y^{(0)}$.

4. Analysis of linear stability

The generating functions of the new implicit schemes NFLMM4.1 and NFLMM4.2 are given by:

$$W_{4.1}(\xi; \beta) = \frac{(1-\xi)^\beta P(\xi)}{Q_{4.1}(\xi)} \quad \text{and} \quad W_{4.2}(\xi; \beta) = \frac{(1-\xi)^\beta P(\xi)}{Q_{4.2}(\xi)} \quad (31)$$

respectively, where $P(\xi)$, $Q_{4.1}(\xi)$ and $Q_{4.2}(\xi)$ are polynomials for which the coefficients are given by (26),(27) and (28) respectively. The following elementary results on complex numbers is useful.

Lemma 4.1 *Let z, w , be two distinct non-zero complex numbers. Then, the following are equivalent.*

- (i) zw is a real.
- (ii) z/w is real.
- (iii) Both z, w are real or z is a real multiple of \bar{w} .

Proof. (i) \Leftrightarrow (ii) and (i) \Leftrightarrow (iii) are obvious. It is enough to prove (i) \Rightarrow (iii).

Suppose that $z = x + iy, w = a + ib$. Then $zw = xa - yb + i(xb + ya)$ is real implies $xb + ya = 0$. Then, for a real $\alpha, x/a = -y/b = \alpha \neq 0$ which gives $x = \alpha a$ and $y = -\alpha b$. Hence $z = \alpha \bar{w}$. ■

In order to analyze the stability properties of the methods, we consider the unstable regions $\{W_{4.x}(\xi; \beta) : |\xi| \leq 1\}$, $x = 1, 2$ and their properties.

Theorem 4.2 *The generating functions $W_{4.x}(\xi; \beta)$, $x = 1, 2$, in (31) have the following properties:*

1. ξ is real if and only if $W_{4.x}(\xi; \beta)$ is real. Moreover, $\xi \in [-1, 1]$ if and only if $0 \leq W_{4.x}(\xi; \beta) \leq W_{4.x}(-1; \beta)$.
2. If $\|\xi\| = 1$ and $\Im(\xi) > 0 (< 0)$, then $\Im(W_{4.x}(\xi; \beta)) < 0 (> 0)$.

Proof. It is enough to prove the sufficiency of both statements.

1. Thanks to Lemma 4.1 that $W_{4.x}(\xi; \beta)$ is real if and only if the factors $(1-\xi)^\beta, P(\xi)$ and $Q_{4.x}(\xi)$ are all real. Hence, ξ is real.
2. If $-1 \leq \xi \leq 1$, we have $0 \leq 1-\xi \leq 2$. Clearly, then, $(1-\xi)^\beta$ is decreasing.

Writing $P(\xi)$, $Q_{4.1}(\xi)$ and $Q_{4.2}(\xi)$ as polynomial of $(1-\xi)$, we get

$$P(\xi) = 1 + \frac{\beta}{2}(1-\xi) + \frac{\beta(\beta+2)}{8}(1-\xi)^2 + \frac{\beta(\beta+2)(\beta+4)}{48}(1-\xi)^3,$$

$$Q_{4.1}(\xi) = 1 + a_2(1-\xi)^2 + a_2(1-\xi)^3,$$

$$Q_{4.2}(\xi) = 1 + a_2(1-\xi)^2 + a_2(1-\xi)^3 - 2a_2(1-\xi)^4,$$

Noticing that $\frac{\beta(\beta+2)(\beta+4)}{48} > a_2$ for NFLMM4.1, we immediately see that $\frac{P(\xi)}{Q_{4.1}(\xi)}$ is also decreasing. Hence, $W_{4.1}(\xi; \beta)$ is decreasing and $W_{4.1}(1; \beta) = 0 \leq W_{4.1}(\xi; \beta) \leq W_{4.1}(-1; \beta)$.

As for NFLMM4.2, $Q_{4.2}(\xi)$ is of degree 4 having an additional term with a negative coefficient. Hence, it is increasing. Therefore, $W_{4.2}(\xi; \beta)$ is decreasing and thus, $W_{4.2}(1; \beta) = 0 \leq W_{4.2}(\xi; \beta) \leq W_{4.2}(-1; \beta)$. ■

Theorem 4.3 *The unstable regions of NFLMM4.1 and NFLMM4.2 are bounded and symmetric about the real axis for $0 < \beta \leq 1$.*

Proof. For the boundedness, we see that the numerator part of $W(\xi; \beta)$, with $|\xi| \leq 1$,

$$|(1-\xi)^\beta P(\xi)| \leq (1+|\xi|)^\beta (|p_0| + |p_1||\xi| + |p_2||\xi|^2 + |p_3||\xi|^3) \leq 2^\beta (p_0 - p_1 + p_2 - p_3) = 2^\beta P(-1),$$

where we have used the facts that $p_0, p_2 > 0$ and $p_1, p_3 < 0$.

For the denominator part for NFLMM4.1,

$$\begin{aligned} |Q_{4.1}(\xi)| &= |1 + a_2(2 - 5\xi + 4\xi^2 - \xi^3)| \geq |1 + 2a_2 - a_2(5 + 4 + 1)| \\ &= 1 - \frac{\beta}{3} > 0 \text{ for } 0 < \beta < 3. \end{aligned}$$

For NFLMM4.2,

$$\begin{aligned} |Q_{4.2}(\xi)| &= |1 + a_2(3\xi - 8\xi^2 + 7\xi^3 - 2\xi^4)| \geq |1 - a_2(3 + 8 + 7 + 2)| \\ &= Q(-1) = 1 - \frac{5\beta}{6} > 0 \text{ for } 0 < \beta < 6/5. \end{aligned}$$

Hence, for $0 < \beta \leq 1$ and for $|\xi| \leq 1$,

$$|W_{4.x}(\xi; \beta)| = \frac{|1-\xi|^\beta |P(\xi)|}{|Q_{4.x}(\xi)|} < \infty, \quad x = 1, 2.$$

Since $W_{4.x}(\bar{\xi}; \beta) = \overline{W_{4.x}(\xi; \beta)}$, we immediately see that the unstable regions are symmetry about the real axis. ■

Since the NFLMM4.x are of order 4, the Dahlquist barrier for FIVPs tells us that they are not A-stable [13].

Therefore, we look for the $A\left(\frac{\pi}{2}\right)$ -stability of these methods, that is, if the methods are stable in the entire left complex plane.

Theorem 4.4 There are threshold values $\beta_{4,x}^* \in (0,1)$ such that the methods NFLMM4.x, $x = 1,2$, are $A\left(\frac{\pi}{2}\right)$ -stable for $0 < \beta < \beta_{4,x}^*$.

Proof: First note that the generations functions $W_{4,x}(\xi; \beta)$ are continuous function in β , where ξ is fixed.

Now, for $|\xi| \leq 1$, from (31) with (21), we have $W_{4,1}(\xi, 0_+) = 1 > 0$. Hence there exists a neighborhood $(0, \epsilon)$ for β such that $W_{4,1}(\xi, \beta) > 0$ for all $|\xi| \leq 1$.

Again, for $\xi_i = i$ and $\beta = 1$, we have

$$W_{4,1}(\xi_i, 1) = \frac{(1-i)(p_0 + ip_1 - p_2 + ip_3)}{1 + \frac{1}{24}(2 - 5i - 4 + i)} = -0.528 - 3.096i.$$

So, $\Re(W_{4,1}(\xi_i, 1)) = -0.528 < 0$. Hence, there is a neighborhood $(1 - \epsilon, 1)$ for β such that $W_{4,1}(\xi_i, \beta) < 0$. Let $\beta_{4,1}^* = \max\{\beta : W_{4,1}(\xi, \beta) \geq 0\}$. Then $0 < \beta_{4,1}^* < 1$.

The proof for $W_{4,2}(\xi, \beta)$ is analogoious with $W_{4,1}(\xi_i, 1) = -0.1927 - 3.358i$. ■

Numerical computation by interval bisection shows that $\beta_{4,1}^* = 0.82960$ and $\beta_{4,2}^* = 0.85024912$ for the NFLMM4.1 and NFLMM4.2 respectively.

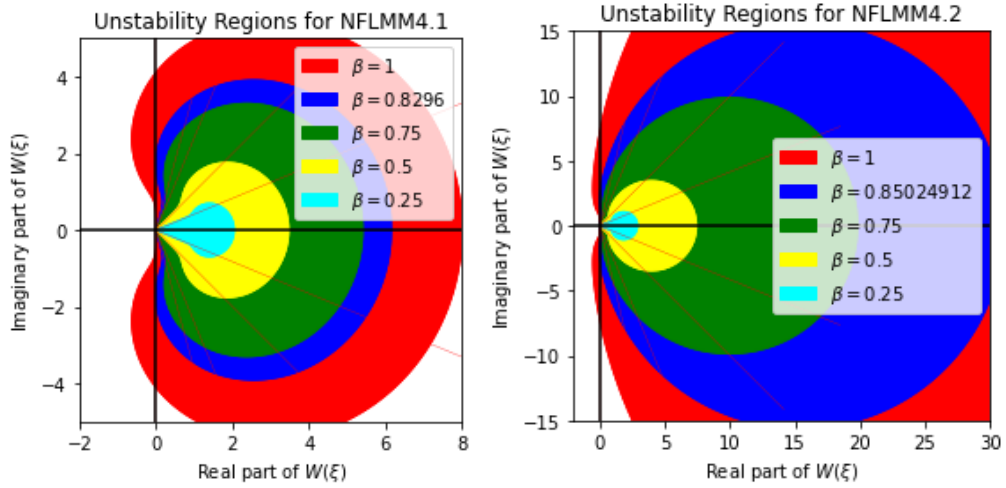


Figure 2. Stability regions of NFLMM4.x for some β values.

In Figure 2, the unstable regions of the two methods NFLMM4.x, $x=1,2$ are shown for different fractional orders $0 < \beta \leq 1$. The straight lines in the figures represent the stability region boundaries of the methods, where the stability regions are shown on the left side of the lines. These lines also correlate to the analytical stability region's boundary Σ_β . It is clear from the figure that the unstable regions surpass the A-stable boundaries for all values of β . Thus, the methods are verified to be not A-stable. The regions in blue are the unstable regions for the threshold values $\beta_{4,x}^*$ which indicate $A\left(\frac{\pi}{2}\right)$ -stable boundaries.

5. Comparisons

In this section, we compare the order 4 NFLMM4.x with FAM3 and FBDF4 for their performances in terms of computations and stability.

5.1 Numerical comparisons

Consider the linear FIVP used in [9].

$$D_t^\beta y(t) = f(t, y(t)) = \lambda y(t) + F(t), \quad 0 \leq t \leq 1, \quad 0 < \beta \leq 1,$$

with the initial condition $y(0) = 0$,

where $F(t) = \frac{\Gamma(n+1)}{\Gamma(n+1-\beta)} t^{n-\beta} - \frac{\Gamma(n)}{\Gamma(n-\beta)} t^{n-1-\beta} + t^n - t^{n-1}$ with $\lambda = -1$.

The exact solution is given by: $y(t) = t^n - t^{n-1}$, where $n = 5$.

The linear equation was solved by using the schems FAM3, FBDF4, NFLMM4.1 and NFLMM4.2 in (23) and (24) with different values of fractional orders $\beta = 0.4, 0.6$ and 0.8 . The problem is computed on the domain $[0,1]$, with

$N_j = 2^j$, $j = 3, 4, \dots, 11$ as the number of subintervals and $\tau_j = \frac{1}{N_j}$ as the step size. The maximum errors E_j for step size τ_j are compared for the methods. The order of the method NFLMM4.1 is computed by the formula

$$p_{j+1} = \frac{\log(E_{j+1}/E_j)}{\log(\tau_{j+1}/\tau_j)}.$$

The orders of other methods are nearly the same and are not presented. The results obtained are listed in Table 1, 2 and 3 respectively.

Table 1. Comparing Maximum errors for $\beta = 0.4$.

N_j	NFLMM4.1	NFLMM4.2	FBDF4	FAM3	Order
8	5.968e-04	2.702e-04	8.327e-04	2.641e-04	-
16	4.171e-05	1.752e-05	5.952e-05	1.785e-05	3.83859
32	2.741e-06	1.115e-06	3.947e-06	1.157e-06	3.92775
64	1.754e-07	7.033e-08	2.537e-07	7.361e-08	3.96556
128	1.109e-08	4.415e-09	1.607e-08	4.641e-09	3.98317
256	6.974e-10	2.766e-10	1.011e-09	2.913e-10	3.99167
512	4.371e-11	1.730e-11	6.341e-11	1.824e-11	3.99585
1024	2.736e-12	1.082e-12	3.972e-12	1.141e-12	3.99789
2048	1.711e-13	6.772e-14	2.523e-13	7.147e-14	3.99843

Table 2. Comparing Maximum errors for $\beta = 0.6$.

N_j	NFLMM4.1	NFLMM4.2	FBDF4	FAM3	Order
8	1.161e-04	6.265e-04	1.361e-03	3.429e-04	-
16	8.129e-05	4.207e-05	9.629e-05	2.288e-05	3.83713
32	5.334e-06	2.715e-06	6.352e-06	1.474e-06	3.92967
64	3.411e-07	1.723e-07	4.072e-07	9.346e-08	3.96670
128	2.156e-08	1.085e-08	2.577e-08	5.884e-09	3.98378
256	1.355e-09	6.809e-10	1.620e-09	3.691e-10	3.99199
512	8.494e-11	4.264e-11	1.016e-10	2.311e-11	3.99602
1024	5.316e-12	2.667e-12	6.370e-12	1.445e-12	3.99812
2048	3.323e-13	1.663e-13	4.168e-13	9.028e-14	3.99975

Table 3. Comparing Maximum errors for $\beta = 0.8$.

N_j	NFLMM4.1	NFLMM4.2	FBDF4	FAM3	Order
8	1.982e-04	1.202e-04	1.972e-03	3.857e-04	-
16	1.386e-05	8.215e-05	1.385e-04	2.546e-05	3.8374
32	9.093e-06	5.336e-06	9.102e-06	1.632e-06	3.93067
64	5.812e-07	3.397e-07	5.823e-07	1.032e-07	3.96753
128	3.672e-08	2.142e-08	3.681e-08	6.492e-09	3.98425
256	2.307e-09	1.345e-09	2.314e-09	4.070e-10	3.99222
512	1.446e-10	8.423e-11	1.450e-10	2.548e-11	3.99611
1024	9.053e-12	5.272e-12	9.094e-12	1.595e-12	3.99776
2048	5.701e-13	3.325e-13	6.024e-13	9.947e-14	3.98928

Since all the four methods are of order 4, the computational solutions for all choices of discretization are expected to be nearly the same.

As for the computational cost, the weights of the NFLMM4.x need only a linear combination of the Grunwald coefficients $g_k^{(\beta)}$, that have the simplest computational cost. The weights of FBDF4 obviously require computations using Miller's formula with four prior weights.

As for the memory requirement, the FAM3 requires keeping all the f_n values stored during the iteration to be used on the right side of scheme (25). The NFLMM4.x require only the last three or four values of f_n as in (23) and (24).

5.2 Comparison of stability

We compare the stability regions of the four implicit FLMMs. The generating functions FBDF4 and FAM3 are provided below:

$$W_{FBDF4}(\xi) = \left(\frac{25}{12} - 4\xi + 3\xi^2 - \frac{4}{3}\xi^3 + \frac{1}{4}\xi^4 \right)^\beta \quad \text{and} \quad W_{FAM3}(\xi) = \frac{(1-\xi)^\beta}{q_0 + q_1\xi + q_2\xi^2 + q_3\xi^3},$$

where $q_i, i = 0,1,2,3$, are given by

$$q_0 = 1 - \frac{5}{6}\beta + \frac{11}{48}\beta^2 - \frac{1}{48}\beta^3, \quad q_1 = \frac{31}{24}\beta - \frac{9}{16}\beta^2 + \frac{1}{16}\beta^3,$$

$$q_2 = -\frac{7}{12}\beta + \frac{7}{16}\beta^2 - \frac{1}{16}\beta^3, \quad q_3 = \frac{1}{8}\beta - \frac{5}{48}\beta^2 + \frac{1}{48}\beta^3.$$

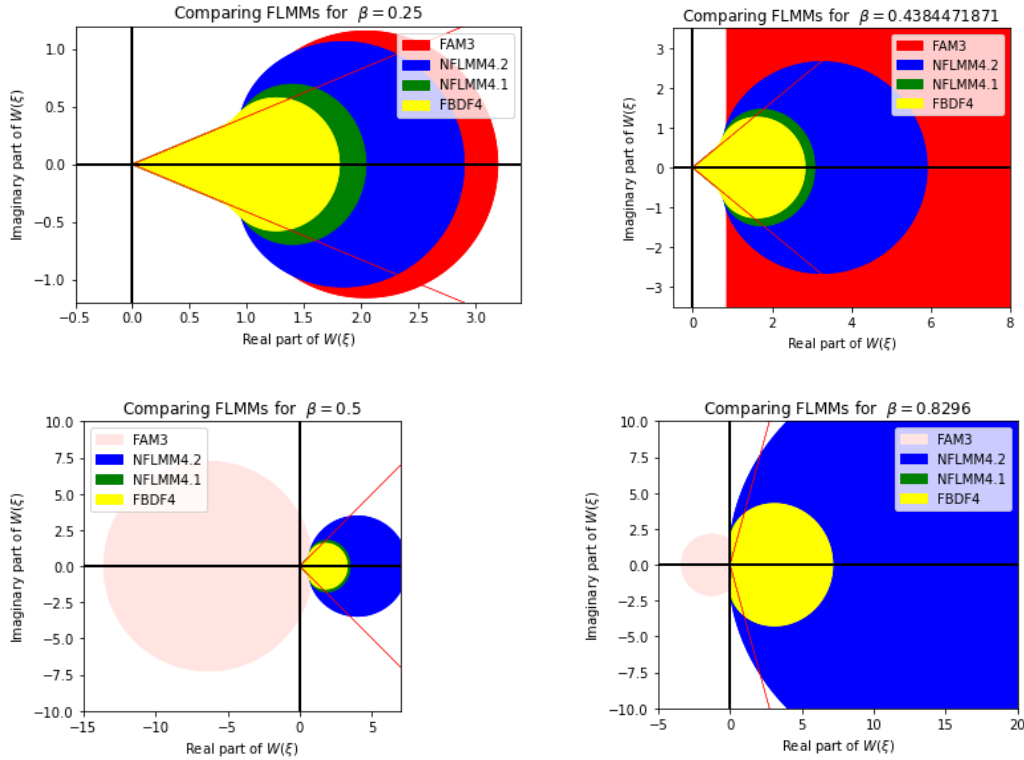


Figure 3. Comparing stability regions for FLMMs of order 4.

Since the FLMM methods with orders greater than 2 are not A-stable, the $A\left(\frac{\pi}{2}\right)$ -stable and $A(0)$ -stable could be used as comparison tools of those methods.

As shown in Figure 3, the unstable region for many values of β is on the right side of the complex plane. However, there are some β values for which the unstable region also extends to the left side, such as $\beta = 1$. The intervals for β where the FLMMs are $A\left(\frac{\pi}{2}\right)$ -stable were calculated numerically. The β^* values for which the intervals $0 < \beta \leq \beta^*$ gives the $A\left(\frac{\pi}{2}\right)$ -stability are given in Table 4.

Table 4. Threshold β^* for $A\left(\frac{\pi}{2}\right)$ -stability.

FAM3	NFLMM4.1	FBDF4	NFLMM4.2
0.4384471	0.82960	0.843895	0.85024912

For the $A\left(\frac{\pi}{2}\right)$ -stability the NFLMM4.2 has the highest interval for β followed by FBDF4, NFLMM4.1 and FAM3. The lower interval size is gained for FAM3. Also note that as β approaches the $A\left(\frac{\pi}{2}\right)$ -stability bound β^* , FAM3's $A(0)$ -stability vanishes. For $\beta > \beta^*$ the stability region becomes bounded and falls on the left complex plane, resulting in only conditional stability.

7. Conclusion

We analyzed and compared the new fractional linear multistep methods NFLMM4.1 and NFLMM4.2 with FAM3 and FBDF4 methods of order 4. We see that NFLMM4.2 is $A\left(\frac{\pi}{2}\right)$ -stable over a wider fractional-order interval while FAM3 displays $A\left(\frac{\pi}{2}\right)$ -stability for a small range of β values. Furthermore, the proposed methods have lower computing cost and minimal storage compared to FAM3.

Conflict of interest

The authors declare no conflict of interest.

Acknowledgment

The authors are grateful to the reviewers for their constructive comments.

References

1. Oldham, K. and Spanier, J. *The fractional calculus theory and applications of differentiation and integration to arbitrary order*. Elsevier, 1974.
2. Diethelm, K. *The analysis of fractional differential equations: An application-oriented exposition using differential operators of Caputo type*. Springer Science and Business Media, 2010.
3. Lubich, C. On the stability of linear multistep methods for Volterra convolution equations. *IMA Journal of Numerical Analysis*, 1983, **3(4)**, 439-465. <https://doi.org/10.1093/imanum/3.4.439>.
4. Lubich, C. Fractional linear multistep methods for Abel-Volterra integral equations of the second kind. *Mathematics of computation*, 1985, **45(172)**, 463-469. <https://www.ams.org/mcom/1985-45-172/S0025-5718-1985-0804935-7/S0025-5718-1985-0804935-7.pdf>.
5. Lubich, C. Discretized fractional calculus. *SIAM Journal on Mathematical Analysis*, 1986, **17(3)**, 704-719. <https://doi.org/10.1137/0517050>.
6. Galeone, L. and Garrappa, R. Fractional Adams-Moulton methods. *Mathematics and Computers in Simulation*, 2008, **79(4)**, 1358-1367. <https://doi.org/10.1016/j.matcom.2008.03.008>.
7. Galeone, L. and Garrappa, R. Explicit methods for fractional differential equations and their stability properties. *Journal of Computational and Applied Mathematics*, 2009, **228(2)**, 548-560. <https://doi.org/10.1016/j.cam.2008.03.025>.
8. Garrappa, R. On some explicit Adams multistep methods for fractional differential equations. *Journal of computational and applied mathematics*, 2009, **229(2)**, 392-399. <https://doi.org/10.1016/j.cam.2008.04.004>.
9. Bonab, Z.F. and Javidi, M. Higher order methods for fractional differential equation based on fractional backward differentiation formula of order three. *Mathematics and Computers in Simulation*, 2020, **172**, 71-89. <https://doi.org/10.1016/j.matcom.2019.12.019>.
10. Aceto, L., Magherini, C. and Novati, P. On the construction and properties of m-step methods for FDEs. *SIAM Journal on Scientific Computing*, 2015, **37(2)**, A653-A675. <https://doi.org/10.1137/140973505>.
11. Al Hasani, K. and Nasir, H.M. New fractional linear multi-step methods of order four with improved stabilities. *C.Q.D. – Revista Eletrônica Paulista de Matemática*, Bauru, 2022, **22(2)**, 178-188. <https://doi.org/10.21167/cqdv22n22022178188>.
12. Nasir, H.M. and Al Hasani, K. Analysis of New Type of Second-order Fractional Linear Multi-step Method with Improved Stability. *SQU Journal for Science*, 2022, **27(2)**, 107-118. <https://doi.org/10.53539/squjs.vol27iss2pp>.
13. Lubich, C. A stability analysis of convolution quadrature for Abel-Volterra integral equations, *IMA J. Numer. Anal.* 1986, **6**, 87-101. <https://doi.org/10.1093/imanum/6.1.87>.
14. Nasir, H.M. and Nafa, K. A new second order approximation for fractional derivatives with applications. *SQU Journal of Science*, 2018, **23(1)**, 43-55. <https://doi.org/10.24200/squjs.vol23iss1pp43-55>.
15. Caputo, M.C. and Torres, D.F. Duality for the left and right fractional derivatives. *Signal Processing*, 2015, **107**, 265-271. <https://doi.org/10.1016/j.sigpro.2014.09.026>.
16. Abdeljawad and Thabet. On Riemann and Caputo fractional differences. *Computers & Mathematics with Applications*, 2011, **62(3)**, 1602-1611. <https://doi.org/10.1016/j.camwa.2011.03.036>.
17. Young, A. The application of approximate product-integration to the numerical solution of integral equations. *Proceedings of the Royal Society of London. Series A. Mathematical and Physical Sciences*, 1954, **224(1159)**, 561-573. <https://doi.org/10.1098/rspa.1954.0180>.
18. Li, C. and Chen, A. Numerical methods for fractional partial differential equations. *International Journal of Computer Mathematics*, 2018, **95(6-7)**, 1048-1099. <https://doi.org/10.1080/00207160.2017.1343941>.
19. Li, C. and Zeng, F. *Numerical methods for fractional calculus*. Chapman and Hall/CRC, 2019.
20. Weilbeer, M. *Efficient numerical methods for fractional differential equations and their analytical background*. *Papierflieger Clausthal-Zellerfeld*, Germany, 2006.
21. Podlubny, I. *Fractional differential equations: an introduction to fractional derivatives, fractional differential equations, to methods of their solution and some of their applications*, volume 198. Academic Press, 1998.
22. Nasir, H.M., Gunawardana, B.L.K. and Abeyrathna, H.M.N.P. A second order finite difference approximation for the fractional diffusion equation. *International Journal of Applied Physics and Mathematics*, 2013, **3(4)**, 237-243. <http://www.ijapm.org/papers/212-P0008.pdf>.
23. Nasir, H.M. and Nafa, K. Algebraic construction of a third order difference approximation for fractional derivatives and applications. *ANZIAM Journal*, 2018, **59(EMAC2017)**, C231-C245. <https://doi.org/10.21914/anziamj.v59i0.12592>.

ANALYSIS OF FRACTIONAL LINEAR MULTI-STEP METHODS OF ORDER FOUR

24. Gunarathna, W.A., Nasir, H.M. and Daundasekera, W.B. An explicit form for higher order approximations of fractional derivatives. *Applied Numerical Mathematics*, 2019, **143**, 51-60.
<https://doi.org/10.1016/j.apnum.2019.03.017>.
 25. Odibat, Z.M. and Momani, S. An algorithm for the numerical solution of differential equations of fractional order. *Journal of Applied Mathematics & Informatics*, 2008, **26(12)**, 15-27.
<https://koreascience.kr/article/JAKO200833338752380.pdf>.
 26. Zhao, J., Long, T. and Xu, Y. Generalised Backward Differentiation Formulae for Fractional Differential Equation. *East Asian Journal on Applied Mathematics*, 2019, **9(3)**, pp.506-521.
<https://doi.org/10.4208/ejam.150618.091018>
 27. Zhao, J., Jiang, X. and Xu, Y. A kind of generalized backward differentiation formulae for solving fractional differential equations. *Applied Mathematics and Computation*, 2022, **419**, p.126872.
<https://doi.org/10.1016/j.amc.2021.126872>.
-

Received 25 March 2023

Accepted 30 May 2023

Knowledge and Attitude Towards COVID-19 and Associated Mental Health Status among Students of Sultan Qaboos University, Oman

M. Mazharul Islam^{1*}, Ronald Wesonga¹, Iman Al Hasani¹, Afra Al Mane²

¹Department of Statistics, College of Science, Sultan Qaboos University, P.O. Box 36, PC 123, Al-Khod, Muscat, Sultanate of Oman; ²Department of Planning and Statistics, Sultan Qaboos University, Muscat, Sultanate of Oman. *Email: mislam@squ.edu.om.

ABSTRACT: This study examined COVID-19-related knowledge and attitude towards COVID-19 and associated mental health status during COVID-19 pandemic among the students of Sultan Qaboos University (SQU), using an online cross-sectional survey conducted from 26 March - 25 April 2021. Both descriptive and inferential statistical techniques, including multiple logistic regression analysis, were used for data analysis. Of the 1,951 respondents, 60% were women, and the mean age of the respondents was 22 ± 4.6 years. Approximately 13% of the students' COVID-19 status was tested and 3.6% were found to be infected with the COVID-19 virus. Overall, students demonstrated a high level (81%) of knowledge and a positive attitude (83%) towards COVID-19. Knowledge appeared as a significant predictor of positive attitude. Despite the high level of knowledge and positive attitudes, some misconceptions and stigma prevailed for a group of students, since approximately one-third of the students opined that COVID-19 was a natural catastrophe and 13% of the students were in favor of keeping it secret if it was infected, which could impede the success of the COVID-19 prevention program. The study documented a high prevalence of mild to severe levels of depression (66.3%), anxiety (69.2%), and stress (71%) among the students. Younger age, female sex, undergraduate students, single marital status, college of study, and good knowledge about COVID-19 appeared as significant predictors of mental health problems among students. For improving the mental health and well-being of the students, the SQU authorities should provide accessible psychological support to the students, with particular attention to the identified sub-group of students. Efforts should be made to remove the COVID-19-related stigma through mass-media campaigns.

Keywords: Knowledge; Attitude; COVID-19; Mental health; Depression; Anxiety; Stress; Students; Oman.

المعرفة والموقف تجاه كوفيد-19 وحال الصحة النفسية المرتبطة بهما لدى طلاب جامعة السلطان قابوس، عمان

م. مظهر الإسلام، رونالد وسونغا، إيمان الحسنی، أفرح المعني

المخلص: تناولت هذه الدراسة المعرفة والمواقف المتعلقة بكوفيد-19 وحال الصحة النفسية المرتبطة بهما أثناء جائحة كوفيد-19 بين طلاب جامعة السلطان قابوس، باستخدام مسح مقطعي عبر الإنترنت تم إجراؤه في 26 مارس - 25 أبريل 2021 بين طلاب جامعة السلطان قابوس. واستخدمت كل من التقنيات الإحصائية الوصفية والإستنتاجية، بما في ذلك تحليل الانحدار اللوجستي المتعدد، لتحليل البيانات. من بين 1951 مشاركاً، 60% كانوا من الإناث، وكان متوسط عمر المشاركين 22 ± 4.6 سنة. تم إختبار حوالي 13% من حالة كوفيد-19 للطلاب وتبين أن 3.6% منهم مصابون بفيروس كوفيد-19. بشكل عام، أظهر الطلاب مستوى عالٍ (81%) من المعرفة وموقفاً إيجابياً (83%) تجاه كوفيد-19. ظهرت المعرفة كمؤشر مهم للموقف الإيجابي. على الرغم من المستوى العالي من المعرفة والمواقف الإيجابية، إلا أن هناك بعض المفاهيم الخاطئة أو الوصمة السائدة لدى مجموعة من الطلاب، حيث رأى حوالي ثلث الطلاب أن فيروس كورونا COVID-19 كان كارثة طبيعية وكان 13% من الطلاب يؤيدون إبقاء الأمر سراً إذا أصيبوا؛ مما قد يعيق نجاح برنامج الوقاية من فيروس كورونا. وثقت الدراسة ارتفاع معدل إنتشار مستويات الإكتئاب من الخفيفة إلى الشديدة (66.3%)، والقلق (69.2%)، والتوتر (71%) بين الطلاب. وظهر أن صغر العمر، وطلاب البكالوريوس، والحالة الإجتماعية العازبة، والكلية الدراسية، والمعرفة الجيدة حول كوفيد-19، تنبئ بشكل مهم بمشاكل الصحة النفسية بين الطلاب. لتحسين الصحة العقلية ورفاهية الطلاب، يجب على هيئة جامعة السلطان قابوس توفير الدعم النفسي الممكن للطلاب، مع إيلاء إهتمام خاص للمجموعة الفرعية المحددة من الطلاب. وينبغي بذل الجهود لإزالة الوصمة المرتبطة بفيروس كورونا (كوفيد-19) من خلال الحملات الإعلامية.

الكلمات المفتاحية: المعرفة؛ الموقف؛ كوفيد-19؛ الصحة النفسية؛ الإكتئاب؛ القلق؛ التوتر؛ الطلبة؛ عُمان.



1. Introduction

The coronavirus disease 2019, in short COVID-19, with different variants emerged as a major public health crisis across the world in December 2019 in the Wuhan region of China and rapidly spread all over the world within three months of time, and the WHO declared it as the pandemic in March 2020 [1, 2]. COVID-19 can cause a range of illnesses in humans, from the common cold to severe acute respiratory syndrome (SARS) [3-5]. It is a highly infectious disease believed to spread through respiratory aerosol generated through coughing and sneezing by an infected person [6], and its main clinical symptoms include fever, dry cough, breathing difficulty, muscle or body aches, fatigue, myalgia, and dyspnea [7,8]. Other symptoms are sore throat, diarrhea, loss of taste or smell, and arthralgia [9-11].

At the outset of the pandemic, there was no proven vaccine or treatment for the disease. Therefore, to contain the spread of the infection within the population, strict infection control measures arising from the knowledge of the transmission mechanisms of the disease were imposed by the countries worldwide [6,12]. The strategies that were established worldwide were largely behavioral, such as social distancing, cleanliness, regular hand washing, and use of face masks in public. The compliance of these initiatives was primarily dependent on one's knowledge and attitudes towards the disease [9,11-13]. In addition, many countries implemented a series of measures, including quarantine, lock-down, suspension of local and international travel flights, bans on large gatherings, mandatory use of face masks, social distancing, closure of schools and universities and of business, home or online education of students, stay-at-home orders, and even curfews [5,14-16]. Despite these efforts, many people tend to ignore them due to poor knowledge and attitudinal issues. Adequate knowledge and positive attitudes of the public are expected to influence the degree of adherence to the personal protective measures, social stigma, clinical outcome and mental health. Hence, it is important to study these domains in any population for developing the effective coping mechanism.

The COVID-19 pandemic has brought into focus the mental health of various sub-groups of the population. Studies have shown that the pandemic created new stressors, including fear of infections, worry for oneself or survival for the loved ones, frustration, boredom, inadequate supplies, inadequate information, financial loss, and stigma [17-20].

Although young adults were found to have a lesser risk of having COVID-19 infection than their older counterparts, they are the most vulnerable group with regards to the deterioration of mental health due to the COVID-19 pandemic [21-24]. Student life, particularly the university student life marks a transitional period for students, during which students have to cope with many social, economic, developmental, and above all academic requirements, making them increasingly vulnerable to stress, anxiety, and depression as well as diabetes, rheumatic diseases and obesity [25-29]. COVID-19 pandemic adds a new dimension to their depression, anxiety, and stress levels.

Knowledge and attitude concerning COVID-19 was found to have significant association with the level of its spread, control and management in many countries across the world [11, 30-32]. Moreover, the situation could be even worse among students at higher institutions of learning because of deteriorating mental health status, resulting in a destabilizing effect on their normal academic performance. Although many studies have been conducted to assess knowledge and attitude of general population and health professionals since the emergence of the COVID-19 pandemic, there is a still scarcity of information regarding knowledge and attitude towards COVID-19 and the associated mental health status among the university students. The aim of this study was to explore the level of knowledge and attitude towards COVID-19 among the university students in Oman, and examined the impact of COVID-19 on mental health of the students. The study also examined the association between knowledge, attitude and mental health status of students and identified the predictors of knowledge and attitude towards COVID-19 and the mental health status during COVID-19. It also tested the hypothesis that COVID-19 elevates the burden of mental health issues among the students than general population. The findings of the study may have important policy implications both at university and national level.

2. Methods

2.1 Study design and participants

The data for this study was obtained through a cross-sectional online survey among the students of Sultan Qaboos University (SQU) in Oman, between 26 March and 25 April 2021. SQU is the only public university in Oman and students from all over the country are admitted on a competitive basis. At the time of the survey, there were 17,019 registered undergraduate and postgraduate students in SQU, of whom 53% were female. Due to strict social distancing measures, stay-at-home orders, and the rapidly evolving pandemic during the study period, the survey was conducted online to collect data in a timely manner. All SQU students had access to social media and institutional e-mail systems.

An online semi-structured questionnaire was developed by using the Questioner platform (<https://www.questionPro.com>) in both English and Arabic, and it was hosted via a unique uniform resource locator (URL). The link to the questionnaire was sent through emails to all students. An information sheet and a consent form were available on the first page of the questionnaire. Participating students were free to withdraw at any time without giving explanations and no personal identification was requested so as to retain information confidentiality. A total of 3,180 students clicked on the survey link, but 1,915 students provided complete responses.

2.2 Data collection tools and measurements

Students’ knowledge about COVID-19 was assessed using 13 true-false questions on three dimension of knowledge: (1) signs and symptoms, (2) mode of transmission, and (3) prevention mechanism (Table 2). Each correct response was scored as 1 point and incorrect response as 0, giving a maximum score of 13 and a minimum score of 0. The higher the points scored, the more knowledgeable the student. The mean score was 9.8. The overall knowledge was then categorized into poor for the scores less than 9 and good for the scores 9 and above.

The attitude was assessed using a 7-item question, each with responses of agree or disagree. A score of 1 was assigned for a response reflecting a positive attitude and 0 for a response reflecting a negative attitude, giving a maximum score of 7 and a minimum score of 0, with mean 5.4. Thus the overall attitude was categorized as negative for the scores less than 5 and positive for the scores 5 and above.

To assess the mental health status, a shorter version of the Depression Anxiety Stress Scale (DASS) has been used [33]. This version, known as the Depression Anxiety Stress Scale 21 (DASS21), has been validated in many countries as a reliable self-administered psychological instrument consisting of 21 items in three domains. Each domain comprises seven items, assessing three dimensions of mental health symptoms: depression, anxiety and stress. Respondents were required to indicate the presence of these symptom(s) over the past week on a 4-point Likert scale scoring from 0 to 3 (0: did not apply at all over the last week, 1: applied to some degree, or some of the time; 2: applied a considerable degree, or a good part of the time; 3: applied very much or most of the time). This instrument is frequently used in clinical and non-clinical trials [33-36], possessing well-established psychometric properties in reliably measuring depression, anxiety, and stress. We performed the Cronbach’s alpha reliability test for the tool, and they were found to be 0.91, 0.84 and 0.90 respectively. The score for each of the DASS21 subscales, seven items per subscale, were summed up which ranges from 0 to 21. The scores were then categorized as “normal”, “mild”, “moderate”, and “severe”, according to the DASS21 manual [33].

2.3 Statistical analysis

The study considered knowledge, attitude and symptoms of depression, anxiety, and stress as the main outcome variables and socio-demographic and COVID-19 related factors as explanatory variables. Both descriptive and inferential statistical techniques as well as relevant statistical tests were employed for data analysis. Descriptive statistics such as frequency, proportion, mean and standard deviation were used to describe the level and pattern of knowledge, attitude, depression, anxiety, and stress. Cross tabulation along with a chi-square test was used to analyze the differentials of the prevalence of good knowledge, positive attitude and mild to severe levels of depression, anxiety, and stress across the socio-demographic and COVID-19 related factors. To identify the significant predictors of the outcome variables such as knowledge, attitude, depression, anxiety, and stress, multiple logistic regression techniques were employed by considering the outcome variables as dichotomous response variables (yes/no). We have dichotomized knowledge scores as good (scores ≥ 9) with coding 1 and poor (scores < 9) with coding 0. Attitude was dichotomized as negative (scores < 5) with coding 0 and positive with coding 1. Participants with a cut-off score of ≥ 10 in depression, ≥ 8 in anxiety, and ≥ 15 in stress dimensions were considered as having mild-severe form of these disorders as referenced by the DASS-21 manual [33]. We coded these cut-off scores of depression, anxiety and stress as 1 and 0 otherwise.

We set up the logistic regression model as follows: As per our study, we define an outcome variable as

$$y = \begin{cases} 1, & \text{if the outcome variable assume value 1} \\ 0, & \text{if the outcome variable assume value 0} \end{cases}$$

and x_1, x_2, \dots, x_n are a set of selected explanatory variables. The logistic regression model is then expressed as

$$\ln \left[\frac{P(y=1|x)}{1-P(y=1|x)} \right] = \beta_0 + \beta_1 x_1 + \beta_2 x_2 + \beta_3 x_3 + \dots + \beta_p x_p$$

where $p(y = 1 | x) = \frac{1}{1 + e^{-(\beta_0 + \beta_1 x_1 + \dots + \beta_n x_n)}}$ is the probability that the outcome variable takes on value 1 and

$\beta_0, \beta_1, \dots, \beta_n$ are the regression coefficients. However, $\beta_0, \beta_1, \dots, \beta_n$ do not have direct interpretation because they measure the effect of a predictor on the log of odds of the outcome variable, not the direct effect on outcome variable. Thus, e^{β_i} which is defined as odds ratio (OR), measuring the amount of change in probability of outcome variable for one unit change in explanatory variable. All the statistical analysis was performed using SPSS Version 23.0. A p-value < 0.05 was considered to be statistically significant.

3. Results

Characteristics of respondents

Of the total 1,915 participants, about 60% were female. More than half (56%) of the participants were young adults of age 20-24 years and were living in city areas (Table 1). The average age of the participants was 22 ± 4.6 years. The participating students were mostly (87%) undergraduate students, while about 10% of participants were postgraduate students. Slightly over half (54%) of the students were from the recent cohorts of 2019 and 2020. About

8% of students were married. The sample included 71 students (3.6%) who had tested COVID-19 positive. However, only 251 (13%) students underwent testing for the COVID-19 infection status.

Table 1. Percentage distribution of students according to demographic and socio-economic characteristics, 2021.

Characteristics	Number	Percent
Total sample	1951	100.0
Age		
< 20	588	30.1
20-24	1096	56.2
25-29	135	6.9
30+	132	6.8
Mean age (SD)	22.01 (4.6)	
Gender		
Male	782	40.1
Female	1169	59.9
College of study (major)		
Arts and Social Sciences	240	12.3
Agricultural & Marine Sciences	146	7.5
Education	318	16.3
Economics and Political Science	300	15.4
Engineering	319	16.4
Law	116	5.9
Medicine & Health Sciences	138	7.1
Science	324	16.6
Nursing	50	2.6
Level of study		
Foundation (pre-major)	49	2.5
Under graduate	1702	87.2
Post-Graduate	200	10.3
Admission cohort		
Before 2016	83	4.3
2016	235	12.0
2017	258	13.2
2018	316	16.2
2019	372	19.1
2020	687	35.2
Place of residence		
Urban	1092	56.0
Rural	859	44.0
Marital status		
Single	1797	92.1
Married	154	7.9
Dwelling type		
Traditional Arabian house	1277	65.5
Flat house	101	5.2
Villa	573	29.4
Monthly HH income (in Omani Rials)		
< 1000	822	42.1
1000 - 2000	785	40.2
>2000	344	17.6
Test for COVID-19		
Not tested	1700	87.1
Tested Negative	180	9.2
Tested positive	71	3.6

Knowledge about COVID-19

Overall students exhibited high levels of knowledge about COVID-19, as 81% of the students had good knowledge. About 82% of the students correctly answered that COVID-19 is a viral disease (Table 2). More than ninety percent (95%) of the students reported coughing/sneezing as signs and symptoms of COVID-19, while difficulty

THE DEUBIQUITYLASE USP5 KNOCKDOWN

in breathing was reported by 85% of the students. Other symptoms like fever and muscle/body aching were mentioned by 78% and 60% students, respectively. About 81% of the students knew that the COVID-19 virus can be transmitted to another person through the mouth, nose and eyes, 83% knew that transmission can happen through touching an infected person and 63% knew that being in close contact with the infected person could be the cause of transmission. About 90% students correctly reported that social distancing, wearing mask and keeping had clean can prevent COVID-19 infection, while about 77% reported that avoiding contact with infected person and avoiding travel or visit to crowded places can prevent COVID-19 infection.

Table 2. Percentage of students providing correct response to the questions related to knowledge about COVID-19, 2021.

Knowledge items	Correct response	
	Number	%
COVID-19 caused by a virus	1606	82.3
The symptoms of COVID-19 are:		
Coughing and sneezing	1856	95.1
Breathing difficulty	1661	85.1
Fever	1522	78.0
Muscle/body aching	1180	60.4
Transmission mechanisms of COVID-19:		
Being in close contact with an infected person	1219	62.5
Touching the infected person	1619	83.0
Mouth, nose and eyes are the routes of entry of coronavirus into human body	1585	81.2
Prevention mechanism of COVID-19:		
Social distancing	1778	91.1
Wearing mask	1737	89.0
Keeping hand clean	1749	89.6
Avoiding contact with infected person	1491	76.4
Avoiding travel and visit to crowded places	1508	77.3
Mean knowledge scores (SD)	9.8 (1.34)	
Overall knowledge about COVID-19		
Good	1589	81.4
Poor	362	18.6

Gender, urban/rural place of residence, cohort of study and college of study showed significant associations with knowledge about COVID-19 (Table 3). Female students were found to be 1.3 times more likely to have good knowledge about COVID-19 (AOR=1.32, 95% CI [1.08 -1.68]). As expected, students from the College of Medicine and Health Sciences (91%) and College of Nursing (90%) exhibited higher knowledge, while students from the College of Arts and Social Sciences (74.6%), as well as students from the College of Education (74.8%) had lower levels of good knowledge about COVID-19. Students from older cohorts were more likely to have good knowledge about COVID-19 compared to the students from recent cohorts (Table 3). Students living in urban areas had 1.43 times higher odds of good knowledge than their rural counterparts (AOR=1.43, 95% CI [1.11 - 1.85]).

Table 3. Percentage of students with poor and good knowledge about COVID-19 according to background characteristics, and results of logistic regression analysis showing odds of good knowledge about COVID-19, 2021.

Characteristics	Knowledge about COVID-19			Logistic regression analysis of good knowledge			
	Poor	Good	p-value [†]	B	AOR	95% CI	p-Value
Total sample	18.6	81.4					
Age			0.621				
< 20	17.7	82.3		0.29	1.33	0.82 - 2.14	0.237
20-24	18.3	81.7		0.25	1.28	0.81 - 2.01	0.283
25-29	20.7	79.3		0.11	1.12	0.61 - 2.05	0.711
30+ (ref.)	22.0	78.0			1.00		
Gender			0.013				
Male (ref.)	20.2	79.8			1.00		
Female	15.5	84.5		0.26	1.30	1.08 - 1.68	0.037
College of study (major)			<0.001				

Arts and Social Sciences	25.4	74.6		-1.17	0.31	0.11 - 0.82	0.018
Agricultural & Marine Sciences	15.1	84.9		-0.54	0.58	0.20 - 1.66	0.316
Education	25.2	74.8		-1.17	0.31	0.12 - 0.82	0.019
Economics and Political Science	18.3	81.7		-0.82	0.44	0.16 - 1.18	0.104
Engineering	15.7	84.3		-0.51	0.60	0.22 - 1.62	0.317
Law	21.6	78.4		-0.92	0.40	0.14 - 1.13	0.085
Medicine & Health Sciences	8.7	91.3		0.15	1.16	0.38 - 3.53	0.794
Science	16.0	84.0		-0.58	0.56	0.21 - 1.50	0.251
Nursing (ref.)	10.0	90.0			1.00		
Level of study			0.423				
Foundation (pre-major)	22.4	77.6		-0.12	0.89	0.37 - 2.12	0.800
Under graduate	18.7	81.3		-0.45	0.64	0.37 - 1.13	0.123
Post-graduate (ref.)	16.0	84.0			1.00		
Admission cohort			0.021				
Before 2016	13.5	86.5		0.33	1.39	1.02 - 2.53	0.018
2016	11.9	88.1		0.63	1.88	1.19 - 2.95	0.006
2017	17.1	82.9		0.20	1.22	0.82 - 1.81	0.320
2018	22.5	77.5		-0.19	0.83	0.59 - 1.17	0.294
2019	20.2	79.8		-0.07	0.93	0.67 - 1.28	0.647
2020 (ref.)	19.2	80.8			1.00		
Place of residence			0.001				
Urban	15.9	84.1		0.36	1.43	1.11 - 1.85	0.005
Rural (ref.)	21.9	78.1			1.00		
Marital status			0.734				
Single	18.6	81.4		0.07	1.07	0.58 - 1.93	0.564
Married (ref.)	17.5	82.5			1.00		
Dwelling type			0.759				
Traditional Arabian house	19.0	81.0		0.10	1.10	0.83 - 1.46	0.592
Flat house	17.8	82.2		-0.17	0.84	0.46 - 1.51	0.497
Villa (ref.)	17.6	82.4			1.00		
Monthly HH income (in OR)			0.042				
< 1000	19.7	80.3		-0.22	0.80	0.56 - 1.16	0.249
1000 - 2000	19.2	80.8		-0.29	0.75	0.52 - 1.08	0.124
>2000 (ref.)	13.2	86.8			1.00		
Test for COVID-19			0.619				
Not tested	18.9	81.1		-0.06	0.94	0.49 - 1.82	0.875
Tested Negative	16.1	83.9		0.01	1.01	0.47 - 2.13	0.453
Tested positive (ref.)	16.9	83.1			1.00		

Note: † p-value relate to Chi-square test to compare the level of knowledge in different sub-groups of respondents. B = Regression coefficient, for reference category it is Zero.

AOR = Adjusted odds ratio, CI = Confidence Interval

ref. = Reference category, Odds ratio is 1.00 for reference category

Attitudes towards COVID-19

About 90% of the students said that COVID-19 is a fatal disease and 93% believed that one can get infected with COVID-19 any time. However, more than one-third (35.2%) of the students believed that COVID-19 is a natural catastrophe, indicating that a group of students were stigmatized to some extent. Majority of students agreed positively to other attitudinal statements. The mean score of positive agreement was found to be 5.4 out of 7. The overall attitude was defined as positive attitude for the scores 5 and above. According to this definition, students were found to have high level of positive attitudes towards COVID-19, as 83% students had positive attitudes.

Students' positive attitudes towards COVID-19 were found to vary significantly with age, gender, college of study, marital status and knowledge about COVID-19. However, logistic regression analysis, after controlling the background characteristics, identified gender, marital status and knowledge about COVID-19 as significant predictors of positive attitudes about COVID-19. Female students were found to be 1.56 time more likely to have positive attitude towards COVID-19 than the male students (AOR=1.56, 95% CI [1.03 - 2.38]). Positive attitude was found to be about 6 times higher among the students with marital status single, compared to married students (AOR= 5.96, 95% CI [2.52 -14.09]), about 3 times higher among the students with good knowledge. Compared to the students with poor knowledge (AOR=3.13, 95% CI [2.04 - 4.76]).

THE DEUBIQUITYLASE USP5 KNOCKDOWN

Prevalence of mental health conditions and their differentials

Table 6 presents the prevalence of 3 mental health conditions namely depression, anxiety, and stress among the students. Overall, the prevalence of mild to moderate levels of depression, anxiety, and stress were found to be 66.3%, 69.2%, and 71.0%, respectively. The prevalence of severe level of depression, anxiety and stress were found to be 37.3%, 40.2% and 23.7%, respectively, which indicates that the severe form of mental conditions explained the major part of the overall prevalence.

Table 6. Prevalence of Depression, Anxiety and Stress among students.

Level	Depression		Anxiety		Stress	
	Number	%	Number	%	Number	%
Normal	657	33.7	601	30.8	566	29.0
Mild	265	13.6	191	9.8	325	16.7
Moderate	302	15.5	375	19.2	598	30.6
Severe	727	37.3	784	40.2	462	23.7
Total	1951	100.0	1951	100.0	1951	100.0

The bivariate analyses presented in Table 7 indicate that students' gender, college of study, level of study, admission cohort, marital status, and knowledge of COVID-19 have significant differential effects on the prevalence of the symptoms of the 3 mental health conditions. The prevalence of symptoms of the 3 mental health conditions was found to be significantly higher among females, undergraduate and single students. Students with good knowledge about COVID-19 were found to have a higher prevalence of depression and anxiety than the students with inadequate knowledge, but the lower prevalence of stress (69.5% vs. 77.3). Students from the College of Arts and Social Sciences showed the higher prevalence of depression, while students from the college of Nursing exhibited the lowest prevalence (54.0%) of depression. On the other hand, the prevalence of anxiety was found to be highest (79.7%) among the students from the College of Medicine and Health Sciences, and lowest among the students from the College of Education (61.9%). Students from the recent cohort showed a higher prevalence of depression, anxiety, distress, and FMD than that of older cohorts.

Determinants of depression, anxiety, and stress

Table 8 presents the results of multiple logistic regression analysis showing the adjusted effects of the characteristics of students on having any symptoms of depression, anxiety, and stress. The adjusted effect of a factor was measured by the adjusted odds ratio (AOR) obtained after controlling the effects of other factors. The results indicate that female students had more than 2 times higher odds of all the 3 mental health conditions compared to male students (AORs and 95% CIs: 2.04 (1.77-2.33) for depression, 2.07(1.67-2.57) for anxiety, 2.51(2.00-3.16) for stress. Students from the College of Arts and Social Sciences, College of Engineering and College of Science were reported to have had more than 2 times higher odds of depression, compared with students from the college of nursing. Students living in the urban area had 27% higher odds of having stress than their rural counterparts (AOR=1.27, 95% CI [1.02-1.61]). Unmarried (single) students were found to have 1.65 times higher odds of being stressed than the married students (AOR=1.65, 95% CI [1.03-2.69]). Knowledge about COVID-19 showed a significant association with the symptom of stress. Students with good knowledge about COVID-19 had 35% lower odds of having stress than the students with no or inadequate knowledge (AOR=0.65, 95% CI [0.44-0.79]). Students from the recent cohorts were more likely to have had mental distress, and anxiety than the older cohorts. However attitudes towards COVID-19 showed no significant association with mental health conditions.

Table 7. Prevalence of mild to severe depression, anxiety and stress by characteristics of students.

Characteristics	Depression ^a		Anxiety ^b		Stress ^c	
	Mild-severe	<i>p-value</i> ^d	Mild-severe	<i>p-value</i> ^d	Mild-severe	<i>p-value</i> ^d
Total sample	66.3		69.2		71.0	
Age		0.672		0.892		0.137
< 20	68.2		69.0		75.0	
20-24	65.7		69.7		71.6	
25-29	63.7		68.1		70.2	
30+	65.9		66.7		71.1	
Gender		<0.001		<0.001		<0.001
Male	60.0		60.6		60.2	
Female	75.3		74.9		78.2	
College of study (major)		0.042		0.017		0.244
Arts and Social Sciences	71.3		69.2		75.8	

Agricultural & Marine Sciences	65.1		71.9		67.1	
Education	60.7		61.9		66.7	
Economics and Political Science	65.7		71.3		73.3	
Engineering	69.6		69.3		68.7	
Law	60.3		62.9		69.8	
Medicine & Health Sciences	68.1		79.7		75.4	
Science	69.4		70.7		71.3	
Nursing	54.0		70.0		76.0	
Level of study		<0.001		<0.001		0.003
Foundation (pre-major)	63.3		61.2		65.3	
Under graduate	67.9		70.8		72.2	
Graduate	56.6		60.7		65.3	
Post-graduate (PhD)	37.0		37.0		44.4	
Admission cohort		0.208		<0.001		0.010
Before 2016	63		63.8		67.4	
2016	67.2		66.0		68.1	
2017	67.8		77.1		75.6	
2018	65.1		74.7		65.1	
2019	66.9		71.0		72.6	
2020	71.2		73.4		76.9	
Place of residence		0.719		0.739		0.137
Urban	66.7		69.5		72.3	
Rural	65.9		68.8		69.3	
Marital status		0.001		<0.001		<0.001
Single	67.4		70.3		72.2	
Married	53.9		56.5		56.5	
Dwelling type		0.663		0.144		0.443
Traditional Arabian house	67.0		69.7		71.4	
Flat house	63.4		60.4		65.3	
Villa	65.4		69.6		71.0	
Monthly HH income (in OR)		0.156		0.125		0.721
< 1000	68.6		69.7		71.9	
1000 - 2000	64.1		67.0		70.1	
>2000	66.0		73.0		70.9	
Test for COVID-19		0.543		0.753		0.175
Not tested	66.2		69.1		71.6	
Tested Negative	66.7		68.9		68.9	
Tested positive	69.0		73.2		62.0	
Knowledge		0.179		0.020		0.003
Good	65.6		68.0		69.5	
Poor	69.3		74.3		77.3	
Attitude		0.784		0,792		
Positive	66.5		69.1		71.2	0.593
Negative	65.7		69.8		69.8	

a Score of 10 or more were defined as mild-to-severe depression;

b Scores of 8 or more were defined as mild-to-severe anxiety;

c Scores of 15 or more were defined as mild-to-severe stress;

d p-value relate to Chi-square tests to compare the prevalence of mild-to-severe mental health symptoms in different sub-groups of populations.

THE DEUBIQUITYLASE USP5 KNOCKDOWN

Table 8. Multiple logistic regression analysis showing the adjusted odds ratios (AORs) and the confidence intervals (CIs) of odds of symptoms of depression, anxiety and stress among students.

Characteristics	Depression			Anxiety			Stress		
	B	AOR(95%CI)	p-value	B	AOR(95%CI)	p-value	B	AOR(95%CI)	p-value
Age									
< 20	0.29	1.34(0.86, 2.08)	0.187	0.28	1.32(0.85, 2.05)	0.204	0.06	1.06(0.62, 1.61)	0.897
20-24	0.22	1.24(0.81, 1.88)	0.317	0.32	1.38(0.91, 2.10)	0.123	0.05	1.05(0.66, 1.64)	0.553
25-29	0.19	1.21(0.69, 2.08)	0.503	0.36	1.43(0.82, 2.50)	0.198	0.03	1.03(0.47, 1.56)	0.346
30+ (ref.)		1.00			1.00			1.00	
Gender									
Male (ref.)		1.00			1.00			1.00	
Female	0.36	1.44(1.16, 1.78)	<0.001	0.73	2.07(1.67, 2.57)	<0.001	0.92	2.51(2.00, 3.16)	<0.001
College of study (major)									
Arts and Social Sciences	0.77	2.16(1.11, 4.22)	0.024	-0.19	0.83(0.41, 1.68)	0.613	-0.24	0.79(0.36, 1.71)	0.559
Agricultural & Marine Sciences	0.42	1.52(0.75, 3.05)	0.240	-0.02	0.98(0.46, 2.05)	0.958	-0.73	0.48(0.21, 1.05)	0.067
Education	0.29	1.34(0.69, 2.58)	0.376	-0.48	0.62(0.31, 1.24)	0.178	-0.65	0.52(0.24, 1.11)	0.094
Economics and Political Science	0.49	1.63(0.85, 3.12)	0.142	-0.01	0.99(0.49, 1.99)	0.995	-0.30	0.74(0.35, 1.57)	0.439
Engineering	0.83	2.30(1.19, 4.43)	0.013	0.10	1.10(0.55, 2.21)	0.780	-0.25	0.78(0.37, 1.66)	0.530
Law	0.28	1.32(0.63, 2.72)	0.118	-0.34	0.71(0.33, 1.52)	0.377	-0.36	0.70(0.31, 1.61)	0.402
Medicine & Health Sciences	0.67	1.95(0.95, 3.99)	0.067	0.51	1.67(0.76, 3.63)	0.196	-0.09	0.91(0.41, 2.08)	0.839
Science	0.70	2.01(1.05, 3.85)	0.032	-0.02	0.98(0.49, 1.95)	0.955	-0.40	0.67(0.32, 1.40)	0.284
Nursing (ref.)		1.00			1.00			1.00	
Level of study									
Foundation (pre-major)	1.30	3.66(1.24, 10.82)	0.018	1.32	3.75(1.27, 11.12)	0.017	0.79	2.20(0.73, 6.59)	0.156
Under graduate	1.06	2.89(1.19, 7.07)	0.021	1.14	3.14(1.27, 7.73)	0.013	0.62	1.85(0.75, 4.52)	0.177
Graduate	0.68	1.97(0.82, 4.74)	0.129	0.92	2.51(1.03, 6.11)	0.041	0.60	1.82(0.75, 4.41)	0.180
Post-graduate (PhD) (ref.)	0.00	1.00			1.00			1.00	
Admission cohort									
Before 2016 (ref.)	0.00	1.00			1.00			1.00	
2016	-0.12	0.89 (0.52, 1.50)	0.661	0.43	1.54(0.88, 2.71)	0.127	-0.16	0.85(0.49, 1.46)	0.566
2017	-0.05	0.95(0.67, 1.35)	0.811	-0.08	0.92(0.65, 1.30)	0.658	-0.17	0.84(0.58, 1.20)	0.344
2018	0.01	1.01(0.73, 1.42)	0.928	0.52	1.69(1.18, 2.43)	0.004	0.26	1.30(0.90, 1.87)	0.157
2019	0.25	1.29(0.94, 1.76)	0.109	0.33	1.39(1.05, 1.92)	0.037	0.37	1.45(1.03, 2.03)	0.030
2020	0.13	1.14(0.85, 1.51)	0.386	0.30	1.35(1.03, 1.81)	0.043	0.21	1.23(0.90, 1.67)	0.179
Place of residence									
Urban	0.11	1.12(0.89, 1.39)	0.321	0.08	1.08(0.86, 1.35)	0.502	0.24	1.27(1.01, 1.61)	0.034
Rural (ref.)	0.00	1.00			1.00			1.00	
Marital status									
Single	0.02	1.02(0.63, 1.62)	0.943	0.07	1.07(0.67, 1.73)	0.756	0.50	1.65(1.02, 2.69)	0.038
Married (ref.)	0.00	1.00			1.00			1.00	
Dwelling type									
Traditional Arabian house	0.06	1.06(0.83, 1.35)	0.623	0.06	1.06(0.82, 1.36)	0.640	0.11	1.12(0.86, 1.45)	0.385
Flat house	0.19	1.21(0.73, 1.98)	0.454	-0.16	0.85(0.52, 1.40)	0.531	0.08	1.08(0.64, 1.81)	0.768
Villa (ref.)	0.00	1.00			1.00			1.00	
Monthly HH income (in OR)									
< 1000	0.18	1.20(0.89, 1.62)	0.224	-0.12	0.89(0.65, 1.23)	0.499	0.10	1.11(0.80, 1.53)	0.533
1000 - 2000	-0.04	0.96(0.72, 1.28)	0.824	-0.24	0.79(0.58, 1.07)	0.128	0.02	1.02(0.74, 1.39)	0.897
>2000 (ref.)	0.00	1.00			1.00			1.00	
Test for COVID-19									
Not tested	0.00	1.00			1.00			1.00	

(ref.)									
Tested Negative	0.08	1.08(0.78, 2.13)	0.514	-0.02	0.98(0.62, 1.12)	0.764	-0.12	0.89(0.68, 1.88)	0.651
Tested positive	0.21	1.23(0.97, 3.12)	0.128	0.11	1.12(0.73, 1.21)	0.286	-0.08	0.92(0.62, 1.98)	0.345
Knowledge									
Good	-0.20	0.82(0.63, 1.06)	0.131	-0.43	0.65(0.50, 0.87)	0.003	-0.49	0.61(0.46, 0.81)	0.001
Poor									
Attitude									
Positive	-0.01	0.99(0.76, 1.28)	0.963	-0.08	0.92(0.71,1.21)	0.565	0.06	1.06(0.81, 1.39)	0.680
Negative									

Note: AOR= Adjusted Odds Ratio, ref= reference category; CI= confidence interval.

a Score of 10 or more were defined as mild-to-severe depression.

b Scores of 8 or more were defined as mild-to-severe anxiety. c Scores of 15 or more were defined as mild-to-severe stress.

4. Discussion

The findings of this study indicate a high rate of effective knowledge about COVID-19 among the university students in Oman. Overall, 81% of the students had good knowledge about COVID-19 which is comparable with the findings in China (82.34%) [31], Saudi Arabia (80%) [37], Iran (87%) [38], and Pakistan (80%) [39]. However, the knowledge level among the students in our study is higher than observed in Bangladesh (50%) [40], Uganda (68%) [41], India (70%) [42], and Ethiopia (76%) [30], but lower than observed in the Philippines (92%) [43] and Iraq (92%) [44]. These differences in knowledge across the countries might be attributed to the differences in the study populations and the measuring tools to assess knowledge about COVID-19.

This study documented a high level of knowledge about COVID-19 etiology, signs and symptoms, main route of transmission, and prevention mechanisms among the university students, which is appreciable and would help in adopting and implementing preventive measures in spreading COVID-19. This finding is similar to that reported among the students in higher educational institution in the Philippines [39], Pakistan [39], Saudi Arabia [37], and Ethiopia [30].

Female students had significantly higher level of good knowledge about COVID-19 than the male students. This might be due to the fact that female students were more concerned about the disease and its preventive mechanisms. There were mixed results about the association between gender and the level of good knowledge about COVID-19. College of the study appeared as a significant predictor of knowledge of students about COVID-19 which was consistent with findings of other studies [30,31,41]. Students from the College of Medicine and Health Sciences and from the College of Nursing showed higher levels of knowledge about COVID-19 than others, which may be attributed to the training of these students about diseases, medicine and public health, as well as their commitment to the medical profession [41]. Students living in urban areas had a higher level of knowledge than their rural counterparts, which is consistent with the findings of previous studies [40,45,46]. This might be due to the fact that students living in urban areas might have higher chance of accessing the main sources of information including social media and internet. Cohort or study year was also another factor affecting knowledge about COVID-19. Students from older cohorts or more years of study had higher level of knowledge than their younger counterparts. The finding is consistent with findings of the studies in Ethiopia [30,47].

The results also indicated high level of positive attitudes towards COVID-19, as more than eighty percent (83%) of the students had a positive attitude towards COVID-19 which was in line with the findings of the studies in Pakistan (82%), Ethiopia (82%), (2021), and Nigeria (80%) [32,48,49]. However, to some extent, there exists a COVID-19 related stigma, as slightly more than one-third (35%) of the students believed that COVID-19 is a natural catastrophe. Regarding factors associated with positive attitude, female students were found to be more likely to have positive attitudes towards COVID-19 than their male counterparts. This finding is consistent with the findings of studies conducted in Saudi Arabia [50], Bangladesh [51], and Pakistan [52]. Good knowledge toward COVID-19 was found to be significantly associated with positive attitude about COVID-19, which is consistent with finding of the previous studies [30,53,54].

The results indicate high prevalence of depression, anxiety, and stress among university students in Oman. The prevalence of mild to severe level of depression, anxiety, and stress, were found to be 66.3%, 69.2%, and 71.0%, respectively. The severe forms of depression, anxiety and distress constituted the major part of the prevalence. More than one-third (37%) of the students exhibited a severe level of depression, while 40.2% exhibited severe anxiety, nearly one-fourth (23.7%) exhibited a severe level of stress.

There is no comparable study in Oman during the current pandemic to check the consistency of our findings of the prevalence of depression, anxiety, and stress among university students. However, a recent study documented that the prevalence of depression, anxiety, and distress were 25%, 22%, and 30%, respectively, among the general adult population of Oman [55]. In another recent multicounty cross-sectional study, Al Omari, *et al.* [56] reported that the prevalence of depression, anxiety, and stress were observed to be 56.2%, 39.4%, and 31%, respectively, among the

THE DEUBIQUITYLASE USP5 KNOCKDOWN

Omani youth of age 15-24 years. All these results indicate that the prevalence of the 3 mental health conditions is substantially higher among the university students in Oman than the Omani general population. Even before the COVID-19 pandemic, many studies across the globe reported higher levels of depression, anxiety, and stress among students than the general population [29,57,58].

Students' mental health can be attributed to a series of factors that range from individual, interpersonal, and institutional levels [59]. On the individual level, students' low self-esteem and lack of coping abilities were correlated with higher levels of depression and even suicide [59,60]. On the institutional level, academic curriculum, campus climate, and faculty interaction largely determined students' experiences at school, which were potential factors that correlated with their mental health [61].

Our findings on mental health status of students in Oman are in close agreement with the findings of the study in Bangladesh [62], Europe and Asia [63], Turkey [64], and the Kingdom of Saudi Arabia [65]. Undergraduate students were found to have had about 3 time higher odds of having mild to severe level of depression and anxiety. This finding is consistent with the findings of the study among university students in Jordan [66], and in Saudi Arabia [65], showing that students with lower educational levels had higher odds of having symptoms of mental disorders.

Female students were found to have had more than 2 times higher risk for anxiety and about 1.5 times higher risk of depression. These findings are consistent with the findings of the multicounty studies of Ochnik et al [63] and Al Omari et al [56]. A recent study in Saudi Arabia also documented a 2.5 times higher risk of anxiety and stress and 1.7 times higher risk of depression among female students than male students [65]. The underlying reasons might be that females are more concerned about their success in a future career, physical appearance, and peer pressure. Also, females are more likely to undergo negative social changes that were brought by social media, consumer culture [67], and cultural expectations [68]. Good knowledge about COVID-19 was found to be negatively associated with anxiety and stress.

The study is not free from limitations. The most important limitations lie with the method of data collection and self-reporting. As the data was collected through online survey, which is associated with an under-coverage problem and lack of proper sampling design, resulting in sampling bias. This could limit the representativeness of the study findings. Under-coverage occurs because many potential respondents do not have easy access to internet or that many students declined to participate in the survey, and thus they were excluded. On the other hand, in an online survey, proper sampling design cannot be maintained as the respondents are self-selected, and thus introduced another kind of bias to the sample. Another limitation is the subjectivity of the students in providing information about knowledge, attitude and symptoms of mental health through a self-administered questionnaire. Despite using a validated and reliable questionnaire, it cannot be assumed that students were totally objective while providing information.

5. Conclusion

This study demonstrates a high prevalence of good knowledge and positive attitude of Omani students towards COVID-19, and at the same time high rate of depression, anxiety, and stress in the university population. Although the findings suggest an overall satisfactory level of knowledge and positive attitude, there still prevails some misconceptions or stigma to a group of students as about one-third of the students opined that COVID-19 is a natural catastrophe and 13% students were in favor of keeping it secret if infected the virus. Also about 18% students had negative attitudes and same percentage had poor knowledge about COVID-19. Positive attitude was found to be highly associated with good knowledge about COVID-19. Good knowledge about COVID-19 appeared as significant predictors of mental health problems. All these findings underscore the need for more educational programs and behavior change communication. It has been observed that the COVID-19 pandemic has increased the mental health issues of university students. More research is needed to identify the reasons for the high prevalence of mental health issues. Younger age, female gender, recent admission cohorts of students, undergraduate students, marital status, college of the study appeared as significant predictors of negative mental health symptoms among the students. The findings of high and elevated mental health symptoms among the university students of this study might have important policy implications for health planners, university administration, faculty members and the healthcare providers in improving the mental health status of university students. Effective mental health services and educational programs need to be designed for the students to meet their mental health needs and development of prevention mechanisms. The mental health services should include educating students about the signs and symptoms of mental illnesses (e.g., anxiety and depression), and their coping mechanisms. Educating students about correct knowledge and stress management methods would help overcome many of the challenges they are facing out of COVID-19 pandemic. Establishing counseling centers and mental health clinics in the university for monitoring and managing psychological problems among university students could be effective and the students should be encouraged to join these centers and clinics when they need such support. Emphasis should also be given to increase the community awareness, particularly among the parents, faculties and healthcare providers about student's mental health and wellbeing.

Conflict of interest

The authors declare no conflict of interest.

Acknowledgment

The authors would like to acknowledge the individuals who participated in the study. The views expressed herein are solely those of the authors and do not necessarily reflect the views of any institution or organization.

Funding

The study received no fund from any organization.

References

1. World Health Organization (WHO). Severe Acute Respiratory Infections Treatment Centre Practical manual to set up and manage a SARI treatment centre and a SARI screening facility in health care facilities. Geneva: World Health Organization; 2020.
2. Wang, C., Pan, R., Wan, X., Tan, Y., Xu, L, Ho, C.S. and Ho, R.C. Immediate psychological responses and associated factors during the initial stage of the 2019 coronavirus disease (COVID-19) epidemic among the general population in China. *International Journal of Environmental Research and Public Health*, 2020, **17(5)**, 1729. <https://doi.org/10.3390/ijerph17051729>.
3. World Health Organization (WHO). Investigation of cases of human infection with Middle East respiratory syndrome coronavirus (MERS-CoV): Interim guidance. Geneva: World Health Organization, 2018.
4. World Health Organization. WHO Director-General's opening remarks at the media briefing on COVID-19 - 11 March 2020. <https://www.who.int/dg/speeches/detail/who-director-general-s-opening-remarks-at-the-mediabriefing-on-COVID-19%2D%2D11-march-2020>.
5. World Health Organization. WHO Coronavirus Disease (COVID-19) Dashboard: World Health Organization, Geneva: WHO, 2020.
6. Li, J.Y., You, Z., Wang, Q., Zhou, Z., Qiu, Y., Luo, R. and Ge, X. The Epidemic of 2019-Novel-Coronavirus (2019-nCoV) Pneumonia and Insights for Emerging Infectious Diseases in the Future. *Microbes and Infection*, 2020, **22**, 80-85. <https://doi.org/10.1016/j.micinf.2020.02.002>.
7. Gao, Q., Hu, Y., Dai, Z., Xiao, F., Wang, J., Wu, J. The epidemiological characteristics of 2019 novel coronavirus diseases (COVID-19) in Jingmen, Hubei, China. *Medicine (Baltimore)*, 2020, **99(23)**, e20605. <https://doi.org/10.1097/MD.00000000000020605> PMID: 32502034.
8. Zhong, B., Huang, Y. and Liu, Q. Mental health toll from the coronavirus: social media usage reveals Wuhan residents' depression and secondary trauma. in the COVID-19 outbreak. *Comput. Hum. Behav.*, 2021, **114**, 106524. doi: 10.1016/j.chb.2020.106524.
9. Zhong, B.L., Luo, W., Li, H.M., Zhang, Q.Q., Liu, X.G, Li, W.T. and Li, W. Knowledge, Attitudes, and Practices towards COVID-19 among Chinese Residents during the Rapid Rise Period of the COVID-19 Outbreak: A Quick Online Cross-Sectional Survey. *International Journal of Biological Sciences*, 2020, **16**,1745-1752.
10. Center for Disease Control (CDC). Coronavirus Disease 2029 (COVID-19). Symptoms of Coronavirus, 2021. <https://www.cdc.gov/coronavirus/2019-ncov/symptoms-testing/symptoms.html>.
11. Abdelhafiz, A.S., Mohammed, Z., Ibrahim, M.E., Ziady, H.H., Alorabi, M., Ayyad, M. and Sultan, E.A. Knowledge, Perceptions, and Attitude of Egyptians towards the Novel Coronavirus Disease (COVID-19). *Journal of Community Health*, 2020, **45**, 881-890. <https://doi.org/10.1007/s10900-020-00827-7>.
12. World Health Organization. Coronavirus Disease (COVID-19) Advice for the Public, Geneva: World Health Organization, 2020. <https://www.who.int/emergencies/diseases/novelcoronavirus-2019/advice-for-public>.
13. Harapan, H., Itoh, N., Yufika, A., Winardi, W., Keam, S., Te, H., Megawati, D., Hayati, Z., Wagner, A.L. and Mudatsir, M. Coronavirious disease 2019 (COVID-19): A literature review. *Journal of Infection and Public Health*, 2020, **13**, 667-673. <https://doi.org/10.1016/j.jiph.2020.03.019> PMID:32340833.
14. Bedford, J., Enria, D., Giesecke, J., Heymann, D.L., Ihekweazu, C. and Kobinger, G., Lane, H.C., Memish, Z., Oh, M., Sall, A.A., Schuchat, A., Ungchusak, K. and Wieler, L.H. WHO Strategic and Technical Advisory Group for Infectious Hazards. COVID-19: towards controlling of a pandemic. *Lancet*, 2020, **395(10229)**, 1015-8. [https://doi.org/10.1016/S0140-6736\(20\)30673-5](https://doi.org/10.1016/S0140-6736(20)30673-5) PMID: 32197103.
15. Khatatbeh, M. Efficacy of nationwide curfew to encounter spread of COVID-19: a case from Jordan. *Frontiers in Public Health*, 2020, **8**, 394.
16. Al Dhaheri, A.S., Bataineh, M.F., Mohamad, M.N., Ajab, A., Al Marzouqi, A., Jarrar, A.H., Carla Habib-Mourad, C., Abu Jamous, D.O., Ali, H.I., Al Sabbah, H., Hasan, H., Stojanovska, L. and Hashim, M. Impact of COVID-19 on mental health and quality of life: Is there any effect? A cross-sectional study of the MENA region. *PLoS ONE*, 2021; **16(3)**: e0249107. <https://doi.org/10.1371/journal.pone.0249107>.
17. Brooks, S.K., Webster, R.K., Smith, L.E., Woodland, L., Wessely, S., Greenberg, N. and Rubin, G.J. The psychological impact of quarantine and how to reduce it: rapid review of the evidence. *Lancet*, 2020, **395(10227)**, 912-920. doi: 10.1016/S0140-6736(20)30460-8.
18. Amerio, A., Brambilla, A., Morganti, A., Aguglia, A., Bianchi, D., Santi, F., Costantini, L., Odone, A., Costanza, A., Signorelli, C., Serafini, G., Amore, M. and Capolongo, S. COVID-19 lockdown: housing built environment's

THE DEUBIQUITYLASE USP5 KNOCKDOWN

- effects on mental health. *International Journal of Environmental Research and public Health*. 2020, **17**, 5973. doi: 10.3390/ijerph1716.
19. Ren, Y., Qian, W., Li, Z., Liu, Z., Zhou, Y., Wang, R., Qi, L., Yang, J., Song, X., Zeng, L. and Zhang, X. Public mental health under the long-term influence of COVID-19 in China: geographical and temporal distribution. *Journal of Affect Disord*. 2020, **277**, 893-900. doi: 10.1016/j.jad.2020.08.045.
 20. Chaturvedi, K., Vishwakarma, D.K. and Singh, N. COVID-19 and its impact on education, social life and mental health of students: A survey. *Children and youth services review*, 2021, **121**, 105866. <https://doi.org/10.1016/j.chilyouth.2020.105866>.
 21. Elmer, T., Mepham, K. and Stadtfeld, C. Students under lockdown: Comparisons of students' social networks and mental health before and during the COVID-19 crisis in Switzerland. *PLoS ONE*, 2020, **15**, e0236337.
 22. Liang, L., Ren, H., Cao, R., Hu, Y., Qin, Z., Li, C. and Mei, S. The Effect of COVID-19 on Youth Mental Health. *Psychiatr. Q*, 2020, **91**, 841-852.
 23. Ibrahim, A.K., Kelly, S.J., Adams, C.E. and Glazebrook, C. A systematic review of studies of depression prevalence in university students. *Journal of Psychiatric Research*, 2013, **47**, 391-400. <https://doi.org/10.1016/j.jpsychires.2012.11.015>.
 24. Robotham, D. and Julian, C. Stress and the higher education student: A critical review of the literature. *Journal of Further High Education*. 2006, **30**, 107-117.
 25. Mikolajczyk, R.T., Maxwell, A.E., El-Ansari, W., Naydenova, V., Stock, C., Ilieva, S., Dudziak, U. and Nagyova, I. Prevalence of depressive symptoms in university students from Germany, Denmark, Poland and Bulgaria. *Social Psychiatry and Psychiatric Epidemiology* 2008. **43(2)**, 105-112. PMID: 18038173.
 26. Al Foukha, M.M., Hamdan-Mansour, A.M. and Banihani, M.A. Social and psychological factors related to risk of eating disorders among high school girls. *The Journal of School Nursing*, 2019, **35(3)**, 169-177. <https://doi.org/10.1177/1059840517737140>.
 27. Read, J.P., Wood, M.D., Davidoff, O.J., McLacken, J. and Campbell, J.F. Making the transition from high school to college: the role of alcohol-related social influence factors in students' drinking. *Substance Abuse*., 2002, **23(1)**, 53-65.
 28. Peric, S. and Stulnig, T.M. Diabetes and COVID-19: Disease-Management-People. *Wiener klinische Wochenschrift*, 2020, **132(13-14)**, 356-361. <https://doi.org/10.1007/s00508-020-01672-3>.
 29. Al Bashir, A. The potential impacts of obesity on COVID-19. *Clinical medicine (London, England)*, 2020, **20(4)**, e109-e113. <https://doi.org/10.7861/clinmed.2020-0239>.
 30. Berihun, G., Walle, Z., Teshome, D., Berhanu, L., Abebe, M., Ademas, A., Gizeyatu, A., Keleb, A., Malede, A., Atikilt, G., Teym, A. and Adane, M. Knowledge, Attitude, and Preventive Practices Towards COVID-19 Among Students of Ethiopian Higher Education Institutions. *Journal of Multidisciplinary Healthcare*, 2021, **14**, 2123-2136.
 31. Peng, YL., Pei, CC., Zheng, Y., Wang, J., Zhang, K., Zheng, ZH. and Zhu, P. Knowledge, Attitude and Practice Associated with COVID-19 among University Students: A Cross-Sectional Survey in China. *BMC Public Health* 2020, **20**, 1292. <https://doi.org/10.1186/s12889-020-09392-z>.
 32. Reuben, R.C., Danladi, M.M.A., Saleh, D.A. and Ejembi, P.E. Knowledge, Attitudes and Practices Towards COVID-19: An Epidemiological Survey in North-Central Nigeria. *Journal of Community Health*, 2021, **46**, 457-470. <https://doi.org/10.1007/s10900-020-00881-1>.
 33. Lovibond, S. and Lovibond, P. *Manual for the Depression Anxiety Stress Scales*. 2nd ed. Psychology Foundation of Australia, 1995. <http://www2.psy.unsw.edu.au/dass/order.htm>.
 34. Wong, J.G., Cheung, E.P., Chan, K.K., Ma, K.K. and Tang, S.W. Web-based survey of depression, anxiety and stress in first-year tertiary education students in Hong Kong. *Aust. N.Z. J. Psychiatry*, 2006, **40**, 777-782.
 35. Gloster, A.T., Rhoades, H.M., Novy, D., Klotsche, J., Senior, A., Kunik, M., M., Wilson, N. and Stanley, M.A. Psychometric properties of the depression anxiety and stress scale-21 in older primary care patients. *Journal of Affect Disord.*, 2008, **110**, 248-259.
 36. Oei, T.P.S., Sawan, g S., Goh, Y.W. and Mukhtar, F. Using the depression anxiety stress scale 21 (DASS-21) across cultures. *International Journal of Psychology*. 2013, **48**, 1018-1029.
 37. Sheeliya, W., Manahil, O. and Ghada, N.M. Knowledge, Attitude and Practice on Prevention of Airborne and Droplet Infections during the Outbreak of Corona Virus among the College Students in University of Bisha, Saudi Arabia. *IJCRR*, 2020, **11**, 20773-20776.
 38. Taghrir, M.H., Borazjani, R. and Shiraly, R. COVID-19 and Iranian Medical Students; a Survey on Their Related-Knowledge, Preventive Behaviours and Risk Perception. *Archives of Iranian Medicine*, 2020, **23**, 249-254. <https://doi.org/10.34172/aim.2020.06>.
 39. Ikhlaq, A., Bint-E-Riaz, H., Bashir, I. and Ijaz, F. Awareness and Attitude of Undergraduate Medical Students towards 2019-Novel Coronavirus. *Pakistan Journal of Medical Sciences* 2020, **36**, S32-S36. <https://doi.org/10.12669/pjms.36.COVID19-S4.2636>.
 40. Patwary, MM., Disha, AS., Bardhan, M., Haque, MZ., Kabir, MP., Billah, SM. Hossain, M.R., Alam, M.A., Browning, M.H.E.M., Shuvo, F.K., Piracha, A., Zhao, B., Swed, S, Shah, J. and Shoib, S. Knowledge, Attitudes, and Practices Toward Coronavirus and Associated Anxiety Symptoms Among University Students: A Cross-Sectional Study During the Early Stages of the COVID-19 Pandemic in Bangladesh. *Front. Psychiatry*, 2022, **13**, 856202. doi: 10.3389/fpsy.2022.856202.

41. Nyeko, R., Amanya, S.B., Aleni, M. and Akello, F. Unsatisfactory COVID-19-Related Knowledge, Attitudes and Practices among Undergraduate University Students in Uganda: An Online Cross-Sectional Survey. *Open Journal of Preventive Medicine*, 2021, **11**, 259-283. <https://doi.org/10.4236/ojpm.2021.116021>.
42. Prasad, S.J., Sewda, A. and Shiv, D.G. Assessing the knowledge, attitude and practices of students regarding the COVID-19 pandemic. *Journal of Health Management*, 2020, **22**, 281-290.
43. Bautista, Jr. AP., Balibrea, D. and Bleza, D.G. Knowledge, Attitude and Practice Toward the Coronavirus Disease (COVID-19) Outbreak Among Selected Employed People in the National Capital Region, Philippines *Asian Journal for Public Opinion Research* 2020, **8(3)**, 2020, 324-350. <http://dx.doi.org/10.15206/ajpor.2020.8.3.324>.
44. Khalil, N.S., Al-yuzbaki, D.B. and Tawfeeq, R.S. COVID-19 knowledge, attitude, and practice among medical undergraduate students in Baghdad City. *Eurasian Journal of Bioscience*. 2020, **14**, 4179-4186.
45. Getawa, S., Aynalem, M., Bayleyegn, B. and Adane, T. Knowledge, attitude and practice towards COVID-19 among secondary school students in Gondar town, Northwest Ethiopia. *PLoS ONE*, 2022, **17(5)**, e0268084. <https://doi.org/10.1371/journal.pone.0268084>.
46. Kumar, B., Pinkey, S.D. and Nurudden, A.M. Knowledge, attitudes and practices towards COVID-19 guidelines among students in Bangladesh. *Social Sciences and Humanities Open*, 2021; **4**:100194. <http://creativecommons.org/licenses/by-nc-nd/4.0/>.
47. Tadesse, S. and Muluye, W. The Impact of COVID-19 Pandemic on Education System in Developing Countries: A Review. *Open Journal of Social Sciences*. 2020, **08(10)**, 159-70.
48. Hussain, I., Majeed, A., Imran, I., Ullah, M., Hashmi, F.K. and Saeed, H., Chaudhry, M.O. and Rasool, M.F. Knowledge, Attitude, and Practices Toward COVID-19 in Primary Healthcare Providers: A Cross-Sectional Study from Three Tertiary Care Hospitals of Peshawar, Pakistan. *Journal of Community Health*, 2021, **46**, 441-449. <https://doi.org/10.1007/s10900-020-00879-9>.
49. Gebretsadik, D., Gebremichael, S. and Belete, M.A. Knowledge, Attitude and Practice Toward COVID-19 Pandemic Among Population Visiting Dessie Health Center for COVID-19 Screening, Northeast Ethiopia. *Infect Drug Resist*, 2021, **14**, 905-15. <https://doi.org/10.2147/IDR.S297047> PMID: 33716509.
50. Al-Hanawi, M.K., Angawi, K., Alshareef, N., Qattan, AMN., Helmy, H.Z., Abudawood, Y., Alqurashi, M., Kattan, W.M., Kadasah, N.A., Chirwa, G.C., Alsharqi, O. Knowledge, Attitude and Practice toward COVID-19 among the Public in the Kingdom of Saudi Arabia: A Cross-Sectional Study. *Frontiers in Public Health*, 2020, **8**, 217. <https://doi.org/10.3389/fpubh.2020.00217>.
51. Ferdous, M.Z., Islam, M.S., Sikder, M.T., Mosaddek, ASM. Zegarra-Valdivia J.A. and Gozal, D. Knowledge, attitude, and practice regarding COVID-19 outbreak in Bangladesh: An online based cross-sectional study. *PLoS One* [Internet], 2020, **15**, 1-17. <http://dx.doi.org/10.1371/journal>.
52. Fatmi, Z., Mahmood, S., Hameed, W., Qazi, I., Siddiqui, M.M. and Dhanwani, A. and Siddiqi, S. Knowledge, attitudes and practices towards COVID-19 among Pakistani residents: information access and low literacy vulnerabilities. *Eastern Mediterranean Health Journal*. 2020, **26(12)**, 1446-1455. <https://doi.org/10.26719/emhj.20.133>.
53. Kassie, B.A., Adane, A., Tilahun, Y.T., Kassahun, E.A., Ayele, A.S. and Belew, A.K. Knowledge and attitude towards COVID-19 and associated factors among health care providers in Northwest Ethiopia. *PLoS One*, 2020, **15(8)**, e0238415. <https://doi.org/10.1371/journal.pone.0238415>.
54. Endriyas, M., Kawza, A., Alano, A., Hussen, M., Mekonnen, E., Samuel, T., Shiferaw, M., Ayele, S., Kelaye, T., Misganaw, T. and Shibru, E. Knowledge and attitude towards COVID-19 and its prevention in selected ten towns of SNNP Region, Ethiopia: Cross-sectional survey. *PLoS ONE*, 2021, **16(8)**, e0255884. <https://doi.org/10.1371/journal.pone.0255884>.
55. Al Sinawia, H., Al Balushi, N., Al-Mahrouqib, T., Al Ghailanib, A., McCallc, R.K. and Sultan, A., Al Sabti, H., Al Maniri, A., Panchatcharam, S.M. and Al-Alawi, M. Predictors of psychological distress among the public in Oman amid coronavirus disease 2019 pandemic: a cross-sectional analytical study. *Psychology, Health & Medicine*, 2021, **26(1)**, 131-144. DOI: 10.1080/13548506.2020.1842473.
56. Al Omari, O., Al Sabei, S., Al Rawajfah, O., Sharour, LA., Aljohani, K. and Alomari, K., Shkman, L., Al Dameery, K., Saifan, A., Al Zubidi, B., Anwar, S. and Alhalaiqa F. Prevalence and Predictors of Depression, Anxiety, and Stress among Youth at the Time of COVID-19: An Online Cross-Sectional Multicountry Study. *Depression Research and Treatment*, 2021, 2020, 1-9. <https://doi.org/10.1155/2020/8887727>.
57. Zeng, W., Chen, R., Wang, X., Zhang, Q. and Deng, W. Prevalence of mental health problems among medical students in China. *Medicine*, 2019, **98**, e15337.
58. Auerbach, RP., Mortier, P., Bruffaerts, R., Alonso, J., Benjet, C., Cuijpers, P., WHO WMH-ICS Collaborators. WHO World Mental Health Surveys International College Student Project: prevalence and distribution of mental disorders. *Journal of Abnormal Psychology*, 2018, **127(7)**, 623-638 [FREE Full text] [CrossRef] [Medline].
59. Byrd, DR. and McKinney, KJ. Individual, interpersonal, and institutional level factors associated with the mental health of college students. *Journal of American College Health*, 2012, **60(3)**, 185-93. <https://doi.org/10.1080/07448481.2011.584334>.
60. Wilburn, V. and Smith, D. Stress, self-esteem, and suicidal ideation in late adolescents. *Adolescence*, 2005, **40**, 33-45.

THE DEUBIQUITYLASE USP5 KNOCKDOWN

61. Hunt, J. and Eisenberg, D. Mental health problems and help seeking behavior among college students. *Journal of Adolescent Health*, 2010, **46**, 3-10.
 62. Islam, M.S., Sujan, MSH., Tasnim, R., Sikder, M.T., Potenza, M.N. and Van, O.J. Psychological responses during the COVID-19 outbreak among university students in Bangladesh. *PLoS ONE*, 2020, **15**(12), e0245083. <https://doi.org/10.1371/journal.pone.0245083>.
 63. Ochnik, D., Rogowska, A.M., Kuśnierz, C., Jakubiak, M., Schütz, A. and Held, M.J., Arzenšek, A., Benatov, J., Berger, R., Korchagina, E.V., Pavlova, I., Blažková, I., Imran Aslan, I., Çınar, O. and Cuero-Acosta, Y.A. Mental health prevalence and predictors among university students in nine countries during the COVID-19 pandemic: a cross-national study. *Scientific Reports*, 2021, **11**, 18644. <https://doi.org/10.1038/s41598-021-97697-3>.
 64. Aslan, I., Ochnik, D. and Çınar, O. Exploring Perceived Stress among Students in Turkey during the COVID-19 Pandemic. *International Journal of Environmental Research and Public Health*, 2020, **17**, 896. doi:10.3390/ijerph17238961.
 65. Al Hadi, A.N. and Al Huwaydi, A.M. The mental health impact of pandemic COVID-19 crisis on university students in Saudi Arabia and associated factors. *Journal of American College Health*, 2021; Publish online. DOI: 10.1080/07448481.2021.1947839.
 66. Nase, A.Y., Dahmash, E.Z., Al-Rousan, R., Alwafi, H., Alrawashdeh, H.M. and Ghoul, I. Abidine, A., Bokhary, M.A., AL-Hadithi, H.T., Ali, D., Abuthawabeh, R., Abdelwahab, G.M., Alhartani, Y., Al Muhaisen, J., Dagash, A. and Alyami, H.S. Mental health status of the general population, healthcare professionals, and university students during 2019 coronavirus disease outbreak in Jordan: A cross-sectional study. *Brain and Behavior*, 2020, **10**(8), e01730. doi: 10.1002/brb3.1730.
 67. Hamilton, M. What's happening to our girls? London: Penguin Books 2008. <https://www.questionPro.com>: Online survey software and tools.
 68. Eckersley, R. Never better or getting worse? The health and wellbeing of young Australians. Canberra: Australia, 2008.
 69. World Medical Association. World Medical Association Declaration of Helsinki: ethical principles for medical research involving human subjects. *Journal of the American Medical Association*. 2013, **310**(20), 2191-4. Epub 2013/10/22. <https://doi.org/10.1001/jama>.
-

Received 1 June 2023

Accepted 18 July 2023

Sultan Qaboos University Journal for Science

Instructions to Authors

Sultan Qaboos University Journal for Science (SQUJS) is an international peer-reviewed journal that publishes original basic and applied research articles in the fields of science. The journal provides a platform for specialists and practitioners and brings together quality papers dealing with mathematics, statistics, chemistry, physics, biology, biotechnology, environmental, earth sciences, and computer sciences as well as related disciplines. All issues of the SQU Journal for Science are freely available online and do not carry any publication charges.

Types of manuscript published

Manuscripts submitted for publication in the SQU Journal for Science must be based on original work and have not been published, accepted or submitted for publication elsewhere. The journal accepts the following types of manuscripts:

1. Editorials (by invitation from the Editorial Board, or papers received of exceptional merit)
2. Review papers
3. Research papers
4. Short communications/Notes
5. Perspectives
6. Case studies

Submission procedure

Manuscripts should be submitted online through the journal management system (<https://journals.squ.edu.om/index.php/squjs>) or electronically to the office of the Journal: squjs@squ.edu.om. To facilitate the preparation of manuscripts that correspond to the Journal format, the Editorial Board has prepared a template, which can be downloaded from the journal website.

Reviewing policy

The SQU Journal for Science uses a blind review process in which the peer reviewers' names are not disclosed to the authors, although the reviewer can make himself known should he choose to do so. Before submitting the papers for review the subject editors will evaluate the suitability of the manuscript for the journal (language, readership, format, etc.), insure the completeness of the submission and make an initial "plagiarism" assessment of the manuscript.

If the manuscript is suitable for the journal, the subject editors will choose 2-3 reviewers among researchers working in a similar field. The selection of reviewers is based on several factors: expertise, reputation, specific recommendations of the author or of a reviewer, and our own previous experience of a reviewer's characteristics. The subject editors will request a minimum of two independent reviews but can if necessary request additional evaluations, particularly if 2 reviewers have severely contradictory opinions on a particular manuscript.

Following the reviews, the subject editor will place the manuscript among one of four categories:

1. *Accepted* with minor modifications; the paper requires mostly editorial and typographic modifications).
2. *Accepted conditionally* to a revision of the papers following the recommendations and specific comments or concerns of the reviewers (the reviewers found incomplete or unclear statements that needs to be revised; some of the results may need to be reinterpreted or some figures redrawn; part of the discussion may need some additional work). The acceptance remains conditional until the editor is satisfied with the revision.
3. *Acceptable* but only after a second round of reviews (the paper cannot be accepted without a major revision of its structure or significant changes in its presentation. The author will receive all comments from the first set of reviewers and requested to resubmit the paper with the suggested modifications and amendments.
4. *Not acceptable*. The paper is not in a relevant area of the journal or is not of a suitable scientific level for publication in the journal.

The editor will then inform the corresponding author of the editorial decision and convey the comments and suggestions of the reviewers to which the author has to respond normally within 2-4 weeks. Authors may contact the editor through the journal email system if they require an extension.

After reception of a revised manuscript, it may be subjected to an additional round of review, particularly if the manuscript was originally placed in the “acceptable” category. The final decision of acceptance or rejection lies with the Editor-in-Chief in coordination with the subject editor, pending approval by the SQUJS editorial board and the Sultan Qaboos University Academic Publication Board.

All communications between authors, editors and reviewers are made using the Journal Management System at: <http://journals.squ.edu.om/index.php/squjs/index>

Authorship

Authorship must be based on all of the following criteria: (1) substantial contribution to the conception and design of the study, data acquisition, analysis and interpretation of the data; (2) drafting the article or revising it critically and; (3) final approval of the version of the manuscript to be published. Contributors who do not meet all 3 of these criteria should be listed in the acknowledgements section of the manuscript. The corresponding author is responsible for taking all necessary coordinating actions for revising the manuscript, receiving authorization from other authors, etc.

Scientific misconduct

According to standard practices in scientific journals, SQU Journal For Science follows the recommendations of the Council of Science Editors (www.councilscienceeditors.org) and defines misconduct as:

1. **Data Corruption:** falsifying data, inventing data, ignoring part of the data purposefully, or any form of omission, suppression or distortion of data.

2. **Plagiarism:** using published or unpublished texts, ideas or thoughts of another writer without acknowledgements and presenting them as one's own. Plagiarism includes duplicate publications or submissions in the same or in another language. The journal will follow COPE guidelines to identify and manage cases of plagiarism or text recycling.

3. **Authorship misconduct:** Exclusion of involved researchers, or inclusion of researchers who have not contributed significantly to the work (see section on authors), or publication without the consent of all authors.

4. **Ethical misconduct:** Failure to follow legal requirements in acquiring the necessary permission to sample, collect, export or import specimens, collect data, use chemicals or obtain ethical permits in the country of the author's institution.

SQU Journal for Science takes all forms of misconduct very seriously. It follows the Committee for Publication Ethics (COPE) recommendations and guidelines (publicationethics.org/resources/guidelines). Final decisions regarding scientific misconducts are taken by the Editor-in-Chief.

Types of articles

The journal accepts several types of articles and recommends the following submission length and subsections:

Editorials (by invitation only)

Editorials should not exceed 2000 words and a maximum of 25 references.

Reviews

Reviews should not exceed 6000 words and 14 pages and approximately 100 references. Authors who would like to submit a review are requested to send to the Editor-in-Chief (squjs@squ.edu.om) a one-page pre-proposal outlining the focus and scope of the projected review before submitting their review online. The abstract of a review paper, although structured, does not have to follow the "5 section template".

Research Articles (original research not exceeding 6000 words)

Research papers should not exceed 6000 words or 14 pages and 50 references. They should be divided into the following 6 sections: Abstract, Introduction, Materials and Methods, Results, Discussion and References. Additional sections such as Acknowledgement, Conclusion or Recommendations can also be included. Although merging results and discussion is possible, it is not a structure encouraged by the editorial board.

Communications/Notes (original research not exceeding 6 printed pages)

Communications/Notes are short original research articles. They should not exceed 3000 words and 30 references or 6 printed pages. They should have the same overall structure as Research Articles including a structured abstract.

Perspectives (short papers, not exceeding 3000 words)

Perspective papers are short papers that present an opinion or novel interpretation of existing ideas or data. They may also present an historical perspective on one of the themes of the journal. These manuscripts should follow a structure and a logical sequence of sections related to the content and purpose of the paper.

Journal language and translation

The Journal publishes papers in English, with the title, author names, abstracts and keywords published in Arabic and English. Where none of the authors are Arabic speaking, an abstract translation service is provided. British English spelling, usage, and punctuation are used throughout the journal.

Editing

Papers accepted for publication will be edited by the Journal editorial office for conciseness, clarity, grammar, spelling and style. Should the editing be extensive and possibly alter the intended meaning of the author(s), queries will be sent by email to the corresponding author requesting clarifications.

Style

The Journal follows the overall evolution of the scientific language. When preparing manuscripts please avoid jargon and long or complex sentences but aim at clear, concise and simple grammatical structures. The editorial board encourages the use of the active voice when it is appropriate.

Abstract

The Editorial board strongly suggests the use of a “structured abstract” not exceeding 300 words. These abstracts, although composed of a single paragraph, include 5 sections that summarize the content of the paper: introduction, experimentals/methodology, results, discussion and conclusion. Each section is introduced by a heading followed by a colon and a series of sentences.

Preparation of the manuscript

All papers will be typeset by the editorial team of the journal at publication time. Therefore, the editorial board requests the authors to follow a clear and simple format for their manuscript thereby facilitating the reviewing and editorial process. Templates for Microsoft Word™ are provided to assist authors in preparing their manuscripts.

The editorial board recommends the use of a classic typeface (Times, Helvetica, Garamond, Myriad-Pro, ...) with 12-point size and at least 14-16 points leading (line spacing) for the text of the manuscript with minimum formatting as most of layout and typographical formats will be applied at the typesetting stage. The manuscript page size should be A4 or US Letter and the editorial board recommends that a margin of at least 3 cm be included on all sides of the paper.

To facilitate the reviewing process, the text of the submission should have line numbers in the left hand margin restarting at 1 on each page and a page number in the footer of the document. Use standard typographic conventions for the text presentation: italic typeface for species names (not

underline), bold face for vectors, true superscript and subscripts when necessary. Emphasis is better marked through italic rather than bold face.

Typography

The journal uses standard typographic convention throughout. The editorial board recommends that you follow these in the preparation of the manuscript.

Italic should be used throughout for the Latin name of species (please do not use underlined text). Emphasis can be placed on some elements of text using bold face.

Abbreviations: Avoid non-standard abbreviations whenever possible, particularly in headings and subheading. If, for the sake of conciseness, the author wishes to use abbreviations, define each abbreviation when they first appear in each section of the manuscript. Standard abbreviation such as RNA, DNA, ATP, ADP, EDTA... do not need to be defined as most readers will be familiar with them. Others such as PAH (Polycyclic Aromatic Hydrocarbon) or ICP (Inductively Coupled Plasma) should be defined as most reader may not be familiar with their meaning.

Units: Always use the International System of Units (SI) for all units. For large or small units use the standard multiplier prefix for the units (k for 1000, M for 1000000, m for 1/1000 and μ for 10⁻⁶). Prefer whenever possible negative exponents to slash: kg·m⁻² rather than kg/m². To separate units, use either a mid-line point (\cdot =ASCII code 183 – Unicode U+00B7) or a non-breaking space. The abbreviated symbols (k, kg, s, P, W, etc.) should be used whenever possible and combined with Arabic numbers (5 kg, 2 m², 5.2 MP, 6.78 MW·h). The only exception is when a number is grammatically placed at the beginning of the sentence. A non-breaking space (Unicode U+00A0) should be used between the number and its units to insure that they stay together in the final document. The SI unit of time is s (second), h stands for hora, min for minuta, d for dies (day) and a for annum (year).

When necessary, non-SI units can be added between parenthesis to allow comparison with older literature or traditional systems of measurements. This includes usual units, such as surface of farming units (faddan, acres, ares, hectares), or traditional depth units (fathoms, brasses, Ba',...) or distance (nautical miles, miles) or other non SI units (gallons, inch, foot, bushels, etc.).

Illustrations

Illustrations should be numbered consecutively and submitted as individual files, not embedded in the article file. To insure compatibility, the journal accepts the following file format: JPEG, TIFF, PNG, PDF, EPS and SVG. Although the journal is normally published in black and white, color illustrations can be used when color is clearly necessary to convey the intended message. Although the authors can suggest the inclusion of color figures in the paper, the final decision to include them or not is left to the editorial board. The editorial team will strive to provide the best possible graphic output from the material submitted by the authors and may in some cases decide to redraw some figures to improve readability. They may also request better quality photographs or color figures if necessary. Typically black and white line figures should have a resolution of at least 600 dpi (at the final printed size) and color figures or photographs 300 dpi (at the final printed size) but should not exceed 10 MB. For line graphics, vector based file formats (SVG, PDF, EPS) are preferred as they are resolution independent.

Each illustration should have at the bottom of the page a brief identifier such as the name of the first author, the word Figure and the sequential number of the figure. (Al-Oufi, Figure 7 for

instance). The full captions of all figures should be presented in numerical order on a separate page at the end of the text manuscript.

In the figure use Helvetica as the standard typeface for all text (axis, legend, axis legend, equations, labels, etc.) and ensure that all text remain legible even after size reduction for final printing. Figures will be printed either as a single column (7 cm wide) or double column (14 cm) figure.

Macro-photographs, micro-photographs, SEM photographs, anatomical drawings, morphological illustrations, should have an appropriately labeled scale bar. Avoid multiplication factors (x100, x10000) as these will change with the rescaling of the figure when printed.

Tables

Tables should be presented in a clear manner and designed to fit on the width of a page. Exceptionally wide tables may be typeset, sideways, along the height of a printed page. All unnecessary decimals should be removed. Tables should be included at the end of the manuscript on separate pages and the legend/caption of each table should be placed on the same page and above the table.

Equations and numbers

Equations should be placed on separate lines and numbered sequentially at the end of the line. They should be typeset using an equation editor. If this is not possible, scan or photograph a clear handwritten version of the equation, which will be typeset by the editorial assistant.

The Journal uses the modern scientific number styles recommended by the Council of Science Editors. This style uses digit numbers (1, 2, 4.5, 7, etc.) for all numeric representations, even single digit ones. The main exceptions are when a digit starts a sentence, or when the single digit number is part of an idiomatic expression such as in “one or both”, a “zero-tolerance policy”, a “one-to-one interview”, “one has to agree that”...

In-text citations:

Please cite references in the text by number only enclosed in parentheses. Citations of unpublished work are listed in parentheses in the text only as follows: ...by J.A. Smith (personal communication); ...(J.A. Smith, personal communication); ...according to J.A. Smith (unpublished data); or ...(J.A. Smith, unpublished data). If the cited individual is not mentioned elsewhere in the references, the individual's full name and address should be provided in a footnote.

End of text references

The bibliographic information for all cited references in the articles are listed at the end of the papers under the heading “References”. Arrange the cited references in the order they appear in the text in sequential numerical order. References should be in full and should provide the reader with needed information to retrieve and examine the cited reference. Please follow the examples shown below, including punctuation. The Journal names follow a “Title case” capitalization - all words are capitalized except for articles (a, an, the); for prepositions (against, of, in, to), for conjunctions (and, for, not, or)-and should NOT be abbreviated. Titles of articles, books, on the other hand follow a sentence case capitalization (i.e. words are capitalized according to the grammar of the language of publication): the first word, the first word that follow a colon or a

semi colon, names of geographic locations, or proper nouns, etc. For articles published in non-English languages, provide the original title if the language uses roman characters or a translation of the title for other languages (Arabic for instance) and add the name of language between 2 periods at the end of the reference.

For online references, follow the overall same standard as for print publication, but include a date of access and a DOI number, if possible. Unpublished results and personal communication are not recommended in the reference list, but may be mentioned in the text. If these references are included in the reference list, they should follow the standard reference style of the journal and should include a substitution of the publication date with either “Unpublished results” or “Personal communication”. Citation of a reference as “in press” implies that the item has been accepted for publication.

Volume and issues, if available, follow directly the Title of the Journal with the issue number between parenthesis. Page numbers follow a colon and are separated by a hyphen. For books, the total page number is used with the abbreviation “pp.” whereas for chapter/section of books, the abbreviation is “p.” followed by the range of pages of the section (p. 25-44). All references end with a period.

Following are some examples of common references:

Single authored paper

Yallaoui, B. Filter representation of normal lattices. *Sultan Qaboos University Journal for Scientific Research - Science and Technology*, 1997, **1**, 63-67.

Multi authored paper

Al-Rumhy, M., Al-Bimani, A. and Boukadi, F. Effect of compositional grading on reservoir performance. *Sultan Qaboos University Journal for Scientific Research - Science and Technology*, 1997, **1**, 37-45.

Book

Steel, R.G. and Torrie, J.H. *Principles and Procedures of Statistics: A Biometrical Approach* (2nd Edition) McGraw-Hill Publishing Co., New York, 1980.

Chapter in a book

Apel, M. and Turkay, M. The Intertidal Crabs and Hermit Crabs (Crustacea: Decapoda: Brachyura: Paguridae) in the Study Area and their Condition After the Oil Spill. In *Establishment of Marine Habitat and Wildlife Sanctuary for the Gulf Region*. Eds. Feltkamp, E. and Krupp, F. Jubail and Frankfurt, 1992.

Bulletin

Page, C.H. and Vigoureaux, P. (Eds). The International System of Units (SI). *National Bureau of Standards Special Publication No. 330 (rev.)*, U.S. Government Printing Office, Washington, DC, 1986.

Conference proceedings

Stirm M., Oceanographic conditions and pelagic biological processes in Omani waters. *Proceedings of FAO Workshop "Mesopelagic Fish Stocks of NW Indian Ocean"*, 29-31 October 1994, Muscat, Oman.

Conference presentation

Elbualy, M.S. Sero-prevalence of *Rubella*, Cytomegalovirus, Measles and Toxoplasmosis among Pregnant Women in Oman. *7th European Congress of Clinical Microbiology and Infectious Diseases*, 12-30 March, 1995, Vienna, Austria.

Submission checklist

1. The current submission has not been previously published nor is it currently submitted to another journal for consideration.
2. The submission text files are in Microsoft Office (.doc, .docx), OpenOffice (.odt), RTF (rtf) or Apple Pages (.pages) document file format.
3. The text of the document uses a 12-point standard font with a 14-16 point leading (space between lines) on A4 or US-Letter format pages with page numbers and line numbers. Manuscript conforms to the journal recommended styles, length and number of sections.
4. The Abstract of the paper follows the structured format described in the guide for authors and includes a single paragraph (<300 words) with 5 inline headings (Introduction, Methodology, Results, Discussion, and Conclusion) and keywords for the manuscript are provided.
5. Photography (or photographic plates) are submitted in the jpeg (.jpg) file format at 300 dots per inch (dpi) with 80% compression quality or better. Line drawings and other figures should be preferably submitted as vector graphics such as pdf, eps or svg files. Alternatively, high resolution (600dpi) image format are acceptable (PNG, TIFF, GIF).
6. All tables including (legend, description and footnotes) and all figure captions are part of the submission main text file.
7. The text adheres to the stylistic and bibliographic requirements outlined in this document which can also be found in the Journal web site.
8. The manuscript has been "spell-checked" and "grammar-checked".

Supplementary material

SQUJS accepts electronic supplementary material to support published manuscripts. These may include high-resolution images, sound-tracks, datasets and will be published online along with the electronic version of the published paper. Data should be provided in one of the supported format (pdf, doc, docx, odt, rtf, pages, jpeg, png, tiff, svg...) for printable documents and standard formats for non-printable documents (AIFF, MP4, MP3, etc.).

Copyrights

The content of the journal is licensed under the Creative Common (CC BY ND) licensing schemes, the details of which can be found at <https://creativecommons.org/licenses/by-nd/4.0/legalcode>.

Proofs

The galley proof of an accepted article is emailed in PDF format to the corresponding author for typographical checking only. It should be returned within 72 hours of receipt.

Publication ethics:

Committee on Publication Ethics (COPE) will be followed. <http://publicationethics.org>

Contact details

The Editor-in-Chief

SQUJS Editorial Office
College of Science
Sultan Qaboos University
P.O. box 36, Postal Code 123
Al-Khod, Muscat
Sultanate of Oman
Tel: (968) 2141 2251

Submission at <https://journals.squ.edu.om/index.php/squjs>

Email: squjs@squ.edu.om

Alternate email: msk@squ.edu.om

المحتويات

الأحياء

- ١ الشجرة المباركة في القرآن - هل هي شجرة الزيتون أم شجرة نخيل الزيت؟
مصطفى قطب
- ٩ تأثير التغيرات المناخية على النباتات الأكثر ندرة في البيئات الجافة
حمادة السيد على

الكيمياء

- ١٧ بناء كاشف فعال بواسطة الأكسدة النشطة لأوكسيد الكرافين لغرض التقدير الإنتقائي والحساس لمادة الدوبامين في
الدم
لمياء الغافري ونسيبة الحاتمي وصلاح الدين جوده وعماد خديش
- ٢٨ تحضير وتوصيف الممتز النانوي لأوكسيد الحديد بواسطة طحلب *Enteromorpha Flexuosa* المستخرج من
ينبع البحر الأحمر، المملكة العربية السعودية
علاء علمي، رأفت عفيفي خطاب، عمر محمد الحربي، جونيل إيمانوففا، عمران علي

الرياضيات

- ٤٤ تحليل طرق كسرية خطية متعددة الخطوات ذات الرتبة الرابعة من التقارب الفائق
خديجة الحسني وحنيفة محمد ناصر

الإحصاء

- ٥٦ المعرفة والموقف تجاه كوفيد -١٩ وحال الصحة النفسية المرتبطة بهما لدى طلاب جامعة السلطان قابوس، عمان
م. مظهر الإسلام، رونالد وسونغفا، إيمان الحسني، أفراح المعني

- i دليل المؤلف

مجلة جامعة السلطان قابوس للعلوم

(سابقاً: مجلة جامعة السلطان قابوس للبحوث العلمية – العلوم والهندسة)

تنشر مجلة جامعة السلطان قابوس للعلوم أبحاثاً أصلية تغطي مجالاً كاملاً من العلوم الأساسية والتطبيقية وتشمل الرياضيات، الإحصاء، الكيمياء، الفيزياء، علوم الأحياء، تقنية (تكنولوجيا) الأحياء، البيئة، علوم الأرض، علوم الحاسب الآلي وكذلك العلوم الأخرى ذات الصلة. كما يجب على الأوراق أن تعرض بحثاً أصلياً لم تنشر مسبقاً. بالإضافة إلى ذلك، فإنّ المجلة تنشر مقالاتٍ محررةً حول مواضيع ذات اهتمامٍ خاصٍ. وترحب المجلة بالمقالات التي لها علاقة بالعلوم التطبيقية ذات الصلة باحتياجات المجتمع المحلي العماني. من الدراسات التطبيقية الهامة نذكر كأمثلة كلاً من البحث عن الحالة الجيولوجية والجيوفيزيائية ونتائج العمل الميداني في مناطق مختلفة من سلطنة عُمان، حيث تكون الدراسات حول البحوث البيولوجية المحلية، توزيعات وحالة الدراسات، تصميم، تنفيذ وتقييم حلول تكنولوجيا المعلومات للصناعات المحلية. وسيتم تحكيم جميع الأوراق البحثية المقدمة.

مجلس النشر العلمي الجامعي

أ.د. عامر الهنائي، رئيس مجلس النشر العلمي الجامعي

أ.د. فاروق صبري مجالي
أ.د. سمير العدوي
أ.د. شافير رحمان
أ.د. سعيد الظفري
د. صالح البراشدي

أ.د. محمد صلاح الدين خان
أ.د. محمد الصقري
د. غازي الرواس
أ.د. سعيد الظفري
الفاضل جمال الغيلاني

مجلس تحرير المجلة

رئيس هيئة التحرير: أ.د. محمد صلاح الدين خان
المحررين: أ.د. رشيد سبيا
د. مايكل بييري

هيئة التحرير

أ.د. عبد الرزاق توزان
د. أحمد السلطان
د. إفتخار أحمد
أ.د. محمد العودات
د. نوال الراسبي
*أ.د. محمد رحمان
أ.د. أحمد الجرا، جامعة اليرموك، الأردن
أ.د. وائل اسماعيل، جامعة الخليج العربية، البحرين
أ.د. إيركان أوزكان، جامعة اسطنبول التقنية، تركيا
أ.د. عمران علي، جامعة المركزية، الهند
*مشرف الموقع الإلكتروني

د. صدقي حسن
أ.د. نظيفة كوجا
أ.د. رشيد سبيا
د. رانجراج سلفراج
د. طلال خليفة الحوسني
أ.د. كيليان داز، المعهد الهندي للتكنولوجيا، بومباي
أ.د. هيكل جيلاسي، المركز الوطني للعلوم والتقنيات النووية، تونس

هيئة المستشارين الدولية

أ.د. أسيف خان، جامعة باث، المملكة المتحدة
أ.د. دينيز سونار، جامعة أديمان، تركيا
أ.د. هدى محمود، جامعة الكويت

أ.د. بول رينبيرري، جامعة باث، المملكة المتحدة
أ.د. يوجندرا باراساد شوبي، جامعة كونكورديا، كندا
أ.د. كوبالابالي فيجيرفلي، جامعة فلوريدا، الولايات المتحدة الأمريكية

مساعد التحرير: ليلي العنبرية

تصميم الغلاف: ليلي العنبرية

تاريخ الإصدار: ديسمبر ٢٠٢٣ م

المجلة غير مسؤولة عن الآراء المنشورة فيها والتي تمثل آراء أصحابها.

جميع الاتصالات مع المجلة تكون عن طريق مكتبها: سلطنة عمان، مسقط، جامعة السلطان قابوس، مجلة جامعة السلطان قابوس للعلوم، ص.ب. ٣٦، الرمز البريدي ١٢٣. هاتف: ٢٤١٤-٢٢٥١ (٩٦٨). البريد الإلكتروني: squjs@squ.edu.om

ISSN (print edition): ١٠٢٧-٥٢٤ X; ISSN (online edition): ٢٤١٤-٥٣٦ X

تحرير وتصميم مكتب تحرير المجلة، كلية العلوم، جامعة السلطان قابوس.

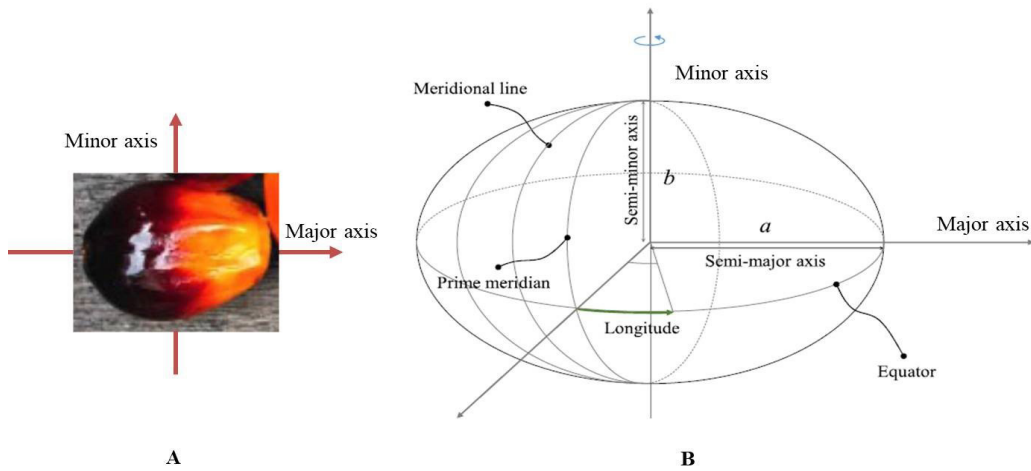
مجلة جامعة السلطان قابوس للعلوم



المجلد ٢٨ ، العدد ٢ ، ٢٠٢٣ م

ISSN (Print Edition): 1027-524 X; ISSN (Online Edition): 2414-536 X

جوجل سكولار، داوج ، كروس جاجيت، لوكس، دار المنظومة والمنهل



أ: ثمرة نخيل الزيت بشكلها البيضاوي والمحور الأكبر والأصغر لها ، ب : حدود النموذج البيضاوي لكوكب الأرض مع المحور الأكبر والأصغر لها (انظر ص.٥)

المحتويات

- الشجرة المباركة في القرآن - هل هي شجرة الزيتون أم شجرة نخيل الزيت؟
- تأثير التغيرات المناخية على النباتات الأكثر ندرة في البيئات الجافة
- بناء كاشف فعال بواسطة الأوكسدة النشطة لأوكسيد الكرافين لغرض التقدير الإنتقائي والحساس لمادة الدوبامين في الدم
- تحضير وتوصيف الممتز النانوي لأوكسيد الحديد بواسطة طحلب *Enteromorpha Flexuosa* المستخرج من ينبع البحر الأحمر ، المملكة السعودية
- تحليل طرق كسرية خطية متعددة الخطوات ذات الرتبة الرابعة من التقارب الفائق
- المعرفة والموقف تجاه كوفيد -١٩ وحال الصحة النفسية المرتبطة بهما لدى طلاب جامعة السلطان قابوس، عمان